FABRICATION OF SELF-ASSEMBLED ZEIN NANOPARTICLES VIA MICROFLUIDIC CHIP AND ULTRASONIC TREATMENT

BY

XUANBO LIU

DISSERTATION

Submitted in partial fulfillment of the requirements
for the degree of Doctor of Philosophy in Food Science and Human Nutrition
with a concentration in Food Science
in the Graduate College of the
University of Illinois at Urbana-Champaign, 2021

Urbana, Illinois

Doctoral Committee:

Professor Feng Hao, Chair
Associate Professor Youngsoo Lee, Director of Research
Research Professor Graciela Wild Padua
Professor Michael J Miller

ABSTRACT

There are many health-promoting and disease-preventing bioactive compounds that are beneficial for human health, such as curcumin, lycopene, lutein, resveratrol, and apigenin. However, these bioactive compounds have some challenges to be used in the food and pharmaceutical industries because of their poor solubility, poor bioavailability, and chemical instability. These limitations can be overcome by encapsulating bioactive compounds into the nanoscale delivery systems (emulsions, liposomes, nanoemulsions, microgels, and nanoparticles). Among these nanoscale delivery systems, nanoparticles have received increasing attention in the food industry for applications like food packaging, sensor, and encapsulation. Zein is a group of prolamines extracted from corn, which is generally recognized as safe in the food industry, and it can form self-assembled nanoparticles in water or a low concentration of ethanol via anti-solvent precipitation. The traditional method to form the zein nanoparticles is dropping the zein ethanol solution into a bulk water phase with mechanical shearing, which creates the heterogeneous shear environment and uncontrolled for nanoparticle formation. In this study, two methods were used to fabricate zein nanoparticles: microfluidic chip and ultrasonic treatment. Microfluidic chips are novel platforms that are used to control the ultra-small volume of fluids going through channels with the dimensions of tens of micrometers. Ultrasound technology has been used in the food industry for many years for bio-compounds extraction, viscosity modification.

The overall objective of this study is to assess the impact of process parameters on the properties of the zein nanoparticles formed via a microfluidic fabrication and ultrasonic treatment and to assess the encapsulation and activities of bioactive compounds, such as nisin and curcumin, in the zein nanoparticles.

First, zein-OSA modified starch nanoparticles were fabricated via a T-junction configuration of the microfluidic chip. The dispersed phase was 1% or 2% zein in 70% (w/v) ethanol and the continuous phase was OSA-modified starch solution at various concentrations: 0%, 1%, 2.5%, 5%, 7.5%, and 10% (w/w). Compared with zein nanoparticles, the zein-OSA starch nanoparticle complexes were stable in various sodium chloride concentrations.

Then, nisin was encapsulated into zein-OSA modified starch and the encapsulation efficiency and the anti-microbial activity of nisin in the zein nanoparticles against *Listeria monocytogenes* in Queso Fresco were measured. As the concentration of OSA modified starch increased, the encapsulation efficiency and anti-microbial activity of nisin increased.

Zein nanoparticles were also formed via ultrasonic treatment with the different initial concentrations of ethanol in the continuous phase, the different ratios of the dispersed phase to continuous phase, and the different ultrasound amplitude. As the initial concentration of ethanol in the continuous phase increased, the particle size increased. PDI results revealed that as the concentration of ethanol in the continuous increased, the PDI decreased and then increased suggesting that there may be a critical ethanol concentration for zein seld-assembly.

Finally, the curcumin was encapsulated into zein nanoparticles via ultrasonic treatment with different initial concentrations of ethanol in the continuous phase and ultrasound amplitude. The findings from this study showed that the presence of zein protected curcumin from degradation under heat and UV light environment, and encapsulation altered the physical state of curcumin from a crystallized state to an amorphous state which may improve the bioaccessibility of the curcumin.

Keywords Zein nanoparticle complexes, the microfluidic chip, ultrasonic treatment

ACKNOWLEDGMENTS

I would like to express my most sincere appreciation to my advisor, Dr. Youngsoo Lee, for his and motivation, enthusiasm, and immense knowledge. Dr. Lee is always patient to listen to my ideas even sometimes are immature. I cannot forget every week's individual meeting and lab meeting, which helped me set up the direction of my research, experiments, and analysis results. Without these individual meetings and lab meetings, I cannot finish these experiments. I cannot forget that Dr. Lee revised my thesis repeatedly from the structure of the thesis to even minor grammar mistakes. Throughout my graduate research, Dr. Lee has given me great freedom to pursue my research, and sometimes even without an objection. This thesis would not have been possible without the support and guidance from him.

Furthermore, I would like to thank my committee members, Dr. Padua, Dr. Feng, and Dr. Miller. The valuable advice they have provided during committee meetings, preliminary exam, and personal conversations have helped me identify the strengths and weaknesses of my study and broadened my scientific view. It has been a pleasure to learn from their expertise and passion for research.

I am also very grateful to Dr. Soo-Yeun Lee, and Dr. Schmidt who has mentored me from every lab meeting. They generously spent their time discussing my research during lab meetings, and brought up insightful and sometimes philosophical perspectives, to help me reflect and solidify my work.

Lastly, I would want to thank my parents, for always supporting me to pursue my dreams. The relentless love from my family and friends has sustained me through the tough days over the past years.

Table of Contents

CHAPTER 1: Introduction

1.1 Significance

Bioactive compounds are receiving much attention in food research because of their various disease-preventing and health-promoting properties (de Vos, Faas, Spasojevic, & Sikkema, 2010). However, bioactive compounds often have limitations to be incorporated into the food matrices due to poor solubility, poor bioavailability, chemical instability (J. Chen & Hu, 2020). These limitations can be overcome by encapsulating bioactive compounds into the nanoscale delivery systems (emulsions, liposomes, nanoemulsions, microgels, and nanoparticles) to reduce the reactivity of the compounds with the environmental factors, such as oxygen, light, or water, and to control the release of bioactive compounds for the maximum efficacy (Ranjan, Dasgupta, & Lichtfouse, 2016) and improve solubility in food matrices (Kamiya, Otani, Fuji, & Miyahara, 2018) . Among these nanoscale delivery systems, nanoparticles have received increasing attention in the food industry for applications like food packaging, sensor, and encapsulation. Nanoparticles are nanometer size (1 nm to 1 μm) ultrafine particles with unique properties due to their large surface area. In general, nanoparticles can be produced by three different methods: 1) top-down that breaks down the larger particles into nanoparticles, such as milling and homogenization; 2) bottom-up that builds the smaller particles into nanoparticles, such as spontaneous emulsification and anti-solvent precipitation; 3) mixed approaches (Mcclements, 2015). The energy used in the top-down methods is higher than the bottom-up methods (Joye & McClements, 2013). Anti-solvent precipitation is an attractive technology to form the nanoparticles in the food delivery system because of the energy-saving and well-controlled environment. Biopolymers associate spontaneously to form nanoparticles when the biopolymers are dropped into the anti-solvent from a solution.

Zein is the plant-based prolamin mixed proteins extracted from corn, and there are more than 50% hydrophobic amino acids in zein. Zein can form the anti-solvent nanoparticles in water or low concentration ethanol solution by shearing (H. Chen & Zhong, 2014), ultrasound (Feng, Zheng, Luan, Shao, & Sun, 2019; Ren et al., 2019), or microfluidic device (Olenskyj, Feng, & Lee, 2017). Because of its unique properties, the zein nanoparticles have been used for encapsulation and delivery of bioactive compounds, such as curcumin, essential fatty acid, carotenoids, etc (Chang, Wang, Hu, & Luo, 2017).

Microfluidic chips are novel platforms that are used to control the ultra-small volume of fluids going through channels with the dimensions of tens of micrometers. For food research, microfluidic chips can be used as tools to form emulsions and microcapsules (Comunian, Ravanfar, Alcaine, & Abbaspourrad, 2018; Priest, Reid, & Whitby, 2011; Ravanfar, Comunian, Dando, & Abbaspourrad, 2018; Zhao-Miao, Yu, & Yan, 2018), micro-detection tools (Guo, Feng, Fang, Xu, & Lu, 2015; Kant et al., 2018; Kim et al., 2015), and micro-reactors (Marze, Algaba, & Marquis, 2014; Nguyen, Marquis, Anton, & Marze, 2019a, 2019b). There are many advantages for the microfluidic chip: small reagent volumes, high selectivity, green credentials, rapid reactions, and small footprints (Elvira, i Solvas, Wootton, & deMello, 2013). However, very few food-grade materials have been successfully adapted in a microfluidic chip and more studies are needed to explore the applications that require food-grade materials. Zein is a food-grade material and can form nanoparticles in the microfluidic chip via self-assembly (Olenskyj et al., 2017). However, zein nanoparticles are not stable in the wide range of pH, especially at and near its isoelectric point. Polysaccharides can be attached to the surface of zein nanoparticles to increase stability. The nanoparticles with protein-polysaccharide complex have gained attention in the food, personal care, and pharmaceutical industries because of the several advantages, such as easy

preparation, biodegradability, and biocompatibility (Chang et al., 2017). Protein-polysaccharide complex has been reported to encapsulate bioactive compounds and increase the encapsulation efficiency and stability of the core materials (Dai et al., 2018). The octenyl-succinic-anhydride (OSA) modified starch is an amphiphilic molecule obtained from the esterification reaction between starch hydroxyl groups and octenyl succinic anhydride and can be used as an emulsion stabilizer and encapsulating agent (Sweedman, Tizzotti, Schäfer, & Gilbert, 2013). OSA–modified starch has been used in the food industry for more than 40 years (Hui, Qi-he, Ming-liang, Qiong, & Guo-qing, 2009). In this project, we aim to fabricate the zein-OSA modified starch nanoparticles using a microfluidic chip and assess the stability of zein nanoparticles in a wide range of pH. For the application of the zein nanoparticles, nisin was encapsulated into zein-OSA modified starch nanoparticles and the encapsulation efficiency and anti-microbial activity of nisin was evaluated.

The microfluidic chip is an effective tool for nanoparticle formation with a small reagent volume, but the sample collection is time-consuming because of the scale of the microfluidic chip. Ultrasound treatment may overcome the challenges of the microfluidic chip in terms of throughput. Ultrasonic energy is generated by a transducer which converts the electrical energy to mechanical vibration. The main driving force of ultrasonic treatment is cavitation by generating the shear force and causing fluid mixing (Kentish & Feng, 2014). Ultrasound technology has been used in the food industry for many years for bio-compounds extraction, viscosity modification, emulsification, surface cleaning, food quality assurance, filtration, tenderization, etc. What's more, ultrasonic treatment can be used to form various nanoparticles and improve the stability of nanoparticles. Ultrasonic treatment increased the yield of the starch nanoparticles (Minakawa, Faria-Tischer, & Mali, 2019) and decreased the particle size of the protein nanoparticles (Zhang et al., 2018). The ultrasound can also help the zein nanoparticle formation (Feng et al., 2019).

However, few studies focused on how the parameters, such as the amplitude of ultrasound and the ethanol concentration of continuous phase, affect the properties of zein nanoparticles via ultrasonic treatment. Therefore, we aim to investigate the impact of ultrasound amplitude and ethanol concentration of continuous phase on the properties of zein nanoparticles. Also, the curcumin was encapsulated in zein nanoparticles using ultrasound treatment, and the encapsulation efficiency and antioxidant activity of curcumin were evaluated.

1.2 Overall goal and hypothesis

The overall objective of this study is to assess the impact of process parameters on the properties of the zein nanoparticles formed via a microfluidic fabrication and ultrasonic treatment and to assess the encapsulation and activities of bioactive compounds, such as nisin and curcumin, in the zein nanoparticles.

The overall hypotheses are 1) Microfluidic device and ultrasonic treatment will provide a well-controlled environment to form zein nanoparticles by adjusting the surface modification of zein particles, the ratio of the dispersed phase and continuous phase, the composition of the continuous phase, and the amplitude of ultrasound wave. The variation of those parameters will allow the control of particle size and stability of zein nanoparticles. 2) The encapsulation efficiency, antimicrobial activity of nisin, and antioxidant activity of curcumin in the zein nanoparticles will increase due to either additional wall material on the zein surface or modification of the morphology and crystallinity of encapsulated bioactive compounds.

1.3 Specific aims and hypotheses

The following four specific aims are proposed to achieve our overall objective and test the hypotheses for this study.

Aim 1: Evaluate the properties and stability of the zein-OSA modified starch nanoparticles via a microfluidic chip.

Hypothesis 1: The particle size of the zein OSA-modified starch complex will increase and the zeta-potential of the nanoparticles will approach to zeta-potential of OSA-modified starch with the increasing concentration of OSA-modified starch. The aggregation of the zein nanoparticles will be decreased by the addition of OSA-modified starch due to its adsorption on the surface of zein nanoparticles.

Aim 2: Evaluate the encapsulation efficiency and antimicrobial activity of nisin in zein-OSA-modified starch nanoparticles formed via a microfluidic chip.

Hypothesis 2: The encapsulation efficiency and antimicrobial activity of nisin in zein-OSA-modified starch nanoparticles will increase with a higher concentration of the modified starch because a thicker layer of OSA-modified starch on the surface of zein nanoparticles provide additional space for nisin to be encapsulated.

Aim 3: Evaluate the effect of ethanol concentration in the continuous phase, the ratio of the dispersed phase and continuous phase, and amplitude of ultrasound waves on the properties of zein nanoparticles.

Hypothesis 3: Increasing ethanol concentration in the continuous phase will increase the particle size of the zein because zein will be easier to become supersaturated and induce nucleation at the lower ethanol concentration. Increasing the ratio of the dispersed phase and continuous phase will increase the particle size of the zein because more zein exists to form nanoparticles. Besides, increasing the amplitude of the ultrasound wave will decrease particle size due to increased cavitation and shear force during the formation of zein nanoparticles.

Aim 4: Assess the encapsulation efficiency and stability of the curcumin encapsulated in the zein nanoparticles by the ultrasonic treatment.

Hypothesis 4: Compared with the shearing treatment, ultrasonic treatment will have higher encapsulation efficiency because the ultrasound will change the morphology and crystallinity of curcumin to trap more core materials in the zein nanoparticles. Compared with the free curcumin, the stability of the encapsulated curcumin via ultrasonic and shearing treatment will be increased because zein prevents curcumin exposure to the adverse environment.

1.4 References

Chang, C., Wang, T., Hu, Q., & Luo, Y. (2017). Caseinate-zein-polysaccharide complex nanoparticles as potential oral delivery vehicles for curcumin: Effect of polysaccharide type and chemical cross-linking. *Food Hydrocolloids*, *72*, 254–262. https://doi.org/10.1016/j.foodhyd.2017.05.039

Chen, H., & Zhong, Q. (2014). Processes improving the dispersibility of spray-dried zein nanoparticles using sodium caseinate. *Food Hydrocolloids*, *35*, 358–366. https://doi.org/10.1016/j.foodhyd.2013.06.012

Chen, J., & Hu, L. (2020). Nanoscale Delivery System for Nutraceuticals: Preparation, Application, Characterization, Safety, and Future Trends. *Food Engineering Reviews*, *12*(1), 14–31. https://doi.org/10.1007/s12393-019-09208-w

Comunian, T. A., Ravanfar, R., Alcaine, S. D., & Abbaspourrad, A. (2018). Water-in-oil-in-water emulsion obtained by glass microfluidic device for protection and heat-triggered release of natural pigments. *Food Research International*, *106*(September 2017), 945–951. https://doi.org/10.1016/j.foodres.2018.02.008

Dai, L., Li, R., Wei, Y., Sun, C., Mao, L., & Gao, Y. (2018). Fabrication of zein and rhamnolipid complex nanoparticles to enhance the stability and in vitro release of curcumin. *Food Hydrocolloids*, *77*, 617–628. https://doi.org/10.1016/j.foodhyd.2017.11.003

de Vos, P., Faas, M. M., Spasojevic, M., & Sikkema, J. (2010). Encapsulation for preservation of functionality and targeted delivery of bioactive food components. *International Dairy Journal*, *20*(4), 292–302. https://doi.org/10.1016/j.idairyj.2009.11.008

Elvira, K. S., i Solvas, X. C., Wootton, R. C. R., & deMello, A. J. (2013). The past, present and potential for microfluidic reactor technology in chemical synthesis. *Nature Chemistry*,

5(11), 905–915. https://doi.org/10.1038/nchem.1753

Feng, S., Zheng, X., Luan, D., Shao, P., & Sun, P. (2019). Preparation and characterization of zein-based phytosterol nanodispersions fabricated by ultrasonic assistant anti-solvent precipitation. *Lwt*, *107*(March), 138–144. https://doi.org/10.1016/j.lwt.2019.03.025

Guo, L., Feng, J., Fang, Z., Xu, J., & Lu, X. (2015). Application of microfluidic "lab-on-a-chip" for the detection of mycotoxins in foods. *Trends in Food Science and Technology*, *46*(2), 252–263. https://doi.org/10.1016/j.tifs.2015.09.005

Hui, R., Qi-he, C., Ming-liang, F., Qiong, X., & Guo-qing, H. (2009). Preparation and properties of octenyl succinic anhydride modified potato starch. *Food Chemistry*, *114*(1), 81–86. https://doi.org/10.1016/j.foodchem.2008.09.019

Joye, I. J., & McClements, D. J. (2013). Production of nanoparticles by anti-solvent precipitation for use in food systems. *Trends in Food Science and Technology*, *34*(2), 109–123. https://doi.org/10.1016/j.tifs.2013.10.002

Kamiya, H., Otani, Y., Fuji, M., & Miyahara, M. (2018). *Characteristics and Behavior of Nanoparticles and Its Dispersion Systems*. *Nanoparticle Technology Handbook*. https://doi.org/10.1016/B978-0-444-64110-6.00003-2

Kant, K., Shahbazi, M. A., Dave, V. P., Ngo, T. A., Chidambara, V. A., Than, L. Q., … Wolff, A. (2018). Microfluidic devices for sample preparation and rapid detection of foodborne pathogens. *Biotechnology Advances*, *36*(4), 1003–1024. https://doi.org/10.1016/j.biotechadv.2018.03.002

Kentish, S., & Feng, H. (2014). Applications of Power Ultrasound in Food Processing. *Annual Review of Food Science and Technology*, *5*(1), 263–284. https://doi.org/10.1146/annurev-food-030212-182537

Kim, M., Jung, T., Kim, Y., Lee, C., Woo, K., Seol, J. H., & Yang, S. (2015). A microfluidic device for label-free detection of Escherichia coli in drinking water using positive dielectrophoretic focusing, capturing, and impedance measurement. *Biosensors and Bioelectronics*, *74*, 1011–1015. https://doi.org/10.1016/j.bios.2015.07.059

Marze, S., Algaba, H., & Marquis, M. (2014). A microfluidic device to study the digestion of trapped lipid droplets. *Food and Function*, *5*(7), 1481–1488. https://doi.org/10.1039/c4fo00010b

Mcclements, D. J. (2015). Nanoscale Nutrient Delivery Systems for Food Applications: Improving Bioactive Dispersibility, Stability, and Bioavailability. *Journal of Food Science*, *80*(7), N1602–N1611. https://doi.org/10.1111/1750-3841.12919

Minakawa, A. F. K., Faria-Tischer, P. C. S., & Mali, S. (2019). Simple ultrasound method to obtain starch micro- and nanoparticles from cassava, corn and yam starches. *Food Chemistry*, *283*(January), 11–18. https://doi.org/10.1016/j.foodchem.2019.01.015

Nguyen, H. T., Marquis, M., Anton, M., & Marze, S. (2019a). Studying the real-time interplay between triglyceride digestion and lipophilic micronutrient bioaccessibility using droplet microfluidics. 2 application to various oils and (pro)vitamins. *Food Chemistry*, *275*(July 2018), 661–667. https://doi.org/10.1016/j.foodchem.2018.09.126

Nguyen, H. T., Marquis, M., Anton, M., & Marze, S. (2019b). Studying the real-time interplay between triglyceride digestion and lipophilic micronutrient bioaccessibility using droplet microfluidics. 2 application to various oils and (pro)vitamins. *Food Chemistry*, *275*(July 2018), 661–667. https://doi.org/10.1016/j.foodchem.2018.09.126

Olenskyj, A. G., Feng, Y., & Lee, Y. (2017). Continuous microfluidic production of zein nanoparticles and correlation of particle size with physical parameters determined using

CFD simulation. *Journal of Food Engineering*, *211*, 50–59. https://doi.org/10.1016/j.jfoodeng.2017.04.019

Priest, C., Reid, M. D., & Whitby, C. P. (2011). Formation and stability of nanoparticle-stabilised oil-in-water emulsions in a microfluidic chip. *Journal of Colloid and Interface Science*, *363*(1), 301–306. https://doi.org/10.1016/j.jcis.2011.07.060

Ranjan, S., Dasgupta, N., & Lichtfouse, E. (2016). *Nanoscience in Food and Agriculture 3* (Vol. 23). https://doi.org/10.1007/978-3-319-48009-1

Ravanfar, R., Comunian, T. A., Dando, R., & Abbaspourrad, A. (2018). Optimization of microcapsules shell structure to preserve labile compounds: A comparison between microfluidics and conventional homogenization method. *Food Chemistry*, *241*(June 2017), 460–467. https://doi.org/10.1016/j.foodchem.2017.09.023

Ren, X., Hou, T., Liang, Q., Zhang, X., Hu, D., Xu, B., … Ma, H. (2019). Effects of frequency ultrasound on the properties of zein-chitosan complex coacervation for resveratrol encapsulation. *Food Chemistry*, *279*(May 2018), 223–230. https://doi.org/10.1016/j.foodchem.2018.11.025

Sweedman, M. C., Tizzotti, M. J., Schäfer, C., & Gilbert, R. G. (2013). Structure and physicochemical properties of octenyl succinic anhydride modified starches: A review. *Carbohydrate Polymers*, *92*(1), 905–920. https://doi.org/10.1016/j.carbpol.2012.09.040

Zhang, Y., Zhou, F., Zhao, M., Lin, L., Ning, Z., & Sun, B. (2018). Soy peptide nanoparticles by ultrasound-induced self-assembly of large peptide aggregates and their role on emulsion stability. *Food Hydrocolloids*, *74*, 62–71. https://doi.org/10.1016/j.foodhyd.2017.07.021

Zhao-Miao, L. I. U., Yu, D. U., & Yan, P. A. N. G. (2018). Generation of Water-In-Oil-In-Water (W/O/W) Double Emulsions by Microfluidics. *Chinese Journal of Analytical Chemistry*,

46(3), 324–330. https://doi.org/10.1016/S1872-2040(17)61072-7

CHAPTER 2: Literature Review

2.1 Bioactive Compounds – Curcumin and Nisin

Bioactive compounds are both essential or non-essential food components that are formed in nature and have the benefit on human health, such as antioxidant effect, anti-inflammatory effect, antibacterial effect, antitumor effect, hypoglycemic effect, gastrointestinal protection, and cardiovascular protection (Biesalski et al., 2009). These include phenolic compounds, essential fatty acids, essential oils, vitamins, and aroma components (Rezaei, Fathi, & Jafari, 2019). The bioactive compounds can be extracted by soxhlet extraction, maceration, hydrodistillation, ultrasound-assisted extraction, pulsed-electric field extraction, enzyme-assisted extraction, microwave-assisted extraction, pressurized liquid extraction, and supercritical fluid extraction (Azmir et al., 2013). Most of the bioactive compounds have the limitation for application in the food industry because of their low water solubility, high sensitivity to heat, light, and oxygen and low bioavailability (Rezaei et al., 2019). Curcumin and Nisin are examples of bioactive compounds.

Curcumin is a natural polyphenolic compound that is extracted from *curcuma longa* (Artiga-Artigas, Lanjari-Pérez, & Martín-Belloso, 2018; Ubeyitogullari & Ciftci, 2019). *Curcuma longa* contains 3-5% curcuminoids (consisting of 77% curcumin, 17% demethoxycurcumin, 3% bisdemethoxycurcumin, and 3% cyclocurcumin) (Araiza-Calahorra, Akhtar, & Sarkar, 2018). As the majority component of curcuminoids in *curcuma longa*, curcumin is a yellowish powder with a high order crystal structure, including monoclinic, orthorhombic, and amorphous structures (Thorat & Dalvi, 2014). As shown in Fig 2.1, the curcumin exists in the equilibrium between the keto and enol form under the different environments. The health benefits of curcumin are widely acknowledged, such as antioxidant, antimicrobial, anticancer. However, the curcumin has the

limitation for application because of biochemical/structural degradation under the external environment such as high light intensity and high temperature (Artiga-Artigas et al., 2018). What's more, the curcumin has a low bioavailability because of a high degree of crystalline and lower water solubility (Ubeyitogullari & Ciftci, 2019). The curcumin has a different solubility in different solvents: water (11 ng/mL), ethanol (5.6 mg/mL), methanol (4.44 mg/mL), acetone (7.75 mg/mL), and isopropanol (3.93 mg/mL) (Araiza-Calahorra et al., 2018). To overcome these limitations, the food delivery systems can be used to carry curcumin, such as O/W emulsions, Pickering emulsions, and nanoemulsions (C. Chang, Wang, Hu, & Luo, 2017; S. Chen, Han, et al., 2020; S. Chen et al., 2018; Dai et al., 2018; Silva et al., 2018; Ubeyitogullari & Ciftci, 2019). The stability and bioavailability of curcumin in the delivery systems can be affected by oil composition, the droplet size of emulsions, and dispersion conditions (Lu, Kelly, & Miao, 2016).

Nisin is another bioactive compound that has been used in the food industry for many years. Nisin is an antimicrobial peptide derived from *Lactococcus lactis*, consisting of nisin A, nisin Z, nisin Q, nisin U, nisin U2, nisin F, and nisin H (Özel, Şimşek, Akçelik, & Saris, 2018). There are four subgroups of bacteriocins, including class I (less than 5 kDa), class II (less than 10 kDa), class III (bigger than 10 kDa), and class IV (contain different compounds). Nisin belongs to class I containing 34 amino acids, which is shown in Fig 2.2 (Bahrami, Delshadi, Jafari, & Williams, 2019). Nisin has been considered as generally recognized as safe (GRAS) in the food system by the Food and Drug Administration (FDA) (Bahrami et al., 2019; Modulation, 2020; Özel et al., 2018; Shin et al., 2016). In the food industry, nisin can be used as the antibacterial agent against Gram-positive bacterial, such as *Listeria monocytogenes* and *Staphylococcus aureus*. However, nisin has some limitations for application in foods, including low stability to the extrinsic environmental stresses (high pH, high temperature), undesirable interactions with other food

components, and low water solubility (de Arauz, Jozala, Mazzola, & Vessoni Penna, 2009). These limitations can be overcome by encapsulating nisin into nanocarriers, including nanoemulsion, nanoparticles, nanoliposomes, and nano-fibers (Bahrami et al., 2019).

2.2 Nanoscale delivery systems

The nanoscale delivery systems are emerging food vehicles with particles in the nanoscales range, including emulsions, liposomes, nanoemulsions, nanogels, and nanoparticles which is shown in Fig 2.3 (Ranjan, Dasgupta, & Lichtfouse, 2016). The nanoscale delivery systems can be used to encapsulate bioactive compounds to reduce the reactivity of the compounds with environmental factors, such as oxygen, light, or water, and to control the release of bioactive compounds for maximum efficacy (J. Chen & Hu, 2020; Joye & McClements, 2013; Mcclements, 2015). Among these nanoscale delivery systems, nanoparticles have received increasing attention in the food industry for applications like food packaging, sensor, and encapsulation. Nanoparticles are nanometer size (1 nm to 1 μm) ultrafine particles with unique properties due to their large surface area. As showed in Fig 2.4, nanoparticles can be produced by two different methods: 1) top-down that breaks down the larger particles into nanoparticles, such as milling and homogenization; 2) bottom-up that builds the smaller particles into nanoparticles, such as spontaneous emulsification and anti-solvent precipitation (Mcclements, 2015). The energy required in the top-down methods is higher than the bottom-up methods (Joye & McClements, 2013). The anti-solvent precipitation is an attractive technology to form nanoparticles in delivery systems because of the low-energy and well-controlled environment. Biopolymers associate spontaneously to form nanoparticles when the biopolymers are dropped into the anti-solvent from a solution to induce supersaturation. There are four stages during the anti-solvent precipitation: Stage I supersaturation, Stage II nucleation, Stage III crystal growth, and Stage IV coagulation. As the concentration of solute

increases, the solute experiences saturation, supersaturation, nucleation, and nuclei growth. (Thorat & Dalvi, 2012). In the anti-solvent precipitation, the particles size and the stability of nanoparticles will be affected by the amount of solute, the ratio of anti-solvent and solvent, temperature, the properties of anti-solvent, and the effect of stabilizers (A. Patel, Hu, Tiwari, & Velikov, 2010). In the food systems, many biopolymers can form nanoparticles by anti-solvent precipitation, such as legumin, gliadin, gelatin, whey protein, and zein.

2.3 Zein

Zein is the prolamine corn storage protein with more than 50% of hydrophobic amino acids including leucine, proline, and alanine. According to the amino sequence and solubility in water, zein can be classified into four distinct types: α-zein, β-zein, γ-zein, and δ-zein (B. Zhang, Luo, & Wang, 2011), and among those types, α-zein is constituted around 70% of the total (Lawton, 2002). Zein is widely used in the food and pharmaceutical industries because it is generally recognized as safe (GRAS), biodegradable, biocompatible and can form self-assembled particles in the low concentration of the ethanol solutions or the water (Lawton, 2002; A. R. Patel & Velikov, 2014). Various methods have been used to form the zein-based nanoscale food delivery systems, including chemical crosslinking, emulsification/solvent evaporation, emulsification/precipitation spray drying, and anti-solvent precipitation. Among these technologies, the anti-solvent precipitation is the most frequently used method to fabricate zein nanoparticles (Y. Wang & Padua, 2012; Yong Zhang et al., 2016). Because zein is amphiphilic, water can be used as an anti-solvent to form self-assembled nanoparticles. As zein aqueous ethanol solution is added to water, zein becomes supersaturated in the anti-solvent/solvent solution. Then zein nucleation will be induced, when the amount of zein is above the critical concentration. After that, the zein nanoparticles will grow by condensation and coagulation (Kasaai, 2018). The particle size and stability of zein

nanoparticles are affected by alcohol type, the initial alcohol concentration, the dilution ratio, the concentration of zein, and mixing methods (Yong Zhang et al., 2016). The concentration of zein and the ratio of water to ethanol tremendously affect the morphology of zein nanoparticles. As the concentration of zein increases, the nanoparticles morphology experiences microspheres, packed spheres, and films (Y. Wang & Padua, 2010). Besides morphology, the secondary structure of zein experiences an α-helix to β-sheet transition during anti-solvent precipitation (Y. Wang & Padua, 2012). Table 2.1 shows examples of using zein nanoparticles as nanoscale food delivery systems to encapsulate the poorly water-soluble bioactive compounds, including β-carotene, cinnamon oil, piperine, quercetin, curcumin, and peppermint oil by magnetic stirring. Besides these conventional mixing methods, microfluidic chips and ultrasonic treatment can be used to fabricate the zein nanoparticles.

2.4 Microfluidic Chip

Microfluidics is an emerging technology intended to manipulate an ultra-small scale of fluids in closed channels with dimensions of tens of micrometers (Whitesides, 2006). To date, scientists have been able to expand the application of microfluidics to a broad spectrum of fields, from biomedical imaging, drug discovery, biomolecule synthesis to diagnostics (Teh, Lin, Hung, & Lee, 2008). The diversity of application of microfluidics is attributed to their superior ability to precisely control a small segment of liquid, which thereby could be used as reaction confinements (Mark, Haeberle, Roth, von Stetten, & Zengerle, 2010). In terms of food-related applications, the utilization of microfluidic devices has been primarily focused on rapid detection to target the issues in food safety (L. Ma, Nilghaz, Choi, Liu, & Lu, 2018; Oscar, Fernando, & del Pilar, 2017; Pu, Xiao, & Sun, 2017), a toolbox to study fundamental physics in emulsion systems (Muijlwijk et al., 2017) and a quantification tool for various chemical compounds (Amine, Boire, Davy, Marquis,

& Renard, 2017; Oscar et al., 2017). And the microfluidic devices also can be used as a tool to fabricate the zein nanoparticles and encapsulate the bioactive compounds (Y. Feng, Ibarra-Sánchez, Luu, Miller, & Lee, 2019; Y. Feng & Lee, 2017).

There are many methods to design microfluidic chips based on the requirements of the device and applications. The traditional methods including bulk micromachining, direct micromachining, replication micromachining (Yazdi et al., 2016). Among these early technologies, soft lithography and photolithography which belong to the replication micromachining are the widely used methods because of the reagents saving and mild reactions. However, these conventional methods even for photolithography can only create 2D or 2.5D chips. And the novel technique that is emerging and gains attention for microfluidic chip fabrication is 3D printing or additive manufacturing (Nielsen, Beauchamp, Nordin, & Woolley, 2020). In this article, photolithography, soft lithography, and 3D-printing technology will be discussed.

2.4.1 The designing of microfluidics

Photolithography and soft lithography

The microfabrication used various patterning techniques, and the most common and powerful methods are photolithography and soft lithography. The table 2.2 listed the difference between soft lithography and photolithography. Both of them can be patterned on the photoresist materials. There are two kinds of photoresist materials, one is negative resist materials and the other is positive resist material. Fig 2.5. Showed the production of these materials. For the negative resist materials, polymer further crosslinks or changes into an insoluble product due to light exposure. The photoresist materials with the absorber layer on the top will be removed and other parts will be retained. SU-8 and KMPR are commonly used as negative resists. And for the positive resist

materials, scission occurs within the polymer chain via light exposure. The photoresist materials exposed to the UV light become more soluble while unexposed areas retain their shapes.

3D-printing technology

These traditional microfluidic chip formation technologies have several disadvantages, such as unable to create complex and precise real 3D-structure, which can be only produced in the cleanroom to ensure no contaminants on the surface of the devices. Besides, the process of the fabrication is expensive, time-consuming, and complex (Amin, Knowlton, Hart, Yenilmez, & Ghaderinezhad, 2016; Macdonald et al., 2017; Nielsen et al., 2020; Weisgrab, Ovsianikov, & Costa, 2019; Yazdi et al., 2016). The 3D-printing technique presents a potential alternative to conventional methods without these drawbacks. Using the 3D-printing, the researchers can create a real, sophisticated 3D-structure microfluidic chip, and not necessary to use the dust-free room, and the cost of the chips are cheaper than the traditional chips. And because the 3D-printing microfluidic chips can provide the actual physiological environment for the cell growth, it can be used as the cell culture platform for the research on nutrients delivery and drug test (Y. He, Wu, Fu, Gao, & Qiu, 2016).

2.4.2 Application of microfluidics chip

2.4.2.1 Microfluidic Chip to form the emulsion and microcapsules

An emulsion is a mixture of the two immiscible heterogeneous systems, one is the continuous phase and the other is the dispersed phase (Bonat Celli & Abbaspourrad, 2018). There are many emulsions in our daily lives, such as milk, mayonnaise, and butter. To improve emulsions stability, preventing droplet coalescence or aggregation, external force should be added during the formation of the emulsion. Emulsification can be achieved by mechanical mixing, including homogenization, high-speed mixers (Bonat Celli & Abbaspourrad, 2018). However, these methods have some

drawbacks, such as uncontrollable formation, insensitiveness, large reagent volumes requirement. Compared with these traditional methods to produce emulsion, the microfluidic chip has many advantages. Firstly, the emulsion can be well-regulated. The microfluidic chip can fabricate the single controllable emulsions, double controllable emulsions, and multicomponent controllable emulsions (M. Zhang et al., 2016). Table 2.3 showed that the microfluidic chips can produce different kinds of emulsion, such as water in oil, oil in water, water-in-oil-in-water, oil-in-water-in-oil, and Pickering emulsions in the micro-scale. By controlling the particle size and polydispersity index (PDI) using a microfluidic system, the stability of the emulsion can be improved, the encapsulated bioactive compound can be preserved, and the shelf life of the products can be extended. For the traditional methods, to produce the emulsions, the researchers should input the extra energy, such as high pressure, ultrasound, and high speed. However, in the microfluidic system, the two immiscible systems merge into the section of the chips to form the emulsion naturally.

2.4.2.2 Microfluidic Chip as the detection tools

Nowadays, consumers are progressively concerned about food quality and security. The foodborne pathogens, chemical contaminants should be detected easily, quickly, accurately, and economically. Using the microfluidic chip has these intrinsic advantages to detect contaminants in foods. The microfluidic chip detector can be designed by paper, PDMS, PMMA, PEG, etc. These materials are cheaper than traditional detection materials. The dimension of the microfluidic chips are smaller than the conventional detector and can be portable. What's more, the volume of the reagent of the chip-based detections is smaller than the traditional detection tools. Because of these advantages, more and more researchers focus on the microfluidic chip detection tool. Table 2.4 listed some examples of the microfluidic chip as the detection tool. Firstly, the microfluidic chip

can be used for foodborne pathogen detections. The most vital to prevent the outbreak of foodborne diseases is to detect the foodborne pathogen rapidly. The conventional methods to detect the foodborne pathogen are time-consuming, labor-intensive, and with poor pathogen detection competencies, which can only be detected in a single type of pathogen with one sample (Kant et al., 2018). However, the chip-based tools have a lower detection limit and a more precise detection profile, such as, increasing the target bacteria detection and lowing the non-target bacterial detection. Besides the foodborne pathogens, the chemical contaminants, such as sulfur dioxide, $Hg^{2+,}$ and Ag^{+}, are also unignorably when it concerns food safety.

2.4.2.3 Microfluidic Chip as reactors

Besides using the microfluidic chip as the emulsion formation tool and the detection tools, the chip devices can be used as the reactor. Compared with traditional reactors, there are many advantages of chip-based reactors. Firstly, the chip-based reactors can produce a well-controlled substrate, such as monodisperse emulsions with the same initial diameter (Marze, Algaba, & Marquis, 2014; Nguyen, Marquis, Anton, & Marze, 2019a). Secondly, because of the high surface-volume ratio, the reaction that happened in the microfluidic chip is faster than in the conventional reactor (A. M. Huebner, Abell, Huck, Baroud, & Hollfelder, 2011; Nguyen, Marquis, Anton, & Marze, 2019b). Thirdly, the surface of the microfluidic chip can be modified. The traditional reactor can be only used in the lipophilic or hydrophilic system, however, the surface of the chip-based reactors can be treated by graft polymerization to modify from the hydrophobic to hydrophilic(Nguyen et al., 2019a). Moreover, the reagent volume of the novel reactors is smaller than the traditional reactors, even reach to micro-scale. Each droplet can be used as the independent reactor in the microfluidic devices (A. Huebner et al., 2009; A. M. Huebner et al., 2011). Finally, the chip-based reactors can be monitored by the confocal fluorescence and optical microscopy (A. Huebner et al., 2009; A. M.

Huebner et al., 2011; Marze et al., 2014; Mongersun, Smeenk, Pratx, Asuri, & Abbyad, 2016; Zheng, Roach, & Ismagilov, 2003).

In conclusion, microfluidic chips are a novel device and can be used to produce well-controlled emulsions, as rapid detection tools and smaller reagent reactors. Microfluidic chips have a potential application in the food and pharmaceutical industries.

2.5 Ultrasonic treatment

Generally, the sound wave can be divided into audile waves (10 Hz-20 kHz), infrasonic waves (<16 Hz), and ultrasonic waves (>20 kHz) (Tiwari, 2015). The frequency of the ultrasound is above the human being's hearing range. For the food industry applications, the ultrasonic treatment can be divided into low-intensity sonication (<1 W/cm^2) and high-intensity sonication (10-1000 W/cm^2). The low-intensity sonication produces a high frequency with the small amplitude waves without material damage and can be used as the non-destructive analytical technique. The high-intensity sonication uses large amplitude waves which can damage/change the structure and properties of the materials and can be employed for processing and extraction (Kadam, Tiwari, Álvarez, & O'Donnell, 2015; Kentish & Feng, 2014). The ultrasonic energy is generated by the transducer that converts the electrical energy to mechanical vibration according to the equation as follow:

$$\text{Energy dissipated} = kf^2 A^2 \qquad (1)$$

Where k is a constant, A is the amplitude and f is the frequency (Leighton, 1994). The ultrasonic baths and ultrasonic horn are two types of ultrasonic devices in the laboratory (Fig 2.7). Compared with the ultrasonic horn, the ultrasonic baths provide a lower energy intensity because this system delivers more evenly diffuse acoustic energy. The ultrasonic horn has a higher energy intensity, however, the intensity decreased dramatically from the center of the horn (Kentish & Feng, 2014).

The main driving force of the ultrasonic waves is cavitation by generating shear forces and fluid mixing. The cavitation bubbles are produced by alternating pressure changes during the ultrasound propagation and can be divided into stable cavitation and transient cavitation (Tiwari, 2015). The bubbles' size is determined by the frequency of the ultrasound, and as the frequency increases the bubbles' size decreases. Once the bubbles reach a certain size, they will collapse to form the shearing force (Kentish & Feng, 2014). The nature of the field generated, the acoustic frequency, temperature, and pressure determine the effectiveness of the ultrasonic treatment. Ultrasound technology has been used in the food industry for many years for bio-compounds extraction, viscosity modification, emulsification, surface cleaning, food quality assurance, filtration, tenderization, etc (Ashokkumar, 2015; Bhaskaracharya, Kentish, & Ashokkumar, 2009; Cárcel, García-Pérez, Benedito, & Mulet, 2012; Chandrapala, Oliver, Kentish, & Ashokkumar, 2012; Chemat et al., 2017; Chemat, Zill-E-Huma, & Khan, 2011; Kadam et al., 2015; Ojha, Mason, O'Donnell, Kerry, & Tiwari, 2017; Tiwari, 2015). Besides, the ultrasound can be used for nanoparticle formation. For the starch nanoparticles, ultrasound increased the yield rate of the cassava, corn, and yam starch nanoparticles and microparticles without any chemical additives, and the particle size was smaller than the native starch granules (Minakawa, Faria-Tischer, & Mali, 2019). There was a minimum water content required for the ultrasound to induce starch nanoparticle formation, and ultrasound increased the amorphous content in the starch nanoparticles (Boufi et al., 2018). What's more, the ultrasonic treatment decreased the viscosity and the average molecular weight of the starch (Y. Chang et al., 2017). For protein nanoparticles, Ren et al. (Ren et al., 2019) compared the different frequencies of the ultrasound that affected the properties of zein-chitosan complex and resveratrol encapsulation. The results showed that the particle size of the zein-chitosan complex treated with dual-frequency (28/40 kHz) was lower than the single or

multi-frequency treatment. The ultrasound increases the stability of zein nanoparticles during the formation (Kamiya, Otani, Fuji, & Miyahara, 2018). The soy peptide nanoparticles which were produced by the ultrasound increased the stability and decreased the lipid oxidation of the emulsion during storage (Yuanhong Zhang et al., 2018). And the encapsulation efficiency of the resveratrol was higher in the dual-frequency than in other frequency treatments.

In this research, the cavitation effect of the ultrasound will be used to control the zein nanoparticles size and increase the stability of the particles and encapsulation efficiency of the curcumin in zein.

2.6 Conclusion

The nanoscale delivery systems are emerging food vehicles with particles in the nanoscales range, including emulsions, liposomes, nanoemulsions, microgels, and nanoparticles. Zein is the prolamine corn storage protein that can be used as the nanoscale food delivery system by anti-solvent precipitation to encapsulate bioactive compounds, such as nisin and curcumin. To well controlled the formation environment, microfluidic chips and ultrasonic treatment can be used as the mixing methods. In this review, we discussed the basic principle of microfluidic devices and ultrasound. Nevertheless, very few studies have been reported using these two techniques to fabricate zein nanoparticles and how the factors of treatment affect the formation of the particles. Also, future studies could focus on these two methods to form uniform nanoscales food delivery systems.

2.7 Tables and figures

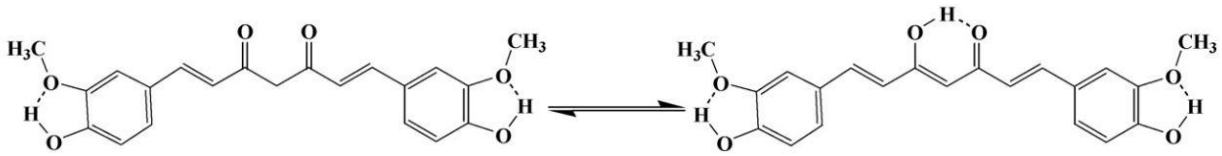

Fig 2.1 The chemical structure of curcumin in keto-enol tautomeric equilibrium (Priyadarsini, 2009).

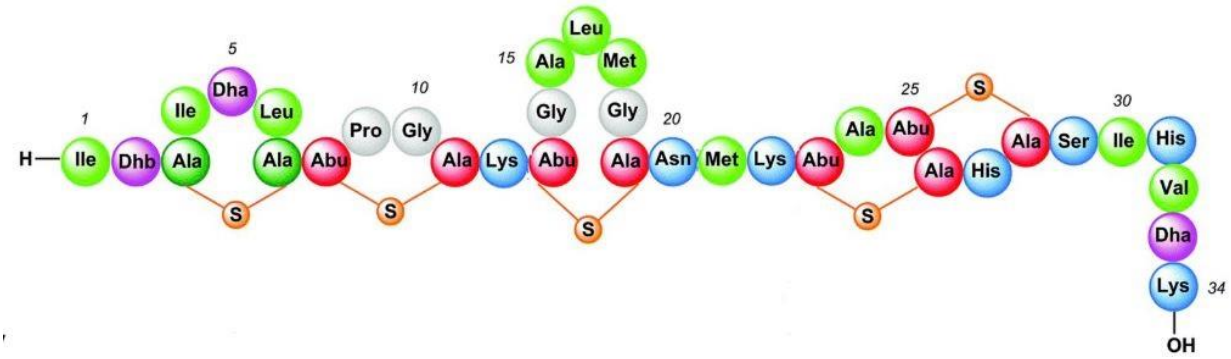

Fig 2.2 The structure of Nisin representing a 34 amino acid chain (Bahrami et al., 2019).

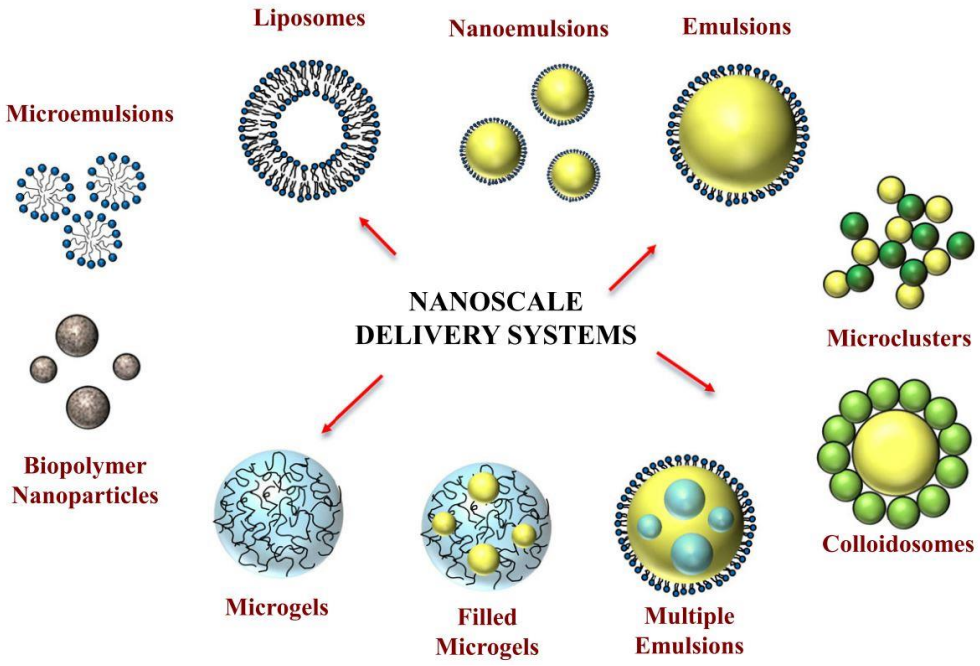

Fig 2.3 Examples of nanoscale delivery systems that can be used to encapsulate, protect and deliver bioactive compounds (Mcclements, 2015).

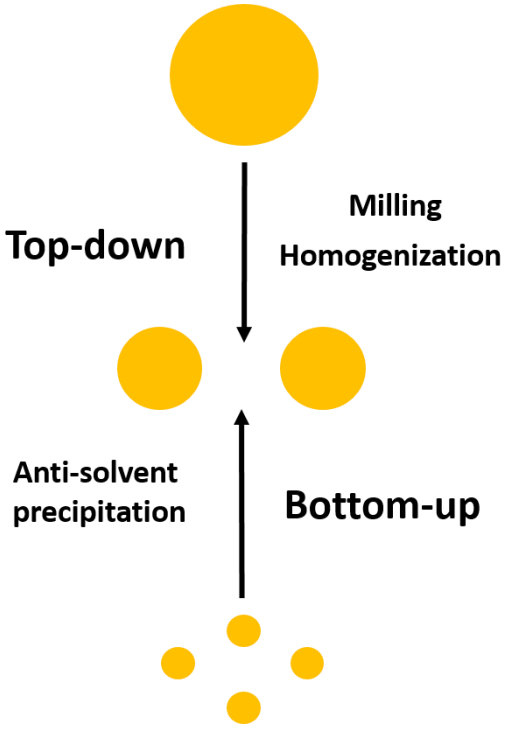

Fig 2.4 Nanoparticles formation can be fabricated from top-down or bottom-up approaches.

Table 2.1 Examples for encapsulation of poorly water-soluble bioactive compounds via zein.

Bioactive Compound	Nanoscale delivery systems	Method	Reference
Origanum vulgare and Thymus vulgaris	Zein nanoparticles	magnetic stirring	(Gonçalves da Rosa et al., 2020)
β-carotene	Zein nanoparticles	magnetic stirring	(Ba et al., 2020)
Cinnamon oil	Zein Pickering emulsion	magnetic stirring	(X. Feng et al., 2020)
Curcumin	Zein nanoparticles	magnetic stirring	(Sun et al., 2020)
Curcumin and Piperine	Zein nanoparticles	magnetic stirring	(S. Chen, Li, et al., 2020)
Luteolin	Zein nanoparticles	magnetic stirring	(Shinde, Agraval, Singh, Yadav, & Kumar, 2019)
Quercetin	Zein nanoparticles	magnetic stirring	(Li et al., 2019)
Propolis	Zein nanoparticles	magnetic stirring	(H. Zhang et al., 2019)
Resveratrol	Zein nanoparticles	magnetic stirring	(Khan et al., 2019)
Curcumin	Zein nanoparticles	magnetic stirring	(Yao, Chen, Song, McClements, & Hu, 2018)
Peppermint Oil	Zein nanoparticles	magnetic stirring	(H. Chen & Zhong, 2015)

Table 2.2 Comparison between photolithography and soft lithography (Xia & Whitesides, 1998).

	Photolithography	Soft lithography
Definition of patterns	Rigid photomask	Elastomeric stamp or mold
Materials that can be patterned directly	Photoresists SAMs on Au and SiO_2	Photoresists SAMs on Au and SiO_2 Unsensitized polymers Precursor polymers Polymer beds Conducting polymers Colloidal materials Sol-gel materials Organic and inorganic salts Biological macromolecules
Surfaces and structures that can be patterned	Planar surface 2-D structures	Both planar and nonplanar Both 2-D and 3-D structures
Current limits to resolution	~ 250 nm (projection) ~ 100 nm (laboratory)	~30 nm, ~60 nm, ~1 μm (laboratory)
Minimum feature size	~ 100 nm	10 -100 nm

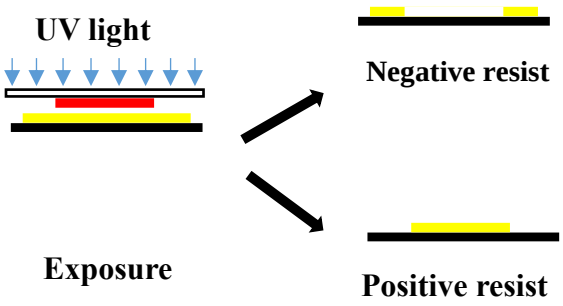

Fig 2.5 The fabrication of negative resist and passive resist material.

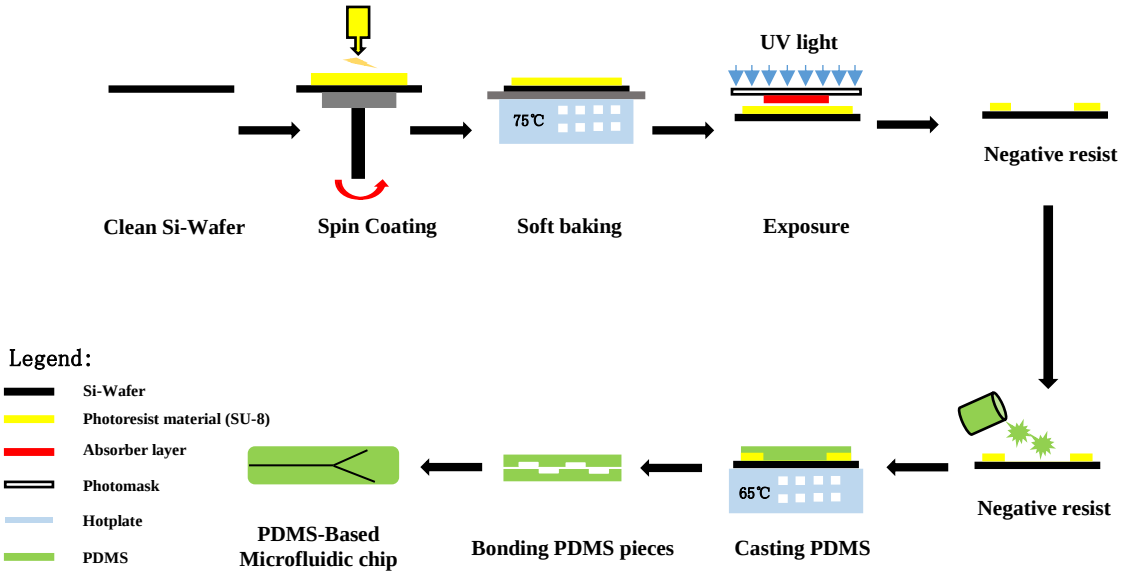

Fig 2.6 The procedure of PDMS-based microfluidic chip fabrication.

Table 2.3 Summary of the Microfluidic Chip to form the emulsion and microcapsules.

Emulsion Category	Material and Design	Purpose	Reference
Water-in-oil-in-water	Glass capillary-based microfluidic chip	Form the β-carotene loaded liposomes for food applications	(Michelon, Huang, de la Torre, Weitz, & Cunha, 2019)
Oil-in-water	Glass microfluidic chip	Stabilize the emulsion	(Comunian, Ravanfar, Selig, & Abbaspourrad, 2018)
Pickering emulsions	Glass microfluidic chip	Understand the mechanism of CLPs in emulsion formation and stabilization	(Schröder, Sprakel, Schroën, Spaen, & Berton-Carabin, 2018)
Microcapsule Oil-in-water	Glass capillary-based microfluidic chip	Preserve labile compounds and improve stability	(Ravanfar, Comunian, Dando, & Abbaspourrad, 2018)
Water-in-water	PDMS microfluidic chip	Improve the biocompatibility and stability of the emulsion	(Abbasi, Navi, & Tsai, 2018)
Oil-in-water-in-oil	Glass microfluidic chip	Improve the stability of echium oil which contains many omega-3 fatty acids in the internal oil phase	(Comunian et al., 2017)
Microcapsule	PDMS microfluidic chip	Produce the controllable zein microcapsule (particle sizes, pore distributions, and permeabilities) via PDMS microfluidic chip	(Y. Feng & Lee, 2017)
Nanoparticle	PDMS microfluidic chip	Demonstrate how effective diameter and PDI of zein nanoparticle can be influenced by the ratio of the continuous and dispersed phase	(Olenskyj, Feng, & Lee, 2017)

Table 2.4 Summary of the Microfluidic Chip to be the detection tools.

Target analyses	Material	Purpose	Reference
Foodborne pathogens			
Staphylococcus aureus and *Vibrio parahaemolyticus*	PDMS/paper hybrid microfluidic chip	Provide an easier fabrication, cheaper way to detect the foodborne pathogens using a microfluidic chip	(Pang et al., 2018)
E. coli O157: H7 and *Staphylococcus aureus*	Polyethylene glycol (PEG) microfluidic chip	Design the novel PEG microfluidic chip to detect the *E. coli O157: H7* and *Staphylococcus aureus*	(Tian, Lyu, Shi, Tan, & Yang, 2016)
Escherichia coli	-	Design the portable, rapid positive DEP-based microorganism detection systems	(Kim et al., 2015)
E. coli O157: H7 and Staphylococcus aureus	PDMS microfluidic chip	Fabricate the PDMS microfluidic chip to detect the *E. coli O157: H7 and Staphylococcus aureus* using *an* antibody-immobilized nanoporous membrane with high sensitivity and lower time cost.	(Tan et al., 2011)
E. coli O157: H7	PMMA microfluidic chip	Design the PMMA microfluidic chip to detect the *E. coli O157: H7* with ease of operation and high throughput.	(Dharmasiri et al., 2010)
E. coli O157: H7	PEG microfluidic chip	Fabricate the PEG microfluidic chip with a nanoporous membrane to increase the detection limit and to be rapid.	(Yu et al., 2009)

Table 2.4 (cont.)

Escherichia coli, Salmonella enterica subsp. enterica serovar Enteritidis, Yersinia enterocolitica, and *Bacillus cereus*	NA	Develop a rapid and simple method to detect the foodborne microorganism via the commercial microfluidic chip.	(Ikeda, Yamaguchi, Tani, & Nasu, 2006)
Chemical contaminants			
Sulfur dioxide	PMMA/paper microfluidic chip	Provide a cheap, compact and reliable way to detect the sulfur dioxide using a microfluidic chip	(Liu, Wang, Fu, & Yang, 2017)
Aflatoxin B_1	Glass microfluidic chip	Design the distance-readout microfluidic chip to low the detection limit	(Y. Ma et al., 2016)
Hg^{2+}, Ag^{+}, aminoglycoside antibiotics	Paper microfluidic chip	Design the kind of paper-based microfluidic chip to detect multiple chemical contaminants in the same microenvironment	(Yali Zhang, Zuo, & Ye, 2015)
Sulfonamide residues in Milk and Chicken Muscle	Cyclic olefin copolymer (COC) microfluidic chip	Design the rapid, sensitive determination of sulfonamide residues by COC-based microfluidic chip	(L. Wang et al., 2012)
Nitrite	PMMA microfluidic chip	Develop the PMMA microfluidic chip to detect nitrite in the food with high reproducibility and sensitivity.	(D. He, Zhang, Huang, & Hu, 2007)
Benzoyl Peroxide	PMMA microfluidic chip	Describe a rapid and sensitive PMMA-based microfluidic chip fabrication for the detection of benzoyl peroxide in flour.	(Wei, Zhujun, & Liu, 2006)

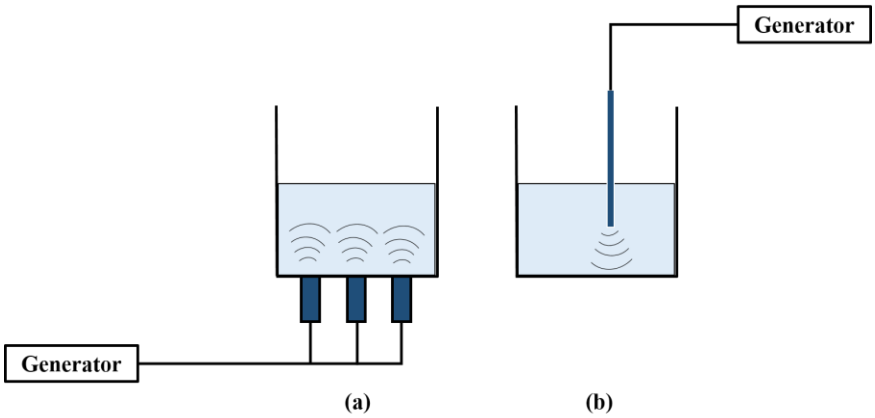

Fig 2.7 The two types of ultrasonic devices in the laboratory. (a) Ultrasonic baths; (b) Ultrasonic horn. (Modified from (Tiwari, 2015))

2.8 References

Abbasi, N., Navi, M., & Tsai, S. S. H. (2018). Microfluidic Generation of Particle-Stabilized Water-in-Water Emulsions. *Langmuir*, *34*(1), 213–218. https://doi.org/10.1021/acs.langmuir.7b03245

Amin, R., Knowlton, S., Hart, A., Yenilmez, B., & Ghaderinezhad, F. (2016). 3D-printed microfluidic devices.

Amine, C., Boire, A., Davy, J., Marquis, M., & Renard, D. (2017). Droplets-based millifluidic for the rapid determination of biopolymers phase diagrams. *Food Hydrocolloids*, *70*, 134–142. https://doi.org/10.1016/j.foodhyd.2017.03.035

Araiza-Calahorra, A., Akhtar, M., & Sarkar, A. (2018). Recent advances in emulsion-based delivery approaches for curcumin: From encapsulation to bioaccessibility. *Trends in Food Science and Technology*, *71*(July 2017), 155–169. https://doi.org/10.1016/j.tifs.2017.11.009

Artiga-Artigas, M., Lanjari-Pérez, Y., & Martín-Belloso, O. (2018). Curcumin-loaded nanoemulsions stability as affected by the nature and concentration of surfactant. *Food Chemistry*, *266*(June), 466–474. https://doi.org/10.1016/j.foodchem.2018.06.043

Ashokkumar, M. (2015). Applications of ultrasound in food and bioprocessing. *Ultrasonics Sonochemistry*, *25*(1), 17–23. https://doi.org/10.1016/j.ultsonch.2014.08.012

Azmir, J., Zaidul, I. S. M., Rahman, M. M., Sharif, K. M., Mohamed, A., Sahena, F., … Omar, A. K. M. (2013). Techniques for extraction of bioactive compounds from plant materials: A review. *Journal of Food Engineering*, *117*(4), 426–436. https://doi.org/10.1016/j.jfoodeng.2013.01.014

Ba, C., Fu, Y., Niu, F., Wang, M., Jin, B., Li, Z., … Li, X. (2020). Effects of environmental stresses on physiochemical stability of β-carotene in zein-carboxymethyl chitosan-tea

polyphenols ternary delivery system. *Food Chemistry*, *311*(November 2019), 125878. https://doi.org/10.1016/j.foodchem.2019.125878

Bahrami, A., Delshadi, R., Jafari, S. M., & Williams, L. (2019). Nanoencapsulated nisin: An engineered natural antimicrobial system for the food industry. *Trends in Food Science and Technology*, *94*(May), 20–31. https://doi.org/10.1016/j.tifs.2019.10.002

Bhaskaracharya, R. K., Kentish, S., & Ashokkumar, M. (2009). Selected applications of ultrasonics in food processing. *Food Engineering Reviews*, *1*(1), 31–49. https://doi.org/10.1007/s12393-009-9003-7

Biesalski, H. K., Dragsted, L. O., Elmadfa, I., Grossklaus, R., Müller, M., Schrenk, D., … Weber, P. (2009). Bioactive compounds: Definition and assessment of activity. *Nutrition*, *25*(11–12), 1202–1205. https://doi.org/10.1016/j.nut.2009.04.023

Bonat Celli, G., & Abbaspourrad, A. (2018). Tailoring Delivery System Functionality Using Microfluidics. *Annu. Rev. Food Sci. Technol*, *921*(21), 1–21. https://doi.org/10.1146/annurev-food-030117

Boufi, S., Bel Haaj, S., Magnin, A., Pignon, F., Impéror-Clerc, M., & Mortha, G. (2018). Ultrasonic assisted production of starch nanoparticles: Structural characterization and mechanism of disintegration. *Ultrasonics Sonochemistry*, *41*(May 2017), 327–336. https://doi.org/10.1016/j.ultsonch.2017.09.033

Cárcel, J. A., García-Pérez, J. V., Benedito, J., & Mulet, A. (2012). Food process innovation through new technologies: Use of ultrasound. *Journal of Food Engineering*, *110*(2), 200–207. https://doi.org/10.1016/j.jfoodeng.2011.05.038

Chandrapala, J., Oliver, C., Kentish, S., & Ashokkumar, M. (2012). Ultrasonics in food processing - Food quality assurance and food safety. *Trends in Food Science and*

Technology, *26*(2), 88–98. https://doi.org/10.1016/j.tifs.2012.01.010

Chang, C., Wang, T., Hu, Q., & Luo, Y. (2017). Caseinate-zein-polysaccharide complex nanoparticles as potential oral delivery vehicles for curcumin: Effect of polysaccharide type and chemical cross-linking. *Food Hydrocolloids*, *72*, 254–262. https://doi.org/10.1016/j.foodhyd.2017.05.039

Chang, Y., Yan, X., Wang, Q., Ren, L., Tong, J., & Zhou, J. (2017). High efficiency and low cost preparation of size controlled starch nanoparticles through ultrasonic treatment and precipitation. *Food Chemistry*, *227*, 369–375. https://doi.org/10.1016/j.foodchem.2017.01.111

Chemat, F., Rombaut, N., Meullemiestre, A., Turk, M., Perino, S., Fabiano-Tixier, A. S., & Abert-Vian, M. (2017). Review of Green Food Processing techniques. Preservation, transformation, and extraction. *Innovative Food Science and Emerging Technologies*, *41*(May), 357–377. https://doi.org/10.1016/j.ifset.2017.04.016

Chemat, F., Zill-E-Huma, & Khan, M. K. (2011). Applications of ultrasound in food technology: Processing, preservation and extraction. *Ultrasonics Sonochemistry*, *18*(4), 813–835. https://doi.org/10.1016/j.ultsonch.2010.11.023

Chen, H., & Zhong, Q. (2015). A novel method of preparing stable zein nanoparticle dispersions for encapsulation of peppermint oil. *Food Hydrocolloids*, *43*, 593e602-602. https://doi.org/10.1016/j.foodhyd.2014.07.018

Chen, J., & Hu, L. (2020). Nanoscale Delivery System for Nutraceuticals: Preparation, Application, Characterization, Safety, and Future Trends. *Food Engineering Reviews*, *12*(1), 14–31. https://doi.org/10.1007/s12393-019-09208-w

Chen, S., Han, Y., Jian, L., Liao, W., Zhang, Y., & Gao, Y. (2020). Fabrication, characterization,

physicochemical stability of zein-chitosan nanocomplex for co-encapsulating curcumin and resveratrol. *Carbohydrate Polymers*, *236*(February), 116090. https://doi.org/10.1016/j.carbpol.2020.116090

Chen, S., Han, Y., Sun, C., Dai, L., Yang, S., Wei, Y., … Gao, Y. (2018). Effect of molecular weight of hyaluronan on zein-based nanoparticles: Fabrication, structural characterization and delivery of curcumin. *Carbohydrate Polymers*, *201*(17), 599–607. https://doi.org/10.1016/j.carbpol.2018.08.116

Chen, S., Li, Q., McClements, D. J., Han, Y., Dai, L., Mao, L., & Gao, Y. (2020). Co-delivery of curcumin and piperine in zein-carrageenan core-shell nanoparticles: Formation, structure, stability and in vitro gastrointestinal digestion. *Food Hydrocolloids*, *99*(August 2019), 105334. https://doi.org/10.1016/j.foodhyd.2019.105334

Comunian, T. A., Ravanfar, R., de Castro, I. A., Dando, R., Favaro-Trindade, C. S., & Abbaspourrad, A. (2017). Improving oxidative stability of echium oil emulsions fabricated by Microfluidics: Effect of ionic gelation and phenolic compounds. *Food Chemistry*, *233*, 125–134. https://doi.org/10.1016/j.foodchem.2017.04.085

Comunian, T. A., Ravanfar, R., Selig, M. J., & Abbaspourrad, A. (2018). Influence of the protein type on the stability of fish oil in water emulsion obtained by glass microfluidic device. *Food Hydrocolloids*, *77*, 96–106. https://doi.org/10.1016/j.foodhyd.2017.09.025

Dai, L., Li, R., Wei, Y., Sun, C., Mao, L., & Gao, Y. (2018). Fabrication of zein and rhamnolipid complex nanoparticles to enhance the stability and in vitro release of curcumin. *Food Hydrocolloids*, *77*, 617–628. https://doi.org/10.1016/j.foodhyd.2017.11.003

de Arauz, L. J., Jozala, A. F., Mazzola, P. G., & Vessoni Penna, T. C. (2009). Nisin biotechnological production and application: a review. *Trends in Food Science and*

Technology, *20*(3–4), 146–154. https://doi.org/10.1016/j.tifs.2009.01.056

Dharmasiri, U., Witek, M., Adams, A., Osiri, J., Hupert, M., Bianchi, T., … Soper, S. (2010). Enrichment and detection of Escherichia coli O157: H7 from water samples using an antibody modified microfluidic chip. *Analytical Chemistry*, *82*(7), 2844–2849. https://doi.org/10.1021/ac100323k.Enrichment

Feng, X., Sun, Y., Yang, Y., Zhou, X., Cen, K., Yu, C., … Tang, X. (2020). Zein nanoparticle stabilized Pickering emulsion enriched with cinnamon oil and its effects on pound cakes. *Lwt*, *122*(January), 109025. https://doi.org/10.1016/j.lwt.2020.109025

Feng, Y., Ibarra-Sánchez, L. A., Luu, L., Miller, M. J., & Lee, Y. (2019). Co-assembly of nisin and zein in microfluidics for enhanced antilisterial activity in Queso Fresco. *Lwt*, *111*(May), 355–362. https://doi.org/10.1016/j.lwt.2019.05.059

Feng, Y., & Lee, Y. (2017). Microfluidic fabrication of hollow protein microcapsules for rate-controlled release. *RSC Advances*, *7*(78), 49455–49462. https://doi.org/10.1039/c7ra08645h

Gonçalves da Rosa, C., Zapelini de Melo, A. P., Sganzerla, W. G., Machado, M. H., Nunes, M. R., Vinicius de Oliveira Brisola Maciel, M., … Manique Barreto, P. L. (2020). Application in situ of zein nanocapsules loaded with Origanum vulgare Linneus and Thymus vulgaris as a preservative in bread. *Food Hydrocolloids*, *99*(August 2019), 105339. https://doi.org/10.1016/j.foodhyd.2019.105339

He, D., Zhang, Z., Huang, Y., & Hu, Y. (2007). Chemiluminescence microflow injection analysis system on a chip for the determination of nitrite in food. *Food Chemistry*, *101*(2), 667–672. https://doi.org/10.1016/j.foodchem.2006.02.024

He, Y., Wu, Y., Fu, J. Z., Gao, Q., & Qiu, J. J. (2016). Developments of 3D Printing Microfluidics and Applications in Chemistry and Biology: a Review. *Electroanalysis*,

28(8), 1658–1678. https://doi.org/10.1002/elan.201600043

Huebner, A., Bratton, D., Whyte, G., Yang, M., Demello, A. J., Abell, C., & Hollfelder, F. (2009). Static microdroplet arrays: A microfluidic device for droplet trapping, incubation and release for enzymatic and cell-based assays. *Lab on a Chip*, *9*(5), 692–698. https://doi.org/10.1039/b813709a

Huebner, A. M., Abell, C., Huck, W. T. S., Baroud, C. N., & Hollfelder, F. (2011). Monitoring a reaction at submillisecond resolution in picoliter volumes. *Analytical Chemistry*, *83*(4), 1462–1468. https://doi.org/10.1021/ac103234a

Ikeda, M., Yamaguchi, N., Tani, K., & Nasu, M. (2006). Rapid and simple detection of food poisoning bacteria by bead assay with a microfluidic chip-based system. *Journal of Microbiological Methods*, *67*(2), 241–247. https://doi.org/10.1016/j.mimet.2006.03.014

Joye, I. J., & McClements, D. J. (2013). Production of nanoparticles by anti-solvent precipitation for use in food systems. *Trends in Food Science and Technology*, *34*(2), 109–123. https://doi.org/10.1016/j.tifs.2013.10.002

Kadam, S. U., Tiwari, B. K., Álvarez, C., & O'Donnell, C. P. (2015). Ultrasound applications for the extraction, identification and delivery of food proteins and bioactive peptides. *Trends in Food Science and Technology*, *46*(1), 60–67. https://doi.org/10.1016/j.tifs.2015.07.012

Kamiya, H., Otani, Y., Fuji, M., & Miyahara, M. (2018). *Characteristics and Behavior of Nanoparticles and Its Dispersion Systems*. *Nanoparticle Technology Handbook*. https://doi.org/10.1016/B978-0-444-64110-6.00003-2

Kant, K., Shahbazi, M. A., Dave, V. P., Ngo, T. A., Chidambara, V. A., Than, L. Q., … Wolff, A. (2018). Microfluidic devices for sample preparation and rapid detection of foodborne pathogens. *Biotechnology Advances*, *36*(4), 1003–1024.

https://doi.org/10.1016/j.biotechadv.2018.03.002

Kasaai, M. R. (2018). Zein and zein -based nano-materials for food and nutrition applications: A review. *Trends in Food Science and Technology*, *79*(July), 184–197. https://doi.org/10.1016/j.tifs.2018.07.015

Kentish, S., & Feng, H. (2014). Applications of Power Ultrasound in Food Processing. *Annual Review of Food Science and Technology*, *5*(1), 263–284. https://doi.org/10.1146/annurev-food-030212-182537

Khan, M. A., Yue, C., Fang, Z., Hu, S., Cheng, H., Bakry, A. M., & Liang, L. (2019). Alginate/chitosan-coated zein nanoparticles for the delivery of resveratrol. *Journal of Food Engineering*, *258*(March), 45–53. https://doi.org/10.1016/j.jfoodeng.2019.04.010

Kim, M., Jung, T., Kim, Y., Lee, C., Woo, K., Seol, J. H., & Yang, S. (2015). A microfluidic device for label-free detection of Escherichia coli in drinking water using positive dielectrophoretic focusing, capturing, and impedance measurement. *Biosensors and Bioelectronics*, *74*, 1011–1015. https://doi.org/10.1016/j.bios.2015.07.059

Lawton, J. W. (2002). Zein: A history of processing and use. *Cereal Chemistry*, *79*(1), 1–18. https://doi.org/10.1094/CCHEM.2002.79.1.1

Li, H., Wang, D., Liu, C., Zhu, J., Fan, M., Sun, X., … Cao, Y. (2019). Fabrication of stable zein nanoparticles coated with soluble soybean polysaccharide for encapsulation of quercetin. *Food Hydrocolloids*, *87*(August 2018), 342–351. https://doi.org/10.1016/j.foodhyd.2018.08.002

Liu, C. C., Wang, Y. N., Fu, L. M., & Yang, D. Y. (2017). Rapid integrated microfluidic paper-based system for sulfur dioxide detection. *Chemical Engineering Journal*, *316*, 790–796. https://doi.org/10.1016/j.cej.2017.02.023

Lu, W., Kelly, A. L., & Miao, S. (2016). Emulsion-based encapsulation and delivery systems for polyphenols. *Trends in Food Science and Technology*, *47*, 1–9. https://doi.org/10.1016/j.tifs.2015.10.015

Ma, L., Nilghaz, A., Choi, J. R., Liu, X., & Lu, X. (2018). Rapid detection of clenbuterol in milk using microfluidic paper-based ELISA. *Food Chemistry*, *246*(July 2017), 437–441. https://doi.org/10.1016/j.foodchem.2017.12.022

Ma, Y., Mao, Y., Huang, D., He, Z., Yan, J., Tian, T., … Yang, C. J. (2016). Lab on a Chip, 3097–3104. https://doi.org/10.1039/c6lc00474a

Macdonald, N. P., Cabot, J. M., Smejkal, P., Guijt, R. M., Paull, B., & Breadmore, M. C. (2017). Comparing Microfluidic Performance of Three-Dimensional (3D) Printing Platforms. *Analytical Chemistry*, *89*(7), 3858–3866. https://doi.org/10.1021/acs.analchem.7b00136

Mark, D., Haeberle, S., Roth, G., von Stetten, F., & Zengerle, R. (2010). Microfluidic lab-on-a-chip platforms: requirements, characteristics and applications. *Chemical Society Reviews*, *39*(3), 1153. https://doi.org/10.1039/b820557b

Marze, S., Algaba, H., & Marquis, M. (2014). A microfluidic device to study the digestion of trapped lipid droplets. *Food and Function*, *5*(7), 1481–1488. https://doi.org/10.1039/c4fo00010b

Mcclements, D. J. (2015). Nanoscale Nutrient Delivery Systems for Food Applications: Improving Bioactive Dispersibility, Stability, and Bioavailability. *Journal of Food Science*, *80*(7), N1602–N1611. https://doi.org/10.1111/1750-3841.12919

Michelon, M., Huang, Y., de la Torre, L. G., Weitz, D. A., & Cunha, R. L. (2019). Single-step microfluidic production of W/O/W double emulsions as templates for B-carotene-loaded giant liposomes formation. *Chemical Engineering Journal*, *366*(July 2018), 27–32.

https://doi.org/10.1016/j.cej.2019.02.021

Minakawa, A. F. K., Faria-Tischer, P. C. S., & Mali, S. (2019). Simple ultrasound method to obtain starch micro- and nanoparticles from cassava, corn and yam starches. *Food Chemistry*, *283*(January), 11–18. https://doi.org/10.1016/j.foodchem.2019.01.015

Modulation, M. (2020). Nisin as a Novel Feed Additive : The E ff ects on Gut.

Mongersun, A., Smeenk, I., Pratx, G., Asuri, P., & Abbyad, P. (2016). Droplet Microfluidic Platform for the Determination of Single-Cell Lactate Release. *Analytical Chemistry*, *88*(6), 3257–3263. https://doi.org/10.1021/acs.analchem.5b04681

Muijlwijk, K., Colijn, I., Harsono, H., Krebs, T., Berton-Carabin, C., & Schroën, K. (2017). Coalescence of protein-stabilised emulsions studied with microfluidics. *Food Hydrocolloids*, *70*, 96–104. https://doi.org/10.1016/j.foodhyd.2017.03.031

Nguyen, H. T., Marquis, M., Anton, M., & Marze, S. (2019a). Studying the real-time interplay between triglyceride digestion and lipophilic micronutrient bioaccessibility using droplet microfluidics. 2 application to various oils and (pro)vitamins. *Food Chemistry*, *275*(July 2018), 661–667. https://doi.org/10.1016/j.foodchem.2018.09.126

Nguyen, H. T., Marquis, M., Anton, M., & Marze, S. (2019b). Studying the real-time interplay between triglyceride digestion and lipophilic micronutrient bioaccessibility using droplet microfluidics. 2 application to various oils and (pro)vitamins. *Food Chemistry*, *275*(July 2018), 661–667. https://doi.org/10.1016/j.foodchem.2018.09.126

Nielsen, A. V, Beauchamp, M. J., Nordin, G. P., & Woolley, A. T. (2020). 3D Printed Microfluidics, 1–21.

Ojha, K. S., Mason, T. J., O'Donnell, C. P., Kerry, J. P., & Tiwari, B. K. (2017). Ultrasound technology for food fermentation applications. *Ultrasonics Sonochemistry*, *34*, 410–417.

https://doi.org/10.1016/j.ultsonch.2016.06.001

Olenskyj, A. G., Feng, Y., & Lee, Y. (2017). Continuous microfluidic production of zein nanoparticles and correlation of particle size with physical parameters determined using CFD simulation. *Journal of Food Engineering*, *211*, 50–59. https://doi.org/10.1016/j.jfoodeng.2017.04.019

Oscar, S. V., Fernando, O. C. L., & del Pilar, C. M. M. (2017). Total polyphenols content in white wines on a microfluidic flow injection analyzer with embedded optical fibers. *Food Chemistry*, *221*, 1062–1068. https://doi.org/10.1016/j.foodchem.2016.11.055

Özel, B., Şimşek, Ö., Akçelik, M., & Saris, P. E. J. (2018). Innovative approaches to nisin production. *Applied Microbiology and Biotechnology*, *102*(15), 6299–6307. https://doi.org/10.1007/s00253-018-9098-y

Pang, B., Fu, K., Liu, Y., Ding, X., Hu, J., Wu, W., … Li, J. (2018). Development of a self-priming PDMS/paper hybrid microfluidic chip using mixed-dye-loaded loop-mediated isothermal amplification assay for multiplex foodborne pathogens detection. *Analytica Chimica Acta*, 1–9. https://doi.org/10.1016/j.aca.2018.07.024

Patel, A., Hu, Y., Tiwari, J. K., & Velikov, K. P. (2010). Synthesis and characterisation of zein-curcumin colloidal particles. *Soft Matter*, *6*(24), 6192–6199. https://doi.org/10.1039/c0sm00800a

Patel, A. R., & Velikov, K. P. (2014). Zein as a source of functional colloidal nano- and microstructures. *Current Opinion in Colloid and Interface Science*, *19*(5), 450–458. https://doi.org/10.1016/j.cocis.2014.08.001

Priyadarsini, K. I. (2009). Photophysics, photochemistry and photobiology of curcumin: Studies from organic solutions, bio-mimetics and living cells. *Journal of Photochemistry and*

Photobiology C: Photochemistry Reviews, *10*(2), 81–95. https://doi.org/10.1016/j.jphotochemrev.2009.05.001

Pu, H., Xiao, W., & Sun, D. W. (2017). SERS-microfluidic systems: A potential platform for rapid analysis of food contaminants. *Trends in Food Science and Technology*, *70*(January), 114–126. https://doi.org/10.1016/j.tifs.2017.10.001

Ranjan, S., Dasgupta, N., & Lichtfouse, E. (2016). *Nanoscience in Food and Agriculture 3* (Vol. 23). https://doi.org/10.1007/978-3-319-48009-1

Ravanfar, R., Comunian, T. A., Dando, R., & Abbaspourrad, A. (2018). Optimization of microcapsules shell structure to preserve labile compounds: A comparison between microfluidics and conventional homogenization method. *Food Chemistry*, *241*(June 2017), 460–467. https://doi.org/10.1016/j.foodchem.2017.09.023

Ren, X., Hou, T., Liang, Q., Zhang, X., Hu, D., Xu, B., … Ma, H. (2019). Effects of frequency ultrasound on the properties of zein-chitosan complex coacervation for resveratrol encapsulation. *Food Chemistry*, *279*(May 2018), 223–230. https://doi.org/10.1016/j.foodchem.2018.11.025

Rezaei, A., Fathi, M., & Jafari, S. M. (2019). Nanoencapsulation of hydrophobic and low-soluble food bioactive compounds within different nanocarriers. *Food Hydrocolloids*, *88*(June 2018), 146–162. https://doi.org/10.1016/j.foodhyd.2018.10.003

Schröder, A., Sprakel, J., Schroën, K., Spaen, J. N., & Berton-Carabin, C. C. (2018). Coalescence stability of Pickering emulsions produced with lipid particles: A microfluidic study. *Journal of Food Engineering*, *234*, 63–72. https://doi.org/10.1016/j.jfoodeng.2018.04.007

Shin, J. M., Gwak, J. W., Kamarajan, P., Fenno, J. C., Rickard, A. H., & Kapila, Y. L. (2016).

Biomedical applications of nisin. *Journal of Applied Microbiology*, *120*(6), 1449–1465. https://doi.org/10.1111/jam.13033

Shinde, P., Agraval, H., Singh, A., Yadav, U. C. S., & Kumar, U. (2019). Synthesis of luteolin loaded zein nanoparticles for targeted cancer therapy improving bioavailability and efficacy. *Journal of Drug Delivery Science and Technology*, *52*(April), 369–378. https://doi.org/10.1016/j.jddst.2019.04.044

Silva, A. C. da, Santos, P. D. de F., Silva, J. T. do P., Leimann, F. V., Bracht, L., & Gonçalves, O. H. (2018). Impact of curcumin nanoformulation on its antimicrobial activity. *Trends in Food Science and Technology*, *72*(January 2017), 74–82. https://doi.org/10.1016/j.tifs.2017.12.004

Sun, X., Pan, C., Ying, Z., Yu, D., Duan, X., Huang, F., … Ouyang, X. kun. (2020). Stabilization of zein nanoparticles with k-carrageenan and tween 80 for encapsulation of curcumin. *International Journal of Biological Macromolecules*, *146*, 549–559. https://doi.org/10.1016/j.ijbiomac.2020.01.053

Tan, F., Leung, P. H. M., Liu, Z. Bin, Zhang, Y., Xiao, L., Ye, W., … Yang, M. (2011). A PDMS microfluidic impedance immunosensor for E. coli O157:H7 and Staphylococcus aureus detection via antibody-immobilized nanoporous membrane. *Sensors and Actuators, B: Chemical*, *159*(1), 328–335. https://doi.org/10.1016/j.snb.2011.06.074

Teh, S.-Y., Lin, R., Hung, L.-H., & Lee, A. P. (2008). Droplet microfluidics. *Lab on a Chip*, *8*(2), 198. https://doi.org/10.1039/b715524g

Thorat, A. A., & Dalvi, S. V. (2012). Liquid antisolvent precipitation and stabilization of nanoparticles of poorly water soluble drugs in aqueous suspensions: Recent developments and future perspective. *Chemical Engineering Journal*, *181–182*, 1–34.

https://doi.org/10.1016/j.cej.2011.12.044

Thorat, A. A., & Dalvi, S. V. (2014). Particle formation pathways and polymorphism of curcumin induced by ultrasound and additives during liquid antisolvent precipitation. *CrystEngComm*, *16*(48), 11102–11114. https://doi.org/10.1039/c4ce02021a

Tian, F., Lyu, J., Shi, J., Tan, F., & Yang, M. (2016). A polymeric microfluidic device integrated with nanoporous alumina membranes for simultaneous detection of multiple foodborne pathogens. *Sensors and Actuators, B: Chemical*, *225*, 312–318. https://doi.org/10.1016/j.snb.2015.11.059

Tiwari, B. K. (2015). Ultrasound: A clean, green extraction technology. *TrAC - Trends in Analytical Chemistry*, *71*, 100–109. https://doi.org/10.1016/j.trac.2015.04.013

Ubeyitogullari, A., & Ciftci, O. N. (2019). A novel and green nanoparticle formation approach to forming low-crystallinity curcumin nanoparticles to improve curcumin's bioaccessibility. *Scientific Reports*, *9*(1), 1–11. https://doi.org/10.1038/s41598-019-55619-4

Wang, L., Wu, J., Wang, Q., He, C., Zhou, L., Wang, J., & Pu, Q. (2012). Rapid and Sensitive Determination of Sulfonamide Residues in Milk and Chicken Muscle by Microfluidic Chip Electrophoresis. https://doi.org/10.1021/jf2036577

Wang, Y., & Padua, G. W. (2010). Formation of zein microphases in ethanol-water. *Langmuir*, *26*(15), 12897–12901. https://doi.org/10.1021/la101688v

Wang, Y., & Padua, G. W. (2012). Nanoscale characterization of zein self-assembly. *Langmuir*, *28*(5), 2429–2435. https://doi.org/10.1021/la204204j

Wei, L., Zhujun, Z., & Liu, Y. (2006). Chemiluminescence microfluidic chip fabricated in PMMA for determination of benzoyl peroxide in flour. *Food Chemistry*, *95*(4), 693–698. https://doi.org/10.1016/j.foodchem.2005.04.005

Weisgrab, G., Ovsianikov, A., & Costa, P. F. (2019). Functional 3D Printing for Microfluidic Chips. *Advanced Materials Technologies*, *4*(10). https://doi.org/10.1002/admt.201900275

Whitesides, G. M. (2006). The origins and the future of microfluidics. *Nature*, *442*(7101), 368–373. https://doi.org/10.1038/nature05058

Xia, Y., & Whitesides, G. M. (1998). Soft lithography. *Annual Review of Materials Science*, *28*(1), 153–184. https://doi.org/10.1146/annurev.matsci.28.1.153

Yao, K., Chen, W., Song, F., McClements, D. J., & Hu, K. (2018). Tailoring zein nanoparticle functionality using biopolymer coatings: Impact on curcumin bioaccessibility and antioxidant capacity under simulated gastrointestinal conditions. *Food Hydrocolloids*, *79*, 262–272. https://doi.org/10.1016/j.foodhyd.2017.12.029

Yazdi, A. A., Popma, A., Wong, W., Nguyen, T., Pan, Y., & Xu, J. (2016). 3D printing: an emerging tool for novel microfluidics and lab-on-a-chip applications. *Microfluidics and Nanofluidics*, *20*(3), 1–18. https://doi.org/10.1007/s10404-016-1715-4

Yu, J., Liu, Z., Liu, Q., Yuen, K. T., Mak, A. F. T., Yang, M., & Leung, P. (2009). A polyethylene glycol (PEG) microfluidic chip with nanostructures for bacteria rapid patterning and detection. *Sensors and Actuators, A: Physical*, *154*(2), 288–294. https://doi.org/10.1016/j.sna.2008.07.005

Zhang, B., Luo, Y., & Wang, Q. (2011). Effect of acid and base treatments on structural, rheological, and antioxidant properties of α-zein. *Food Chemistry*, *124*(1), 210–220. https://doi.org/10.1016/j.foodchem.2010.06.019

Zhang, H., Fu, Y., Xu, Y., Niu, F., Li, Z., Ba, C., … Li, X. (2019). One-step assembly of zein/caseinate/alginate nanoparticles for encapsulation and improved bioaccessibility of propolis. *Food and Function*, *10*(2), 635–645. https://doi.org/10.1039/c8fo01614c

Zhang, M., Wang, W., Xie, R., Ju, X., Liu, Z., Jiang, L., … Chu, L. (2016). Controllable microfluidic strategies for fabricating microparticles using emulsions as templates. *Particuology*, *24*, 18–31. https://doi.org/10.1016/j.partic.2015.08.001

Zhang, Yali, Zuo, P., & Ye, B. C. (2015). A low-cost and simple paper-based microfluidic device for simultaneous multiplex determination of different types of chemical contaminants in food. *Biosensors and Bioelectronics*, *68*, 14–19. https://doi.org/10.1016/j.bios.2014.12.042

Zhang, Yong, Cui, L., Li, F., Shi, N., Li, C., Yu, X., … Kong, W. (2016). Design, fabrication and biomedical applications of zein-based nano/micro-carrier systems. *International Journal of Pharmaceutics*, *513*(1–2), 191–210. https://doi.org/10.1016/j.ijpharm.2016.09.023

Zhang, Yuanhong, Zhou, F., Zhao, M., Lin, L., Ning, Z., & Sun, B. (2018). Soy peptide nanoparticles by ultrasound-induced self-assembly of large peptide aggregates and their role on emulsion stability. *Food Hydrocolloids*, *74*, 62–71. https://doi.org/10.1016/j.foodhyd.2017.07.021

Zheng, B., Roach, L. S., & Ismagilov, R. F. (2003). Screening of protein crystallization conditions on a microfluidic chip using nanoliter-size droplets. *Journal of the American Chemical Society*, *125*(37), 11170–11171. https://doi.org/10.1021/ja037166v

CHAPTER 3: Fabrication of zein-modified starch nanoparticle complexes via microfluidic chip

3.1 Abstract

A microfluidic chip is a micro-reactor that precisely manipulates and controls fluidic reagents. There are many advantages to using a microfluidic chip including small reagent volume, selectivity, and rapid reaction. Zein is a group of prolamines extracted from corn that can form self-assembled nanoparticles in water or a low concentration of ethanol in a microfluidic chip. However, the zein nanoparticles are not stable, especially in a neutral pH solution due to their isoelectric point. The objective of this research was to increase the stability of zein nanoparticles by incorporating octenyl-succinic-anhydride (OSA) -modified starch via a microfluidic chip. A T-junction configuration of the microfluidic chip was used to fabricate the zein nanoparticle complexes. The dispersed phase was 1% zein or 2% zein in 70% (w/v) ethanol and the continuous phase was OSA-modified starch solution at various concentrations: 0%, 1%, 2.5%, 5%, 7.5%, and 10% (w/w). pH was adjusted to 3 for both phases. The flow rates were 10 ml/h and 30 ml/h, respectively. Effective diameter, polydispersity index, and circular dichroism spectroscopy of the zein nanoparticle suspensions were measured. Sodium chloride (0 mM, 25 mM, 50 mM, and 125 mM) was added to the nanoparticle suspensions to show the stability of the nanoparticles in various ionic strength environments. The effective diameter increased from 117.8±14.5 to 198.7±13.9 nm as the concentration of the modified starch increased from 0 to 10% (w/w). The polydispersity indexes did not show a significant difference between samples. Hydrogen bonding, electronic interaction, and hydrophobic interaction were the main driving force to form the zein nanoparticles. Compared with zein nanoparticles, the nanoparticle complexes were more stable without precipitation in various sodium chloride concentrations.

Keywords Zein nanoparticle complexes, modified starch, the microfluidic chip, stability

3.2 Introduction

Microfluidic chips are novel tiny reactors that are used to control ultra-small volume fluids with the dimensions of tens of micrometers. Nowadays, researchers have been able to expand the application of microfluidic chips in many fields, including drug discovery, biomedical imaging, and biomolecule synthesis, etc. (Teh, Lin, Hung, & Lee, 2008). For food-related research, the microfluidic chip can be used as the tools for forming emulsion (Comunian, Ravanfar, Alcaine, & Abbaspourrad, 2018; Priest, Reid, & Whitby, 2011; Ravanfar, Comunian, Dando, & Abbaspourrad, 2018; Zhao-Miao, Yu, & Yan, 2018), micro-detections (Guo, Feng, Fang, Xu, & Lu, 2015; Kant et al., 2018; Kim et al., 2015), and micro-reactors (Marze, Algaba, & Marquis, 2014; Nguyen, Marquis, Anton, & Marze, 2019a, 2019b). There are many advantages for the microfluidic chip: small reagent volumes, selectivity, green credentials rapid reactions, and small footprints (Elvira, I Solvas, Wootton, & deMello, 2013). However, very few food-grade materials have been successfully adapted in a microfluidic chip and more studies are needed to explore the applications that require food-grade materials.

Zein is the prolamine corn storage mixed protein. More than 50% of its amino acids are hydrophobic such as leucine, proline, and alanine. Based on the amino sequence and solubility in water, zein can be classified into four distinct types: α-zein, β-zein, γ-zein and δ-zein (Zhang, Luo, & Wang, 2011) and among of those types, α- is constituted around 70% in total (Lawton, 2002). Zein is widely used in the food and pharmaceutical industries because it is generally recognized as safe (GRAS), biodegradable, and biocompatible. Zein can form self-assembled particles with a process called anti-solvent precipitation in the low concentration of the ethanol solutions (Lawton, 2002; Patel & Velikov, 2014). However, zein nanoparticles are not stable in the wide range of pH,

especially at the isoelectric point. Polysaccharides can be attached to the surface of zein nanoparticles to increase stability. The nanoparticles with protein-polysaccharide complex have gained attention in the food, personal care, and pharmaceutical industries because of several advantages, such as easy preparation, biodegradability, and biocompatibility (Chang, Wang, Hu, & Luo, 2017). Protein-polysaccharide complex has been reported to encapsulate bioactive compounds and increase the encapsulation efficiency and stability of the core materials (Dai et al., 2018). As shown in Fig 3.1, the polysaccharides and protein can be interactive or not be interactive when the aqueous solutions of polysaccharides and protein are mixed. For the zein nanoparticles, polysaccharides can be attached to the surface of zein nanoparticles and increase stability.

The octenyl-succinic-anhydride (OSA) modified starch is an amphiphilic molecule obtained from the esterification reaction between starch hydroxyl groups and octenyl succinic anhydride, which is showed in Fig 3.2. It can be used as an emulsion stabilizer and encapsulating agent (Sweedman, Tizzotti, Schäfer, & Gilbert, 2013). OSA–modified starch has been used in the food industry for more than 40 years (Hui, Qi-he, Ming-liang, Qiong, & Guo-qing, 2009). In this study, we aimed to fabricate the zein-OSA modified starch nanoparticles using a microfluidic chip and to improve the stability of zein nanoparticles in a wide range of pH.

3.3 Materials and methods

3.3.1 Materials

Zein (purified) was purchased from Sigma–Aldrich (St. Louis, MO). Ethanol (200 proof) was purchased from Decon Labs (King of Prussia, PA). And OSA-modified starch was obtained from Ingredion company (Ingredion, Westchester, IL).

3.3.2 Sample preparation and characterization of nanoparticles

The dispersed phase was 1% or 2% zein dissolved in 70% (w/v) ethanol by stirring at 200 rpm overnight and then centrifuged at 4000 rpm for 10 min to remove undissolved materials. The continuous phase was a OSA-modified starch solution at various concentrations: 0%, 1%, 2.5%, 5%, 7.5%, and 10% (w/w). The starch was dissolved into deionized (DI) water by stirring at 200 rpm overnight. pH was adjusted to 3 for both phases. The 1% or 2% zein solution was loaded into a 10 ml syringe (Hamilton Robotics, Reno, NV) and the flow rate was set at 10 ml/h which was controlled by a syringe pump (Harvard Apparatus, Holliston, MA). The different concentrations of the modified starch solutions were loaded into the 10 ml syringe (Hamilton Robotics, Reno, NV) and the flow rate was set at 30 ml/h which were controlled by a syringe pump (Harvard Apparatus, Holliston, MA). The T junction, 100 μm microfluidic chip (Dolomite Ltd., Royston, UK) was used to collect samples and each sample was created with triplicates. The nanoparticle dispersions were collected in 20 mL glass vials (Thermo Fisher Scientific, Inc., Waltham, MA) for analyses.

Particle size and polydispersity index determination

All the samples were diluted at 1:40 using the DI water and the effective diameter was measured by a Dynamic Light Scattering (DLS) particle size analyzer (Brookhaven Instruments, Holtsville, NY). The effective diameters were reported as the surface average diameter (D3,2) and the equation was expressed as follow:

$$D_{3,2} = \frac{\Sigma nidi^3}{\Sigma nidi^2} \qquad (1)$$

where ni is the number of particles with diameter di. The three replicated readings were collected for each sample. The polydispersity index (PDI) was also measured by the DLS and three replicated readings were averaged.

Zeta-potential measurements

The zeta-potential of the freshly prepared samples were measured by the zeta-potential analyzer (Brookhaven Instruments, Holtsville, NY) at various pH values from 3 to 8. The suspensions were diluted by 80 times to minimize the electrokinetic potential not a contribution from inter-colloidal interaction.

Interactions related to particle formation

The contributions of hydrogen bonding, hydrophobic interaction, and disulfide bonding for particle formation were evaluated by urea, sodium dodecyl sulfate (SDS), and dithiothreitol (DTT), respectively based on the previously published method (Akbari & Wu, 2016). The zein-nanoparticle dispersions with different concentrations of the modified starch were mixed with the agents at various concentrations to assess the driving force for the complex formation. For the urea, the concentration was varied from 1M to 7 M, and from 0.25% to 1% (w/w) for SDS, and from 10 mM to 60 mM for DTT. After 6 h, the turbidity of the solutions was measured by the UV-visible spectrophotometer (Genesys5, Thermo Scientific Co., Waltham, MA) at 600 nm wavelengths. T_0 was the initial turbidity of the solutions and T was the turbidity of the solutions 6 hours after adding the dissociation agents. The ratio of the T/ T_0 was used to indicate the dissociation of the particles.

The stability of the particles in the salt solution

The stability of the zein-nanoparticles was measured by adding them into sodium chloride solution at different concentrations and sedimentation of particles was observed (H. Chen & Zhong, 2015). The same volume of NaCl solution was combined with the freshly prepared zein-nanoparticles solution with different concentrations of the modified starch (0%, 1%, 2.5%, 5%, 7.5%, and 10%). The final concentrations of the salt solution were 0 mM, 25 mM, 50 mM, and 125 mM.

Circular Dichroism (CD) Spectroscopy

CD spectra were collected using JASCO J-715 spectropolarimeter (Jasco Inc., Easton, MD) using the published method with some modifications (Feng & Lee, 2017). The 100 times diluted samples were placed in an 1 cm path length quartz cell with wavelength ranging from 200 to 250 nm at 25 ℃ with a scanning speed of 50 nm/min. The ratio of α-helix, β-sheet, and the random coil was calculated by the BeStSel software (Micsonai et al., 2015).

Statistical analysis

All the experiments were conducted in triplicate. The results were expressed as mean±standard deviation (n=3). The significant differences of the results among the different treatments assessed by ANOVA ($P< 0.5$) and the averages were compared using Tukey's test.

3.4 Results and Discussion

Particle size and polydispersity index

The particle size and polydispersity index (PDI) of the 1% and 2% zein nanoparticles with the various concentration of the OSA-modified starch (0%, 1%, 2.5%, 5%, 7.5%, and 10%) are shown in Fig 3.3. As the concentration of OSA-modified starch increased, the particle size of the zein-nanoparticles increased. The particle size of the zein-nanoparticle without the modified starch was around 117.8 nm, which is in good agreement with the previously reported results (H. Chen & Zhong, 2015; Gonçalves da Rosa et al., 2020). As the concentration of modified starch increased from 1% to 10%, the effective diameter increased from 117.8±14.5 to 198.7±13.9 nm with the 1% of zein solution and from 150.53±3.48 to 317.6±3.4 nm with the 2% of zein solutions. The particle size was significantly higher with 2% zein than 1% zein. The effective diameter increased as the concentration of OSA-modified starch increased because the added modified starch attached to the surface of zein nanoparticles to enlarge the particle size. Although there were statistical

differences in the PDI in the zein-nanoparticle with various concentrations of the modified starch, there was no clear trend for the PDI. The PDI describes the degree of "non-uniformity" of the distribution and the addition of modified starch did not change the uniformity of the zein nanoparticles fabricated in the microfluidic chip.

Zeta-potential measurements

The zeta-potential of the 1% and 2% zein nanoparticles with the various concentrations of OSA-modified starch are shown in Fig 3.4. For the zein nanoparticles without OSA-modified starch, as the pH increased from 3 to 8, the zeta-potential changed from the positive to the negative, and the isoelectric point (pI) of the zein was around 6.4, which is in good agreement with the published results (H. Chen & Zhong, 2015; Hu & McClements, 2015; Li et al., 2019). The zeta-potential of OSA-modified starch is negative in the range of pH from 3 to 8 because the branch chain of OSA-modified starch has negative charges in the wide range of pH (Lin, Liang, Zhong, Ye, & Singh, 2018). The concentration of modified starch can be categorized in three levels: low concentration (1% and 2.5%), medium concentration (5% and 7.5%), and high concentration (10%). For the 1% zein solution with the low concentration of modified starch, as the pH increased, the zeta-potential changed from positive to negative, and the pI was around 4 which is lower than the zein-only nanoparticles. With the medium and high concentration of modified starch, the zeta-potential was negative in the entire pH range from 3 to 8. For the 2% zein solution with the low and medium concentration of modified starch, as the pH increased, the zeta-potential changed from positive to negative, and the pI was around 3.3. With the high concentration of modified starch, the zeta-potential was negative in the entire pH range from 3 to 8. At the low modified starch concentration, the modified starch only partially covered the surface of the zein nanoparticles, and as the concentration increased, the modified starch gradually covered more surface of the zein

nanoparticles. The results also suggested that the electrostatic interaction was one of the main driving forces to form the zein OSA-modified starch nanoparticles (S. Chen et al., 2020).

Interactions related to the formation of the particle

Different interactions such as hydrogen bonding, electrostatic interaction, disulfide bonding, and hydrophobic interactions could affect the zein OSA-modified starch nanoparticles formation. To assess the driving force between zein and OSA-modified starch interaction, different dissociation agents were used as SDS disrupted hydrophobic interactions, urea disrupted hydrogen bonding, and DTT disrupted disulfide bonding between zein and modified starch. The ratio of T/T_0 was used to indicate the dissociation of the particles. As the reagents were added, the zein OSA-modified starch dissociated and the turbidity of the suspension decreased. As shown in Fig 3.5, T/T_0 decreased as the concentration of SDS and urea increased. However, T/T_0 did not change as the concentration of the DTT increased. The results indicated that the hydrophobic interactions and hydrogen bonding were the main driving force to form the zein-modified starch nanoparticles via microfluidic chip (Akbari & Wu, 2016).

The stability of the particles in the salt solution

Fig 3.6 shows the pictures of the zein-modified starch nanoparticles in a series of NaCl solutions. As the concentration of the NaCl increased, the stability of the nanoparticles decreased and aggregated more. At the same concentration of NaCl, as the concentration of the modified starch increased, the stability of the zein nanoparticles increased and aggregated less. The modified starch could increase the stability of the zein nanoparticles via a microfluidic chip within 0 to 125 mM of NaCl solution.

Circular Dichroism (CD) Spectroscopy

The circular dichroism (CD) spectroscopy of the 1% and 2% zein nanoparticles with different concentrations of the modified starch (0%, 5%, and 10%) are shown in Table 3.2 and Fig 3.7. In the CD spectra, individual zein nanoparticles and zein OSA-modified starch exhibited two troughs at 210 nm and 225 nm. For the untreated zein nanoparticles, the percentages of α-helix, β-sheet, and random coil were around: 14%, 43%, and 43% which are in good agreement with the published data (Feng & Lee, 2017). Compared with the zein nanoparticles, there was no significant difference in the ratio of α-helix, β-sheet, and random coil among the various concentration of the zein OSA-modified starch complex. The results showed that the modified starch did not change the secondary protein structure of zein in the nanoparticles.

3.5 Conclusions

In summary, the 1% or 2% zein OSA-modified starch nanoparticles were prepared by the microfluidic chip with the fixed flow rate at pH 3. As the concentration of the modified starch increased, the particle size increased, so the particle size could be controlled by adjusting the formulation. The impact of zein or modified starch concentrations on the PDI was not significant. The main driving forces to form the complex nanoparticles were hydrophobic interaction, electrostatic interaction, and hydrogen bonding. The modified starch did not change the secondary protein structure of the zein nanoparticles during formation. These results can be used for the zein nanoparticles formation as the nanoscale food delivery system via the microfluidic system.

3.6 Tables and figures

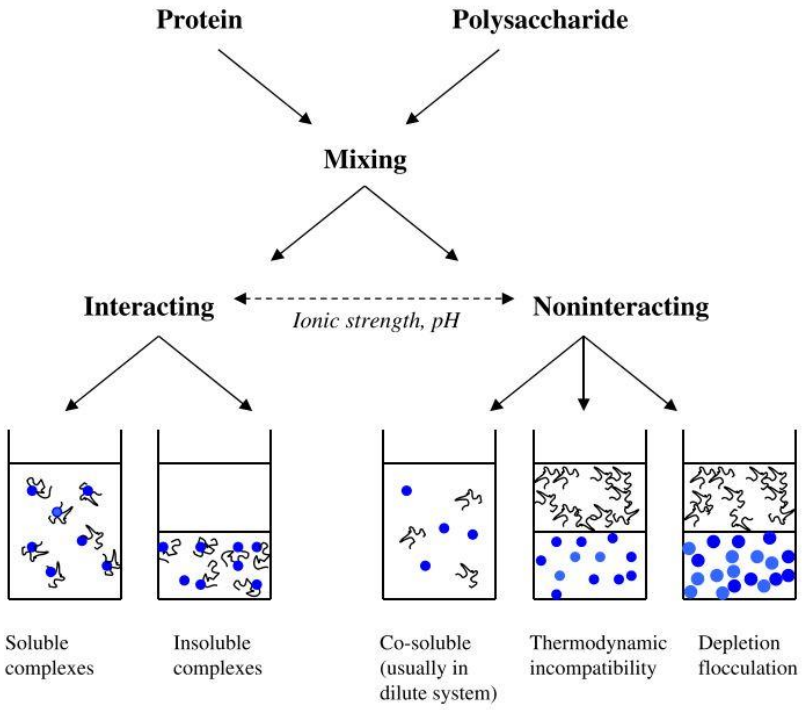

Fig 3.1 Different types of interactions between proteins and polysaccharides in aqueous solutions (Goh, Teo, Sarkar, & Singh, 2020).

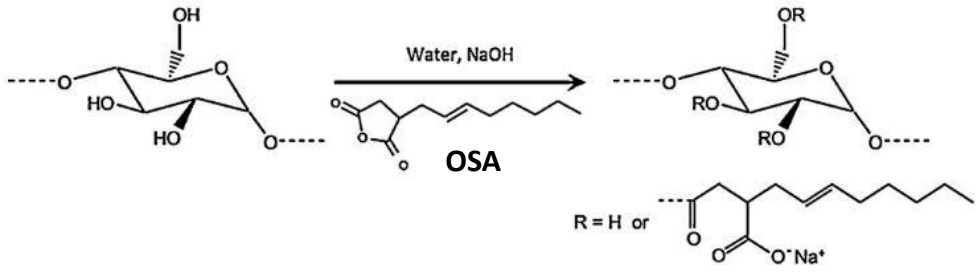

Fig 3.2 Structure of OSA-modified starches (Sweedman et al., 2013).

Table 3.1 The sample codes of zein-modified starch nanoparticles formation via microfluidic chip.

The sample code	OSA-Modified Starch Concentration% (w/w)	Zein Concentration% (w/w)
MS0-Zein1	0	1
MS1-Zein1	1	
MS2.5-Zein1	2.5	
MS5-Zein1	5	
MS7.5-Zein1	7.5	
MS10-Zein1	10	
MS0-Zein2	0	2
MS1-Zein2	1	
MS2.5-Zein2	2.5	
MS5-Zein2	5	
MS7.5-Zein2	7.5	
MS10-Zein2	10	

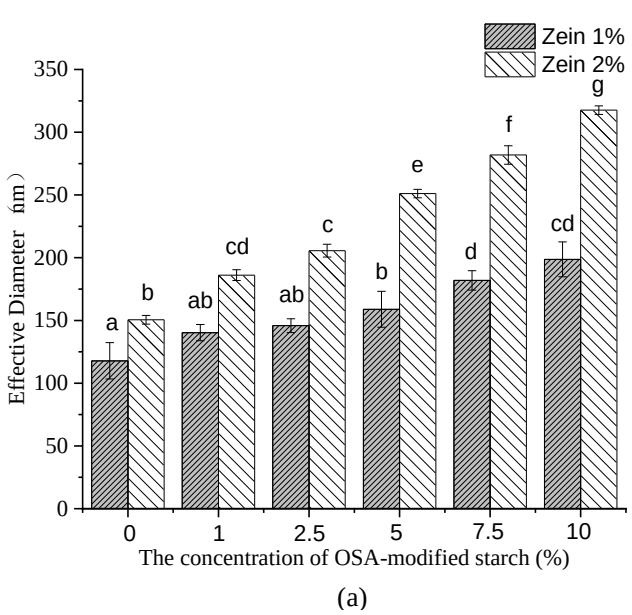

(a)

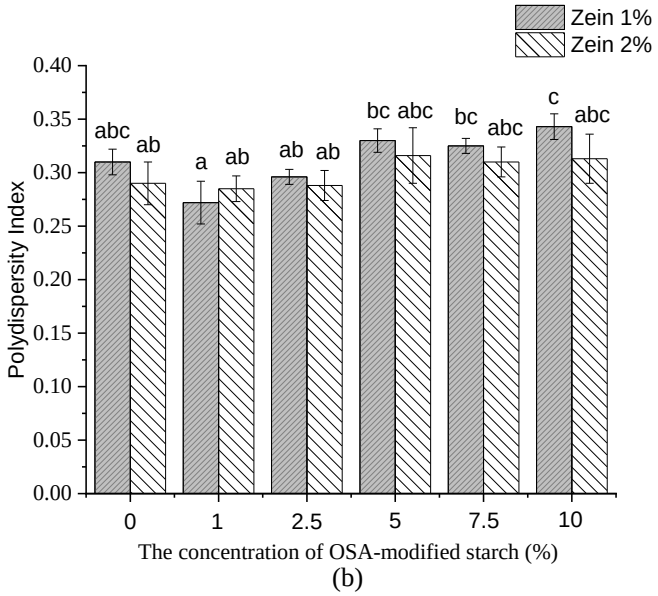

(b)

Fig 3.3 The effective diameter (a) and PDI (b) of the 1%, and 2% zein nanoparticles with various concentrations of modified starch.

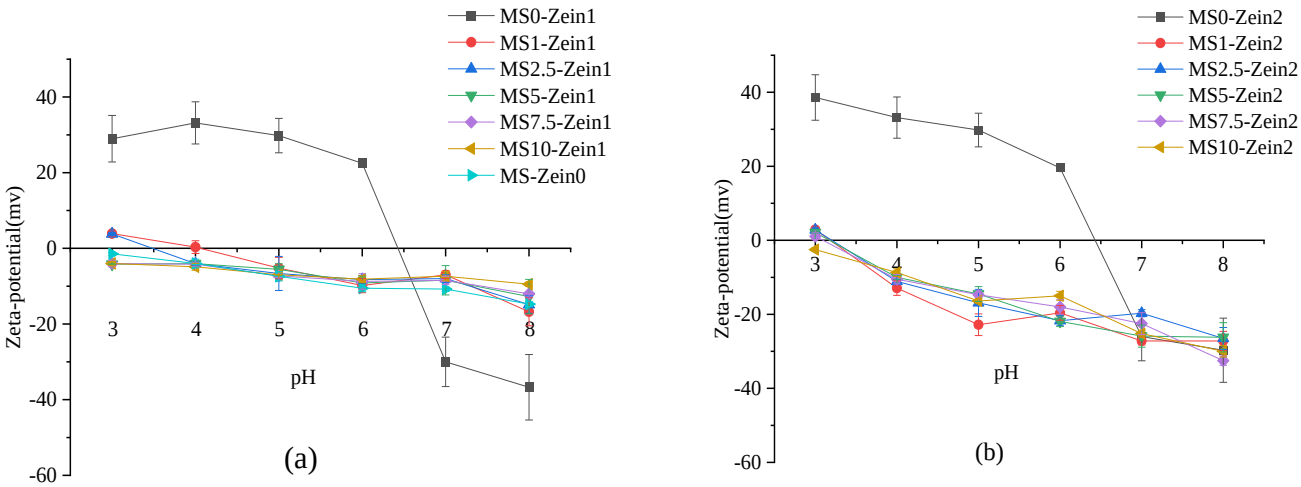

Fig 3.4 The zeta-potential of zein nanoparticles with different concentrations of modified starch. (a) 1% zein nanoparticles; (b) 2% zein nanoparticles.

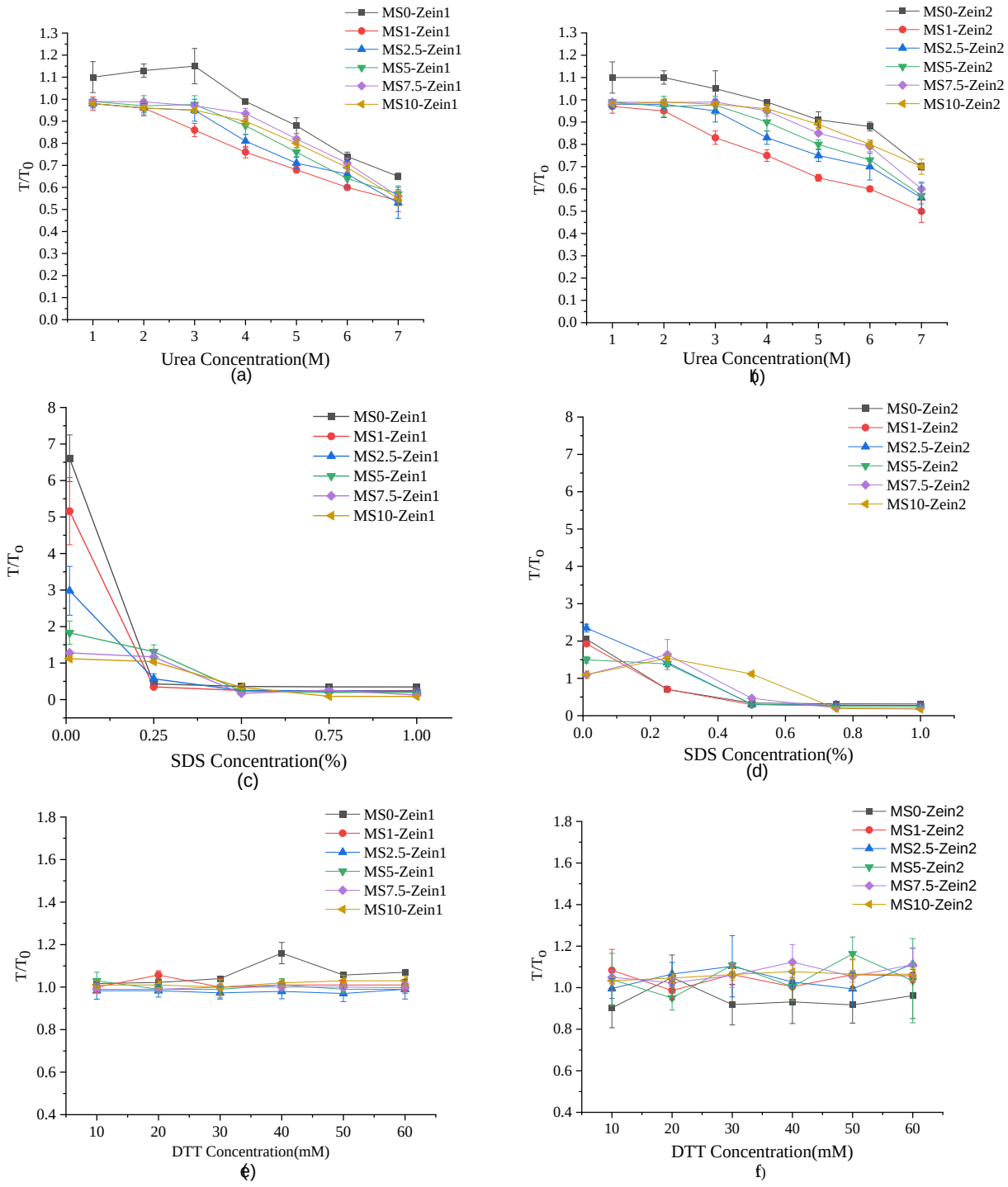

Fig 3.5 The effect of the Urea, SDS, and DTT on change of the turbidity of the zein-modified starch nanoparticle. (a), (c), (e) 1% zein nanoparticles; (b), (d), (f) 2% zein nanoparticles.

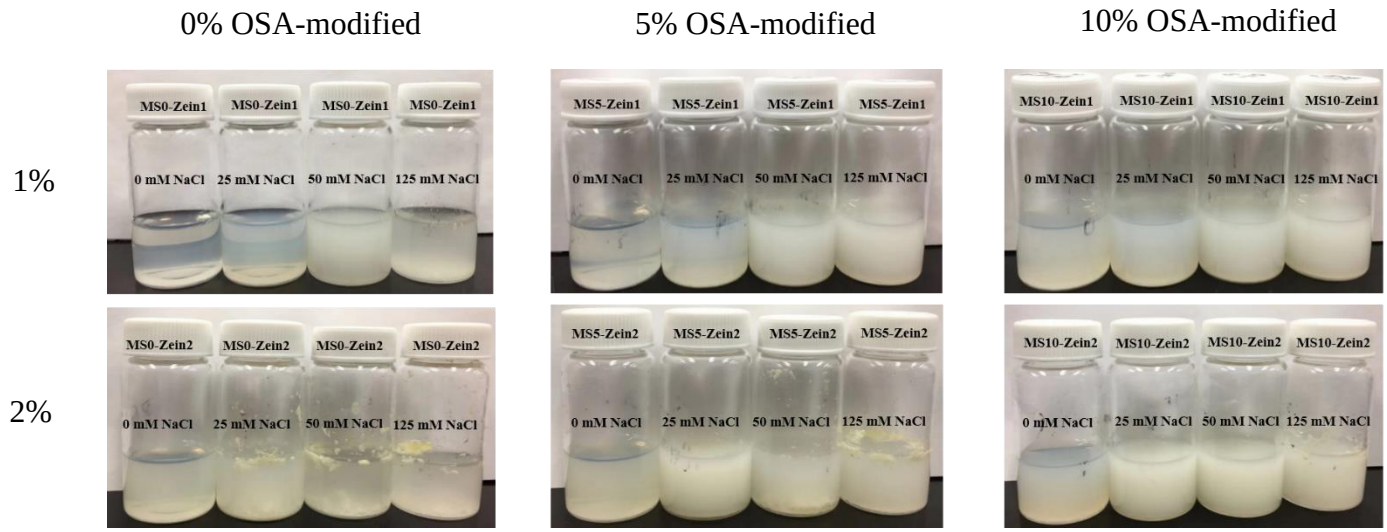

Fig 3.6 The pictures of the zein-modified starch nanoparticles with a series of NaCl concentrations.

Table 3.2 The CD Spectroscopy of the zein-nanoparticle with the different concentrations of the modified starch.

The sample	α-helix (%)	β-sheet (%)	Random coil (%)
MS_0-$Zein_1$	14.8±1.35[a]	43±2.69[a]	42.2±2.35[a]
MS_5-$Zein_1$	12.8±1.07[a]	44.2±1.52[a]	43±1.65[a]
MS_{10}-$Zein_1$	11±0.96[a]	43.5±0.78[a]	45.5±2.17[a]
MS_0-$Zein_2$	14±0.86 [a]	41.2±1.45[a]	44.8±1.07[a]
MS_5-$Zein_2$	13.6±0.93 [a]	47.9±2.96[b]	38.5±2.78[b]
MS_{10}-$Zein_2$	11.9±0.65 [a]	42.6±1.02[a]	45.5±1.98[a]

Values with different letters in the same column are significantly different (P< 0.05).

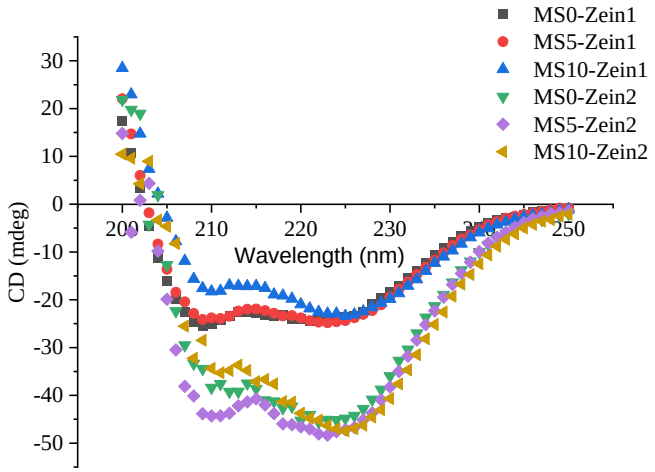

Fig 3.7 The CD Spectroscopy of the zein-nanoparticle with the different concentrations of the modified starch.

3.7 References

Akbari, A., & Wu, J. (2016). Cruciferin nanoparticles: Preparation, characterization and their potential application in delivery of bioactive compounds. *Food Hydrocolloids*, *54*, 107–118. https://doi.org/10.1016/j.foodhyd.2015.09.017

Chang, C., Wang, T., Hu, Q., & Luo, Y. (2017). Caseinate-zein-polysaccharide complex nanoparticles as potential oral delivery vehicles for curcumin: Effect of polysaccharide type and chemical cross-linking. *Food Hydrocolloids*, *72*, 254–262. https://doi.org/10.1016/j.foodhyd.2017.05.039

Chen, H., & Zhong, Q. (2015). A novel method of preparing stable zein nanoparticle dispersions for encapsulation of peppermint oil. *Food Hydrocolloids*, *43*, 593e602-602. https://doi.org/10.1016/j.foodhyd.2014.07.018

Chen, S., Li, Q., McClements, D. J., Han, Y., Dai, L., Mao, L., & Gao, Y. (2020). Co-delivery of curcumin and piperine in zein-carrageenan core-shell nanoparticles: Formation, structure, stability and in vitro gastrointestinal digestion. *Food Hydrocolloids*, *99*(August 2019), 105334. https://doi.org/10.1016/j.foodhyd.2019.105334

Comunian, T. A., Ravanfar, R., Alcaine, S. D., & Abbaspourrad, A. (2018). Water-in-oil-in-water emulsion obtained by glass microfluidic device for protection and heat-triggered release of natural pigments. *Food Research International*, *106*(September 2017), 945–951. https://doi.org/10.1016/j.foodres.2018.02.008

Dai, L., Li, R., Wei, Y., Sun, C., Mao, L., & Gao, Y. (2018). Fabrication of zein and rhamnolipid complex nanoparticles to enhance the stability and in vitro release of curcumin. *Food Hydrocolloids*, *77*, 617–628. https://doi.org/10.1016/j.foodhyd.2017.11.003

Elvira, K. S., i Solvas, X. C., Wootton, R. C. R., & deMello, A. J. (2013). The past, present and

potential for microfluidic reactor technology in chemical synthesis. *Nature Chemistry*, *5*(11), 905–915. https://doi.org/10.1038/nchem.1753

Feng, Y., & Lee, Y. (2017). Microfluidic fabrication of hollow protein microcapsules for rate-controlled release. *RSC Advances*, *7*(78), 49455–49462. https://doi.org/10.1039/c7ra08645h

Goh, K. K. T., Teo, A., Sarkar, A., & Singh, H. (2020). *Milk protein-polysaccharide interactions*. *Milk Proteins* (3rd ed.). Elsevier Inc. https://doi.org/10.1016/b978-0-12-815251-5.00013-x

Gonçalves da Rosa, C., Zapelini de Melo, A. P., Sganzerla, W. G., Machado, M. H., Nunes, M. R., Vinicius de Oliveira Brisola Maciel, M., … Manique Barreto, P. L. (2020). Application in situ of zein nanocapsules loaded with Origanum vulgare Linneus and Thymus vulgaris as a preservative in bread. *Food Hydrocolloids*, *99*(August 2019), 105339. https://doi.org/10.1016/j.foodhyd.2019.105339

Guo, L., Feng, J., Fang, Z., Xu, J., & Lu, X. (2015). Application of microfluidic “lab-on-a-chip” for the detection of mycotoxins in foods. *Trends in Food Science and Technology*, *46*(2), 252–263. https://doi.org/10.1016/j.tifs.2015.09.005

Hu, K., & McClements, D. J. (2015). Fabrication of biopolymer nanoparticles by antisolvent precipitation and electrostatic deposition: Zein-alginate core/shell nanoparticles. *Food Hydrocolloids*, *44*, 101–108. https://doi.org/10.1016/j.foodhyd.2014.09.015

Hui, R., Qi-he, C., Ming-liang, F., Qiong, X., & Guo-qing, H. (2009). Preparation and properties of octenyl succinic anhydride modified potato starch. *Food Chemistry*, *114*(1), 81–86. https://doi.org/10.1016/j.foodchem.2008.09.019

Kant, K., Shahbazi, M. A., Dave, V. P., Ngo, T. A., Chidambara, V. A., Than, L. Q., … Wolff, A. (2018). Microfluidic devices for sample preparation and rapid detection of foodborne

pathogens. *Biotechnology Advances*, *36*(4), 1003–1024. https://doi.org/10.1016/j.biotechadv.2018.03.002

Kim, M., Jung, T., Kim, Y., Lee, C., Woo, K., Seol, J. H., & Yang, S. (2015). A microfluidic device for label-free detection of Escherichia coli in drinking water using positive dielectrophoretic focusing, capturing, and impedance measurement. *Biosensors and Bioelectronics*, *74*, 1011–1015. https://doi.org/10.1016/j.bios.2015.07.059

Lawton, J. W. (2002). Zein: A history of processing and use. *Cereal Chemistry*, *79*(1), 1–18. https://doi.org/10.1094/CCHEM.2002.79.1.1

Li, H., Wang, D., Liu, C., Zhu, J., Fan, M., Sun, X., … Cao, Y. (2019). Fabrication of stable zein nanoparticles coated with soluble soybean polysaccharide for encapsulation of quercetin. *Food Hydrocolloids*, *87*(August 2018), 342–351. https://doi.org/10.1016/j.foodhyd.2018.08.002

Lin, Q., Liang, R., Zhong, F., Ye, A., & Singh, H. (2018). Physical properties and biological fate of OSA-modified-starch-stabilized emulsions containing β-carotene: Effect of calcium and pH. *Food Hydrocolloids*, *77*, 549–556. https://doi.org/10.1016/j.foodhyd.2017.10.033

Marze, S., Algaba, H., & Marquis, M. (2014). A microfluidic device to study the digestion of trapped lipid droplets. *Food and Function*, *5*(7), 1481–1488. https://doi.org/10.1039/c4fo00010b

Micsonai, A., Wien, F., Kernya, L., Lee, Y. H., Goto, Y., Réfrégiers, M., & Kardos, J. (2015). Accurate secondary structure prediction and fold recognition for circular dichroism spectroscopy. *Proceedings of the National Academy of Sciences of the United States of America*, *112*(24), E3095–E3103. https://doi.org/10.1073/pnas.1500851112

Nguyen, H. T., Marquis, M., Anton, M., & Marze, S. (2019a). Studying the real-time interplay

between triglyceride digestion and lipophilic micronutrient bioaccessibility using droplet microfluidics. 2 application to various oils and (pro)vitamins. *Food Chemistry*, *275*(July 2018), 661–667. https://doi.org/10.1016/j.foodchem.2018.09.126

Nguyen, H. T., Marquis, M., Anton, M., & Marze, S. (2019b). Studying the real-time interplay between triglyceride digestion and lipophilic micronutrient bioaccessibility using droplet microfluidics. 2 application to various oils and (pro)vitamins. *Food Chemistry*, *275*(July 2018), 661–667. https://doi.org/10.1016/j.foodchem.2018.09.126

Patel, A. R., & Velikov, K. P. (2014). Zein as a source of functional colloidal nano- and microstructures. *Current Opinion in Colloid and Interface Science*, *19*(5), 450–458. https://doi.org/10.1016/j.cocis.2014.08.001

Priest, C., Reid, M. D., & Whitby, C. P. (2011). Formation and stability of nanoparticle-stabilised oil-in-water emulsions in a microfluidic chip. *Journal of Colloid and Interface Science*, *363*(1), 301–306. https://doi.org/10.1016/j.jcis.2011.07.060

Ravanfar, R., Comunian, T. A., Dando, R., & Abbaspourrad, A. (2018). Optimization of microcapsules shell structure to preserve labile compounds: A comparison between microfluidics and conventional homogenization method. *Food Chemistry*, *241*(June 2017), 460–467. https://doi.org/10.1016/j.foodchem.2017.09.023

Sweedman, M. C., Tizzotti, M. J., Schäfer, C., & Gilbert, R. G. (2013). Structure and physicochemical properties of octenyl succinic anhydride modified starches: A review. *Carbohydrate Polymers*, *92*(1), 905–920. https://doi.org/10.1016/j.carbpol.2012.09.040

Teh, S. Y., Lin, R., Hung, L. H., & Lee, A. P. (2008). Droplet microfluidics. *Lab on a Chip*, *8*(2), 198–220. https://doi.org/10.1039/b715524g

Zhang, B., Luo, Y., & Wang, Q. (2011). Effect of acid and base treatments on structural,

rheological, and antioxidant properties of α-zein. *Food Chemistry*, *124*(1), 210–220. https://doi.org/10.1016/j.foodchem.2010.06.019

Zhao-Miao, L. I. U., Yu, D. U., & Yan, P. A. N. G. (2018). Generation of Water-In-Oil-In-Water (W/O/W) Double Emulsions by Microfluidics. *Chinese Journal of Analytical Chemistry*, *46*(3), 324–330. https://doi.org/10.1016/S1872-2040(17)61072-7

CHAPTER 4: Encapsulation of Nisin in zein-modified starch nanoparticle complexes via microfluidic chip

4.1 Abstract

Nisin is an antimicrobial peptide derived from *Lactococcus lactis* with 34 amino acids and is considered generally recognized as safe (GRAS) in food systems. However, nisin is not stable, especially in extrinsic environmental stresses (high pH, high temperature) and it has low water solubility. Nisin can be encapsulated into the zein nanoparticle to increased stability and solubility. The objective of this study was to increased the encapsulation efficiency and anti-microbial activity of the nisin encapsulated into the zein nanoparticles using a microfluidic chip. A T-junction configuration of a microfluidic chip was used to fabricate the zein-nisin nanoparticle complexes. The dispersed phase was 1% zein or 2% zein in 70% (w/v) ethanol and the continuous phase was octenyl-succinic-anhydride (OSA) starch solution at various concentrations: 0%, 5%, and 10% (w/w). pH was adjusted to 3 for both phases. The flow rates were 10 ml/h for the dispersed phase and 30 ml/h for the continuous phase. The encapsulation efficiency and the anti-microbial activity of nisin in the zein nanoparticles against the *Listeria monocytogenes* in the Queso Fresco were measured. The encapsulation efficiency was higher with 2% zein than 1% zein and increased as the concentration of the modified starch increased. The encapsulated nisin showed more anitlisterial activity than free nisin, especially for the first three days.

Keywords: Zein nanoparticle complexes, the microfluidic chip, Nisin

4.2 Introduction

Zein is the corn storage mixed protein containing more than 50% hydrophobic amino acid. There are four distinct types of zein: α-zein, β-zein, γ-zein, and δ-zein with different amino sequence and solubility (Zhang, Luo, & Wang, 2011). Zein is widely used in food and pharmaceutical and it is generally recognized as safe material (GRAS). Because zein has different solubility between the water and ethanol, it can form anti-solvent precipitation under the low ethanol concentration solution (Lawton, 2002; Patel & Velikov, 2014). Base on this property, it can be used as a nanoscale food delivery system to encapsulate bioactive compounds. However, zein nanoparticles are not stable in the wide range of pH, especially at the isoelectric point. Polysaccharides can be attached to the surface of zein nanoparticles to increase stability. The nanoparticles with protein-polysaccharide complex have gained attention in the food, personal care, and pharmaceutical industries because of the several advantages, such as easy preparation, biodegradability, and biocompatibility (Chang, Wang, Hu, & Luo, 2017). Protein-polysaccharide complex has been reported to encapsulate bioactive compounds and increase the encapsulation efficiency and stability of the core materials (Dai et al., 2018). In this study, OSA-modified starch was complexed with zein as described in Chapter 3.

Nisin is a 34-amino acid antimicrobial peptide produced by *Lactococcus lactis ssp. Lactis* (Ibarra-Sánchez, El-Haddad, Mahmoud, Miller, & Karam, 2020). Nisin has been considered as generally recognized as safe (GRAS) in the food system by the US Food and Drug Administration (FDA) (21CFR184.1538). In the food industry, nisin can be used as the antibacterial agent against Gram-positive pathogens, such as *Listeria monocytogenes* and *Staphylococcus aureus*. However, nisin has some limitations, such as instability at high temperature, and reduced activity in low acidity and high fat-containing foods, undesirable interactions with other food components, and low water

solubility (de Arauz, Jozala, Mazzola, & Vessoni Penna, 2009; Ibarra-Sánchez et al., 2020). These limitations can be overcome by encapsulating nisin into nanocarriers, including nanoemulsion, nanoparticles, nanoliposomes, and nano-fibers (Bahrami et al., 2019). In this study, the zein-OSA modified starch nanoparticles were fabricated using the microfluidic chip, and nisin was encapsulated into the zein-OSA modified starch complex. The objective of this study was to evaluate the encapsulation efficiency and antilisterial activity of nisin when incorporated into Queso Fresco.

4.3 Materials and methods

4.3.1 Materials

Zein (purified) was purchased from Sigma–Aldrich (St. Louis, MO). Ethanol (200 proof) was purchased from Decon Labs (King of Prussia, PA). OSA-modified starch was obtained from Ingredion company (Ingredion, Westchester, IL). Nisin (Nisaplin, Danisco, New Century, KS) was extracted with 70% ethanol at pH 3 overnight to prepare the stock solution.

4.3.2 Sample preparation and characterization of nanoparticles

Nisin was dissolved to reach 0.5 mg/ml in 1% or 2% zein in 70% (w/v) ethanol solution as the dispersed phase by stirring at 200 rpm overnight and then centrifuged at 4000 rpm for 10 min to remove unsolvable materials. The continuous phase was prepared by dissolving OSA-modified starch into the DI water to reach various concentrations (0%, 5%, and 10% (w/w)) by stirring the solution at 200 rpm overnight to ensure complete hydration of the modified starch. (Table 4.1). pH was adjusted to 3 for both phases. The 1% or 2% zein solution with nisin was loaded into the 10 ml syringe (Hamilton Robotics, Reno, NV) and the flow rate was 10 ml/h which was controlled by a syringe pump (Harvard Apparatus, Holliston, MA). The different concentrations of the modified starch solutions were loaded into the 10 ml syringe (Hamilton Robotics, Reno, NV) and

the flow rates were 30 ml/h which were controlled by the syringe pump (Harvard Apparatus, Holliston, MA). The T junction 100 μm microfluidic chip was used to collect samples and each sample was created with three batch replicates. The microfluidic system was purchased from Dolomite (Dolomite Ltd., Royston, UK). The nanoparticle dispersions were collected in 20 mL glass vials (Thermo Fisher Scientific, Inc., Waltham, MA) for analyses.

4.3.3 The encapsulation efficiency of nisin

Nisin Encapsulation Efficiency

To quantify nisin in the nanocapsules suspensions, 300 μL of nanocapsule suspension was mixed with 700 μL of 100% ethanol to disrupt nanocapsules and release nisin for total nisin, or mixed with 700 μL of deionized water to maintain nanocapsules integrity to measure free nisin in the supernatant. The samples were passed sequentially through 0.45, 0.22, and 0.1 μm filters (PES Syringe Filter, Sartorius) to separate polymer fractions or microcapsules from the solution before injecting into an HPLC for nisin quantification. The encapsulation efficiency was calculated as follows:

$$Encapsulation\ efficiency\ (\%) = \frac{(total\ amount\ of\ nisin\ -free\ nisin\ in\ the\ supernant)}{total\ amount\ of\ nisin} \times 100$$

Nisin Quantification with HPLC

Nisin was quantified utilizing HPLC as previously described with minor modifications (Feng et al., 2019). Briefly, a Waters 2695 Alliance HPLC system (Waters, Milford, MA) equipped with a Hewlett-Packard series 1050 photodiode array detector (Hewlett-Packard, Palo Alto, CA) was used. The analytical column was a reversed-phase Hypersil GOLD C18 (175 A, 250 x 4.6 mm, 5 μm) (Thermo Scientific, San Diego, CA). Solvent A was 0.1 % (v/v) trifluoroacetic acid (TFA) in ultra-pure water, and solvent B was 90% (v/v) HPLC-grade acetonitrile (Thermo Fisher Scientific) containing 0.1% TFA (v/v) in ultra-pure water. The column temperature was maintained at 40 °C,

sample injection volume was 20 µL, and samples were measured at UV absorption of 214 nm. A linear gradient from 31% B to 43% B over 16 min was run at a flow rate of 1.0 mL/min. The standard curve was plotted using 10, 50, 100, 200, and 300 µg/mL nisin (Nisaplin®, 2.5% nisin w/w), and the amount of nisin was calculated from the area of the peak at 214 nm. HPLC analysis was performed in duplicate for each sample.

4.3.4 The antimicrobial activity test

Microorganisms and culture conditions

Listeria monocytogenes strains (Agricultural Research Service Culture Collection Northern Regional Research Laboratory strains B-33104, B33419, B-33420, B-33424, and B-33513) were recovered from frozen glycerol stock (-80 °C) and grown in brain heart infusion (BHI; Difco, Becton Dickinson and Co., Sparks, MD) broth, at 37 °C for 24 h with 250-rpm agitation to obtain cell concentrations of ~9 Log CFU/mL. *L. monocytogenes* cocktails were prepared by combining equal volumes of stationary phase cultures of the five different foodborne outbreak-associated strains. The serial dilutions of the *L. monocytogenes* cocktail were further prepared in PBS (KCl 200 mg/L; KH_2PO_4, 200 mg/L; NaCl, 8 g/L; Na_2HPO_4, 1.15 g/L, pH 7.2) to obtain the desired cell concentrations. Listeria enumeration was carried out on PALCAM Listeria-Selective agar (EMDMillipore) supplemented with 20 mg/mL ceftazidime (Tokyo Chemical Industry Co. Ltd.) and incubated for 48 h at 37 °C.

Antilisterial properties in Queso Fresco

The antimicrobial activity of free and encapsulated nisin was evaluated by their addition to Queso Fresco (QF) as previously described with minor modifications (Van Tassell et al., 2015). Aliquots of microcapsule suspensions containing 37.5 µg nisin were vacuum concentrated in a Vacufuge Concentrator 5301 (Eppendorf North America, Westbury, NY, USA) for 45 min at room

temperature. Batches of QF were prepared with Nisaplin® and concentrated microcapsules suspension to an equivalent amount of 37.5 µg of nisin/mL of milk added into the milk before renneting. This corresponded to approximately 250 µg of nisin/g of cheese, the maximum permissible concentration in the United States. Sample cheeses were inoculated with a five-strain *L. monocytogenes* cocktail directly into the curd before pressing, for a final concentration of approximately 3.5 Log CFU/g. All cheeses were stored at 4 °C for up to 14 days until sampled for *Listeria* enumeration. Cheeses were individually homogenized and serially diluted in PBS and spread plated on PALCAM Listeria-Selective agar supplemented with 20 µg/mL ceftazidime to enumerate *L. monocytogenes*. Plates were incubated at 37 °C for 48 h.

4.3.5 Statistical analysis

All the experimental results were conducted in triplicate. The results were expressed as mean ± standard deviation (n=3). The significant differences of the results among the different treatments were assessed by ANOVA ($P < 0.5$), and the averages were compared using Tukey's test.

4.4 Results and Discussion

Encapsulation efficiency of nisin

The encapsulation efficiency of the nisin in the 1% and 2% zein nanoparticles with various concentrations of modified starch (0%, 5%, and 10%) was shown in Fig 4.1. As the concentration of the modified starch increased, the encapsulation efficiency of nisin increased. For the 1% zein nanoparticles, as the OSA-modified starch increased, the encapsulation efficiency enhanced from 10% to 40%. And for the 2% zein nanoparticles, as the OSA-modified starch increased, the encapsulation efficiency increased from 23% to 50%. The results are likely due to the increased wall thickness on the zein surface as well as increased wall material, i.e. zein. When the OSA-modified starch attached to the surface of zein nanoparticles, the particle size increased and the

thicker layer of OSA-modified starch provides more space as well as a barrier for nisin to be encapsulated thus encapsulation efficiency increased.

Antimicrobial activity

Nisin is known to inhibit Gram-positive bacteria, such as *L. monocytogenes*, a foodborne pathogen that has been associated with listeriosis outbreaks linked to fresh cheeses (Ibarra-Sánchez et al., 2017). The antimicrobial activity of nisin encapsulated in zein-modified starch against *L. monocytogenes* was evaluated in Queso Fresco (Fig 4.2). *L. monocytogenes* counts in control cheeses reached approximately 5.5 Log CFU/g by day 14 of storage at 4°C, an increase of about 2 Log CFU from the initial inoculum. Similar to our previous studies (Feng, Ibarra-Sánchez, Luu, Miller, & Lee, 2019; Ibarra-Sánchez, Kong, Lu, & Miller, 2021; Ibarra-Sánchez, Van Tassell, & Miller, 2018; Martínez-Ramos, Ibarra-Sánchez, Amaya-Llano, & Miller, 2020), a discreet reduction in the pathogen counts was observed in cheeses added with free nisin compared to control cheeses. The limited antilisterial efficacy of nisin in Queso Fresco is the result of nisin's instability at near neutral pH, and interactions with milk fat, caseins, and cations (Ibarra-Sánchez et al., 2020). All cheeses added with nisin encapsulated in zein-modified starch exhibited overall lower pathogen counts during storage. The antilisterial effect was evident until day 3. From day 5 and until day 14, a difference of approximately 0.5 and 0.8 Log CFU/g relative to control cheeses, was observed in cheeses with nisin in 1% and 2% zein nanoparticles, respectively. The effect of the concentrations of modified starch (0%, 5%, and 10%) was not evident in enhancing the efficacy of encapsulated nisin to reduce *L. monocytogenes* counts in Queso Fresco samples. Although we observed that increasing the concentration of modified starch increased the encapsulation efficiency of nisin in zein nanoparticles (Fig 1), it is possible that nisin was mostly encapsulated on or near the surface (layer of OSA modified starch) being released quickly and showed larger

impact than the nisin encapsulated into the deeper section of zein nanoparticles. Both 1% and 2% zein nanoparticles with 10% modified starch showed the highest antilisterial effect from each zein concentration until day 3, which suggests that the fast released encapsulated nisin was effective in controlling the growth of *L. monocytonese* but there may not be enough slow released encapsulated nisin to extend the antibacterial effect.

4.5 Conclusions

The nisin encapsulated into 1% or 2% zein-OSA-modified starch nanoparticles were prepared by the microfluidic chip with a fixed flow rate at pH 3. As the concentration of the modified starch increased, the encapsulation efficiency of the nisin increased. The encapsulated nisin showed more anitlisterial activity than free nisin, especially for the first three days. The impact of the starch concentration on the antimicrobial activity against *L. monocytogenes* was not conclusive. There should be a study to accomplish the sustained release of nisin from micro- and nano-capsules to extend the antibacterial activity of nisin.

4.6 Tables and figures

Table 4.1 The experimental design of encapsulation of Nisin in zein-modified starch nanoparticles formation via microfluidic chip.

The sample code	OSA-Modified Starch Concentration (%)	Zein Concentration (%)
MS0-Zein1	0	
MS5-Zein1	5	1
MS10-Zein1	10	
MS0-Zein2	0	
MS5-Zein2	5	2
MS10-Zein2	10	

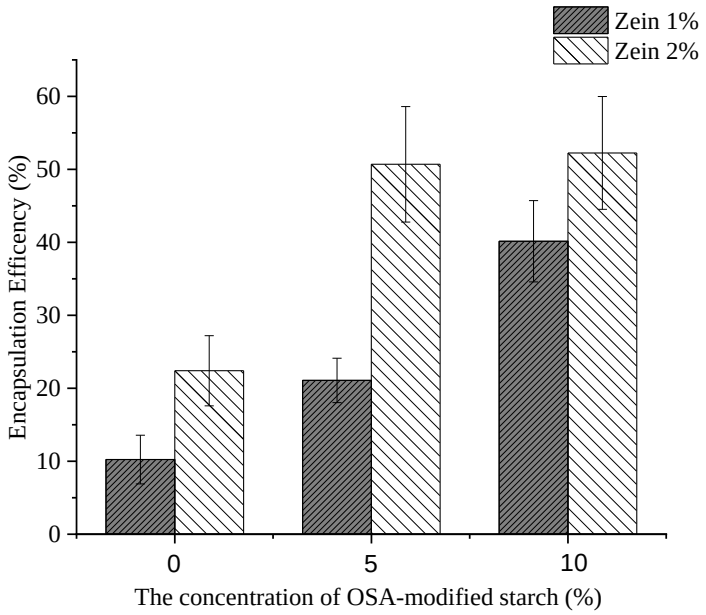

Fig 4.1 The encapsulation efficiency of the nisin encapsulated zein nanoparticle with 0, 5, and 10% modified starch.

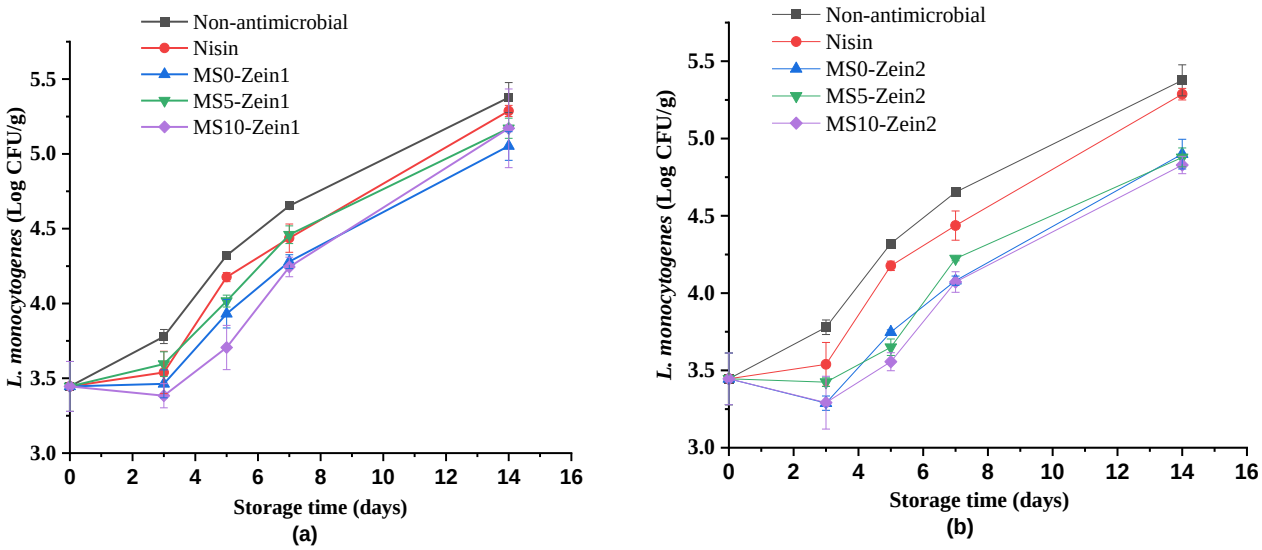

Fig 4.2 Antimicrobial activity nisin encapsulated zein nanoparticle with 0, 5, and 10% modified starch. (a) 1% zein nanoparticles; (b) 2% zein nanoparticles.

4.7 References

Bahrami, A., Delshadi, R., Jafari, S. M., & Williams, L. (2019). Nanoencapsulated nisin: An engineered natural antimicrobial system for the food industry. *Trends in Food Science and Technology*, *94*(May), 20–31. https://doi.org/10.1016/j.tifs.2019.10.002

Chang, C., Wang, T., Hu, Q., & Luo, Y. (2017). Caseinate-zein-polysaccharide complex nanoparticles as potential oral delivery vehicles for curcumin: Effect of polysaccharide type and chemical cross-linking. *Food Hydrocolloids*, *72*, 254–262. https://doi.org/10.1016/j.foodhyd.2017.05.039

Dai, L., Li, R., Wei, Y., Sun, C., Mao, L., & Gao, Y. (2018). Fabrication of zein and rhamnolipid complex nanoparticles to enhance the stability and in vitro release of curcumin. *Food Hydrocolloids*, *77*, 617–628. https://doi.org/10.1016/j.foodhyd.2017.11.003

de Arauz, L. J., Jozala, A. F., Mazzola, P. G., & Vessoni Penna, T. C. (2009). Nisin biotechnological production and application: a review. *Trends in Food Science and Technology*, *20*(3–4), 146–154. https://doi.org/10.1016/j.tifs.2009.01.056

Feng, Y., Ibarra-Sánchez, L. A., Luu, L., Miller, M. J., & Lee, Y. (2019). Co-assembly of nisin and zein in microfluidics for enhanced antilisterial activity in Queso Fresco. *Lwt*, *111*(February), 355–362. https://doi.org/10.1016/j.lwt.2019.05.059

Ibarra-Sánchez, L. A., El-Haddad, N., Mahmoud, D., Miller, M. J., & Karam, L. (2020). Invited review: Advances in nisin use for preservation of dairy products. *Journal of Dairy Science*, *103*(3), 2041–2052. https://doi.org/10.3168/jds.2019-17498

Ibarra-Sánchez, L. A., Kong, W., Lu, T., & Miller, M. J. (2021). Efficacy of nisin derivatives with improved biochemical characteristics, alone and in combination with endolysin PlyP100 to control Listeria monocytogenes in laboratory-scale Queso Fresco. *Food*

Microbiology, *94*(July 2020). https://doi.org/10.1016/j.fm.2020.103668

Ibarra-Sánchez, L. A., Van Tassell, M. L., & Miller, M. J. (2018). Antimicrobial behavior of phage endolysin PlyP100 and its synergy with nisin to control Listeria monocytogenes in Queso Fresco. *Food Microbiology*, *72*, 128–134. https://doi.org/10.1016/j.fm.2017.11.013

Lawton, J. W. (2002). Zein: A history of processing and use. *Cereal Chemistry*, *79*(1), 1–18. https://doi.org/10.1094/CCHEM.2002.79.1.1

Martínez-Ramos, A. R., Ibarra-Sánchez, L. A., Amaya-Llano, S. L., & Miller, M. J. (2020). Evaluation of combinations of nisin, lauric arginate, and ε-polylysine to control Listeria monocytogenes in queso fresco. *Journal of Dairy Science*, *103*(12), 11152–11162. https://doi.org/10.3168/jds.2020-19001

Modulation, M. (2020). Nisin as a Novel Feed Additive : The E ff ects on Gut.

Özel, B., Şimşek, Ö., Akçelik, M., & Saris, P. E. J. (2018). Innovative approaches to nisin production. *Applied Microbiology and Biotechnology*, *102*(15), 6299–6307. https://doi.org/10.1007/s00253-018-9098-y

Patel, A. R., & Velikov, K. P. (2014). Zein as a source of functional colloidal nano- and microstructures. *Current Opinion in Colloid and Interface Science*, *19*(5), 450–458. https://doi.org/10.1016/j.cocis.2014.08.001

Shin, J. M., Gwak, J. W., Kamarajan, P., Fenno, J. C., Rickard, A. H., & Kapila, Y. L. (2016). Biomedical applications of nisin. *Journal of Applied Microbiology*, *120*(6), 1449–1465. https://doi.org/10.1111/jam.13033

Van Tassell, M. L., Ibarra-Sánchez, L. A., Takhar, S. R., Amaya-Llano, S. L., & Miller, M. J. (2015). Use of a miniature laboratory fresh cheese model for investigating antimicrobial activities. *Journal of Dairy Science*, *98*(12), 8515–8524. https://doi.org/10.3168/jds.2015-

9967

Zhang, B., Luo, Y., & Wang, Q. (2011). Effect of acid and base treatments on structural, rheological, and antioxidant properties of α-zein. *Food Chemistry, 124*(1), 210–220. https://doi.org/10.1016/j.foodchem.2010.06.019

CHAPTER 5: Fabrication of zein-nanoparticles via ultrasonic treatment

5.1 Abstract

Zein is the corn storage protein, which contains more than 50% hydrophobic amino acid. It can be used as a nanoscale food delivery system by anti-solvent precipitation in the water-ethanol solution. The properties of zein nanoparticles formed by anti-solvent precipitation are affected by alcohol type, the concentration of zein, mixing methods, initial ethanol concentration, and dilution ratio. Ultrasound is an emerging and non-thermal technology in the food industry and can be used to assist zein nanoparticles fabrication. The objective of this research was to evaluate the effect of ethanol concentration in the continuous phase, the ratio of the dispersed phase and continuous phase, and the amplitude of ultrasound waves on the properties of zein nanoparticles. Zein nanoparticles were fabricated by ultrasonic treatment with the different initial ethanol concentration (0%, 10%, 20%, and 30%) in the continuous phase, the different ratio of the dispersed phase to continuous phase (1:2, 1:5, and 1: 10), and different ultrasound amplitude (20%, 30%, 40%, and 50%). The particle size, polydispersity, and morphological structure of zein nanoparticles were analyzed. The particle size increased as the concentration of ethanol concentration in the continuous phase increased. As the ratio of the dispersed to continuous phase decreased, the particle size decreased. The ultrasound amplitude did not show a significant effect on the particle size. The polydispersity index (PDI) results revealed that as the concentration of ethanol in the continuous increased, the PDI first decreased and then increased, suggesting that there is a critical ethanol concentration for zein self-assembly. The findings of this study provide insights and means for manipulating zein nanoparticles by adjusting ethanol concentration in the continuous phase and the ratio of the dispersed phase to the continuous phase.

Keywords zein, anti-solvent precipitation, ultrasound, particle size

5.2 Introduction

Zein is the prolamine corn storage protein with more than 50% of hydrophobic amino acids including leucine, proline, and alanine (Shukla & Cheryan, 2001). Zein is widely used in the food and pharmaceutical industries because it is generally recognized as safe (GRAS), biodegradable, and biocompatible (Lawton, 2002; A. R. Patel & Velikov, 2014). Because zein is amphiphilic, it has been used as nanoscale food delivery systems to encapsulate lipophilic bioactive compounds, including β-carotene (Ba et al., 2020), cinnamon oil (Feng et al., 2020), curcumin (Sun et al., 2020), and quercetin (Li et al., 2019). Various methods have been used to form the zein-based nanoscale food delivery systems, including chemical crosslinking, emulsification/solvent evaporation, emulsification/precipitation spray drying, and anti-solvent precipitation. Among these technologies, the anti-solvent precipitation is the most frequently used to fabricate zein nanoparticles (Wang & Padua, 2012; Yong Zhang et al., 2016). Anti-solvent precipitation, which is also called liquid-liquid dispersion, can be achieved by adding a solution to a non-solvent to induce supersaturation and form nanoparticles (Joye & McClements, 2013). For the zein nanoparticle fabrication, 55%-95% (v/v) ethanol or other organic solvents can be used as primary solvent, and water can be used as the non-solvent (H. Zhang et al., 2019). As showed in Fig 5.1, the composition of zein, water, and ethanol should be located in the precipitation area or coacervation area to cause zein anti-solvent precipitation. As the concentration of ethanol decreasing, nucleation of zein may occur because of supersaturation. In this process, the particle size and stability of zein nanoparticles are affected by alcohol type, the concentration of zein, mixing methods, the initial ethanol concentration, and the dilution ratio (Yong Zhang et al., 2016). Zein has a different solubility in different solvents (ethanol, methanol, and isopropanol) so different supersaturation points. As the degree of supersaturation increased, the particle size of the

final product decreased (A. Patel, Hu, Tiwari, & Velikov, 2010). However, few studies have been published on the effect of the initial ethanol concentration and the dilution ratio on the properties of zein nanoparticles. Often, zein nanoparticles were fabricated using magnetic stirring. In this study, emerging green and non-thermal technology, ultrasound will be used to form the zein nanoparticles.

Generally, the sound wave can be divided into audile waves (10 Hz-20 kHz), infrasonic waves (<16 Hz), and ultrasonic waves (>20 kHz) (Tiwari, 2015). The frequency of the ultrasound is above the human being's hearing. The main driving force of the ultrasonic waves is cavitation by generating shear forces and fluid mixing. The cavitation bubbles are produced by alternating pressure changes during the propagation of ultrasound waves (Tiwari, 2015). Once the bubbles reach a certain size, they will collapse to form the shearing force (Kentish & Feng, 2014). Ultrasound technology has been used in the food industry for many years for bio-compounds extraction, viscosity modification, emulsification, surface cleaning, food quality assurance, filtration, tenderization (Ashokkumar, 2015; Bhaskaracharya, Kentish, & Ashokkumar, 2009; Cárcel, García-Pérez, Benedito, & Mulet, 2012; Chandrapala, Oliver, Kentish, & Ashokkumar, 2012; Chemat et al., 2017; Chemat, Zill-E-Huma, & Khan, 2011; Kadam, Tiwari, Álvarez, & O'Donnell, 2015; Ojha, Mason, O'Donnell, Kerry, & Tiwari, 2017; Tiwari, 2015). In addition, ultrasound can be used for nanoparticle formation. For the starch nanoparticles, ultrasound increased the yield rate of the cassava, corn, and yam starch nanoparticles and microparticles without any chemical additives, and the particle size was smaller than the native starch granules (Minakawa, Faria-Tischer, & Mali, 2019). There was a minimum water content required for the ultrasound to induce starch nanoparticle formation, and ultrasound increased the amorphous content in the starch nanoparticles (Boufi et al., 2018). What's more, the ultrasonic treatment

decreased the viscosity and the weight average molecular weight of the starch (Chang et al., 2017). For the protein nanoparticles, Ren et al. (Ren et al., 2019) compared the different frequencies of the ultrasound to evaluate the effect of ultrasound on the properties of zein-chitosan complex and resveratrol encapsulation. The results showed that the particle size of the zein-chitosan complex treated with dual-frequency (28/40 kHz) was smaller than the single or multi-frequency treatment. The ultrasound treatment increased the stability of zein nanoparticles during the formation. The soy peptide nanoparticles which were produced by an ultrasound treatment increased the stability and decreased the lipid oxidation of the emulsion during storage (Yuanhong Zhang et al., 2018). However, few studies focus on the effect of ultrasound amplitude, the initial concentration of ethanol, and the ratio of the dispersed phase and continuous phase on the properties of zein nanoparticle formation.

Herein, the objective of this research was to investigate the effect of ethanol concentration in the continuous phase, the ratio of the dispersed phase and continuous phase, and amplitude of ultrasound on the properties of zein nanoparticles by particle size, polydispersity, and morphological structure. The results fro this study can provide the reference for the formation and application of the zein nanoparticles in food delivery systems in the food industry.

5.3 Materials and methods

5.3.1 Materials

Zein (Z3625, Sigma-Aldrich, St. Louis, MO) dissolved in 70% (v/v) ethanol (200 Proof, Decon Laboratories, King of Prussia, PA) was used as the dispersed phase. Different concentration of ethanol solution: 0% (v/v), 10% (v/v), 20% (v/v), and 30% (v/v) were used as the continuous phase.

5.3.2 Sample preparation and characterization of nanoparticles

The zein nanoparticles were prepared by ultrasonic treatment and stirring treatment. 2 g zein was dissolved into 100 mL 70% ethanol overnight to reach 2% w/w, and pH was adjusted 3. The 3 mL, 6 mL, or 15 mL of zein solutions were dropped into 30 mL of 0 % (DI water), 10 %, 20 %, or 30% ethanol using a 20 ml syringe, and pH was adjusted 3. The volume ratios of dispersed phase to continuous phase were 1:10, 1:5, and 1:2, respectively. The needle (23G: 0.6 mm×25 mm) was located directly above the center of a 100 mL beaker. The flow rates were: 0.3 mL/min, 0.6 mL/min, and 1.5 mL/min for the ratios of 1:10, 1:5, and 1:2, respectively and the amplitude setting were 20%, 30%, 40%, and 50% using a Q125 ultrasonic homogenizer (QSonica, Newton, CT). For the stirring treatment, the various volume of zein solutions was dropped into 30 mL of DI water at 600 rpm. The amplitude was limited to 50% due to heating of the sample when the amplitude was more than 50%, which negatively impacted the formation of the zein nanoparticles. The sample preparation setup is shown in Fig 5.2. A rotary evaporator (Heidolph 2-Collegiate, Germany) was used at 40 ℃ for 10 min to remove the remained ethanol in the zein nanoparticles solution.

Particle size and polydispersity index (PDI)

All the samples were diluted to the 1:50 ratio using DI water so that the suspensions were not cloudy. The effective diameter was measured by a Dynamic Light Scattering (DLS) particle size analyzer (Brookhaven Instruments, Holtsville, NY). The effective diameters were reported as the surface average diameter (D3,2) and the equation is expressed as follow:

$$D_{3,2} = \frac{\Sigma nidi^3}{\Sigma nidi^2} \qquad (1)$$

where ni is the number of particles with diameter di. The three replicated readings were collected for each sample. The polydispersity index (PDI) was also collected using the DLS and three replicated readings were averaged.

Scanning electron microscopy

Freshly prepared nanoparticle dispersions were converted into a powder using freeze-drying (Harvest Right, Salt Lake City, Utah). The dried nanoparticles were analyzed using scanning electron microscopy (Hitachi S-4800, CA, U.S.) with an acceleration potential of 10 kV using a high vacuum mode. A layer of gold coating (15 nm) was applied to the mounted sample before analysis.

5.4 Results and Discussion

The pictures of the zein nanoparticles

The pictures of the zein nanoparticle suspensions with the various initial concentration of ethanol in the continuous phase and the ratio of dispersed phased to continuous phase and different are presented in Fig 5.3. At the same initial concentration of ethanol in the continuous, as the zein concentration increased, the zein nanoparticle suspension became cloudier and darker due to more particles present in the suspension. For the sample of 1:2 ratio at 30% ethanol, the suspension appeared to be similar to 2% zein solution. The final concentration of zein, water, and ethanol were: 0.67%, 56.33%, and 43% (Table 5.3) for this sample. Based on the ternary diagram of zein in the water and ethanol solution (Fig 5.7), this sample was located close to the solution region causing a similar appearance as the zein solution. Furthermore, the zein nanoparticle suspension became cloudier as the initial concentration of ethanol in the continuous phase increased at the same ratio of dispersed phase to the continuous phase. It is because that as the initial concentration

of ethanol in the continuous phase increased, the degree of supersaturation S decreased and the size of zein nanoparticles increased.

Particle size and polydispersity index

The particle size and polydispersity index of the zein nanoparticles with the different initial ethanol concentration (0%, 10%, 20%, and 30%) in the continuous phase, the volume ratio of the dispersed phase to continuous phase (1:2, 1:5, and 1: 10), and the ultrasound amplitude (20%, 30%, 40%, and 50%) are shown in Fig 5.4, 5, and 6. From the figures, at the same ratio of the dispersed phase and continuous phase and the same ultrasound amplitude, as the initial concentration of ethanol in the continuous phase increased, the particle size increased. The particle size increased as the ratio of the dispersed phase to continuous phase decreased when the concentration of ethanol in the continuous and ultrasound amplitude was constant. There was no significant impact of the ultrasound amplitude on the zein particle size. Zein anti-solvent precipitation can be achieved by adding the zein ethanol solution to the water to induce supersaturation and form zein nanoparticles. During this processing, several factors can affect particle formation and particle size. The results can be explained by the equation of anti-solvent precipitation. The driving force of the anti-solvent precipitation is supersaturation ratio (S), the degree of supersaturation S can be described as follow (Joye & McClements, 2013):

$$S = \frac{C}{C^*} \qquad (1)$$

Where C is the zein concentration in ethanol solution and C* is the saturation concentration of zein in the ethanol-water mixture. In this study, the zein concentration was controlled by the ratio of the dispersed phase and continuous phase. At the same ratio, the zein concentration is the same. Based on the zein ternary phase diagram in water-ethanol binary solvent (Fig 5.1), as the

concentration of ethanol increased, the solubility of zein increased, and the saturation concentration of zein increased:

$$C_{0\%*} < C_{10\%*} < C_{20\%*} < C_{30\%*}$$

The degree of supersaturation, S decreased as the concentration of ethanol increased:

$$S_{0\%} > S_{10\%} > S_{20\%} > S_{30\%}$$

Using the Ostwald-Freundlich equation, the $\ln(s)$ can be described as follow (A. Patel et al., 2010) :

$$\ln(s) = \frac{2\gamma}{rkT} \qquad (2)$$

Where γ is the solid-liquid interfacial tension, k is the Boltzmann constant, and T is the temperature, r is the radius of particles. The $\ln(s)$ decreased as the concentration of ethanol increased:

$$\ln(S_{0\%}) > \ln(S_{10\%}) > \ln(S_{20\%}) > \ln(S_{30\%})$$

So, based on the equation (2), the radius of zein nanoparticles increased as the concentration of ethanol increased:

$$r_{0\%} < r_{10\%} < r_{20\%} < r_{30\%}$$

As the results, at the same ratio of the dispersed phase to the continuous phase when the concentration of zein in the ethanol is constant, the particle size of zein nanoparticles will be affected by the ethanol concentration. As the initial concentration of ethanol in the continuous increased, the particle size of zein nanoparticles increased.

As shown in Table 5.3, the final concentration of water, zein, and ethanol was dependant on the initial concentration of ethanol in the continuous phase and the ratio of the dispersed phase to continuous treatment. Based on the final composition, the different treatments can be tagged into the ternary diagram of zein in the water and ethanol solution in Fig 5.7.

The polydispersity index (PDI) is the ratio of the mass average molar mass and the number averaged molar mass, and it can reflect the uniformity of the sample. Generally, it is considered as a monodispersed particle when PDI is less than 0.2. For perfectly uniform particles, the PDI would be 0.0. As the final concentration of ethanol increased, the PDI decreased first and then increased. The PDI reached the lowest value of less than 1.5 at the final concentration of ethanol around 28%, which is shown in Fig 5.8. The results indicated that there may be a critical ethanol concentration on the ternary diagram. The zein nanoparticles reached a lower PDI value meaning the formation of more uniform particles when the treatment condition was approaching this critical ethanol concentration. There may be a balance between the kinetics of the zein self-assembly and the shear force generated by the ultrasound waves to form uniform zein particles. Away from the critical ethanol concentration, the self-assembly may be either too fast or too slow for the ultrasound wave to effectively control the particle size.

Scanning electron microscopy

The images of zein nanoparticles by scanning electron microscopy were showed in Fig 5.9, Fig 5.10, and Fig 5.11. For Fig 5.9, the ratio of the dispersed phase to continuous phased was 1:2 and as the initial concentration of ethanol in the continuous phase increased, the particle size increased. The results showed the same trend when the ratio of dispersed phased and continuous phased was 1:5 (Fig 5.10) and 1:10 (Fig 5.11).

5.5 Conclusions

In this study, zein nanoparticles were fabricated by ultrasonic treatment with different concentrations of ethanol in the continuous phase, different ratios of the dispersed phase, and continuous and different amplitude. The properties of zein nanoparticles were characterized by particle size, polydispersity index, and SEM. The results showed that as the concentration of

ethanol in the zein nanoparticle suspension increased, the particle size increased and the PDI decreased and then increased; indicating that the concentration of ethanol is a critical factor affecting the zein nanoparticle formation and there may be a critical ethanol concentration. As the ratio of dispersed phase increased, the particle size increased. The amplitude did not significantly influence the particle size and PDI. These results can be used for the zein nanoparticles formation as designing of the nanoscale food delivery system via ultrasonic treatment.

5.6 Tables and figures

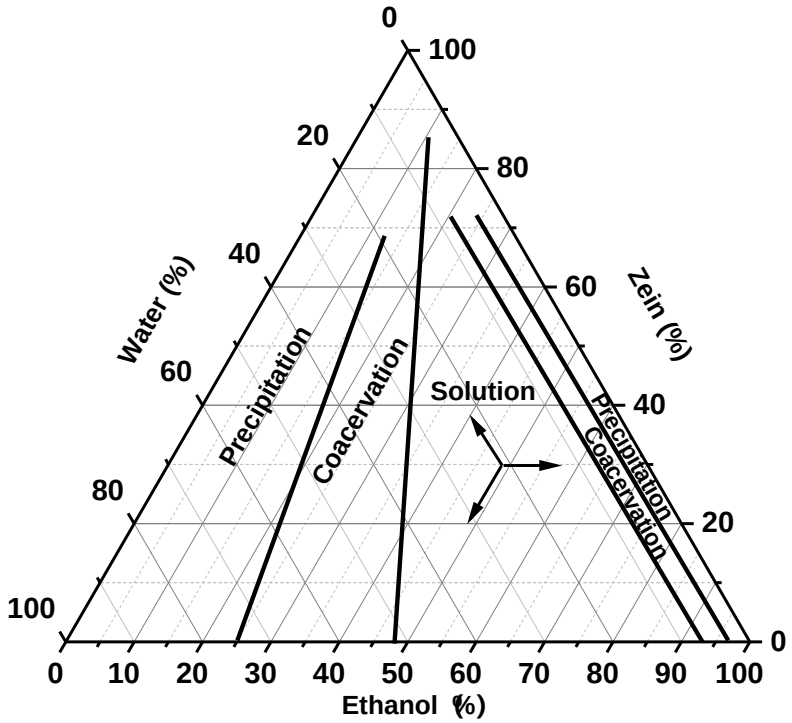

Fig 5.1 The ternary diagram of the zein was modified from Moosé (Shukla & Cheryan, 2001).

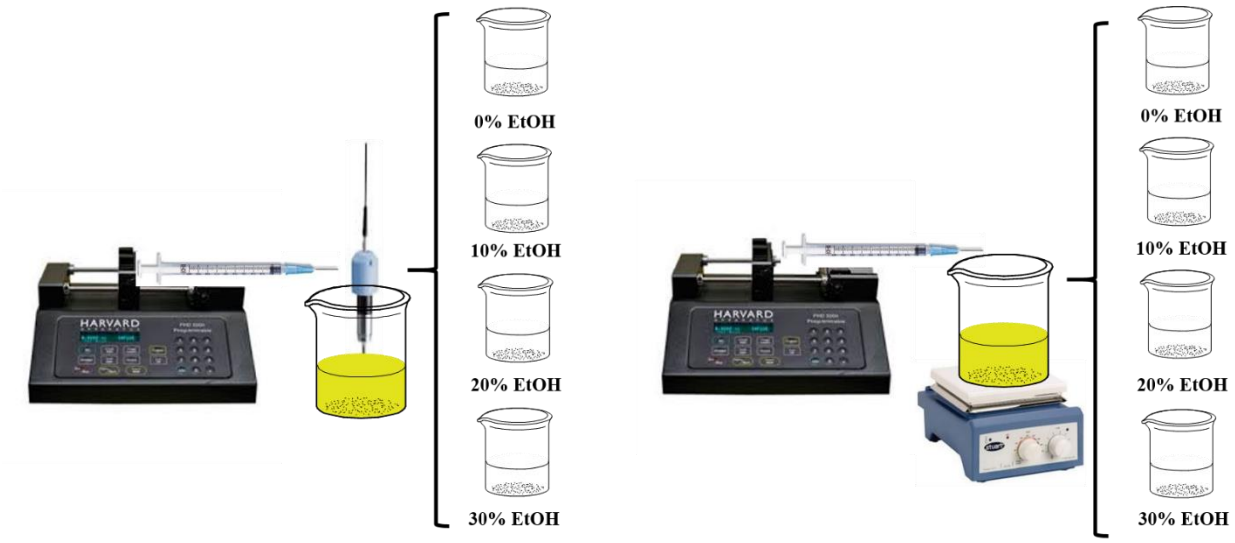

Fig 5.2 The experimental setup of the ultrasonic and shearing treatment zein nanoparticles.

Table 5.1 Experimental design of the 2% zein nanoparticles production via shearing treatment.

Treatment	Ethanol Concentration (%, w/v)	Dispersed phase: Continuous phase Volume ratio
Shearing	0	1:2
	10	
	20	
	30	
	0	1:5
	10	
	20	
	30	
	0	1:10
	10	
	20	
	30	

Table 5.2 Experimental design of the 2% zein nanoparticles production via ultrasonic treatment.

Treatment	Amplitude	Ethanol Concentration (%, w/v)	Dispersed phase: Continuous phase Volume ratio
Ultrasound	20%	0	1:2
		10	
		20	
		30	
	30%	0	
		10	
		20	
		30	
	40%	0	
		10	
		20	
		30	
	50%	0	
		10	
		20	
		30	
Ultrasound	20%	0	1:5
		10	
		20	
		30	
	30%	0	
		10	
		20	
		30	
	40%	0	
		10	
		20	
		30	
	50%	0	
		10	
		20	
		30	

Table 5.2 (cont.)

Treatment	Amplitude	Ethanol Concentration (%, w/v)	Dispersed phase: Continuous phase Volume ratio
Ultrasound	20%	0	1:10
		10	
		20	
		30	
	30%	0	
		10	
		20	
		30	
	40%	0	
		10	
		20	
		30	
	50%	0	
		10	
		20	
		30	

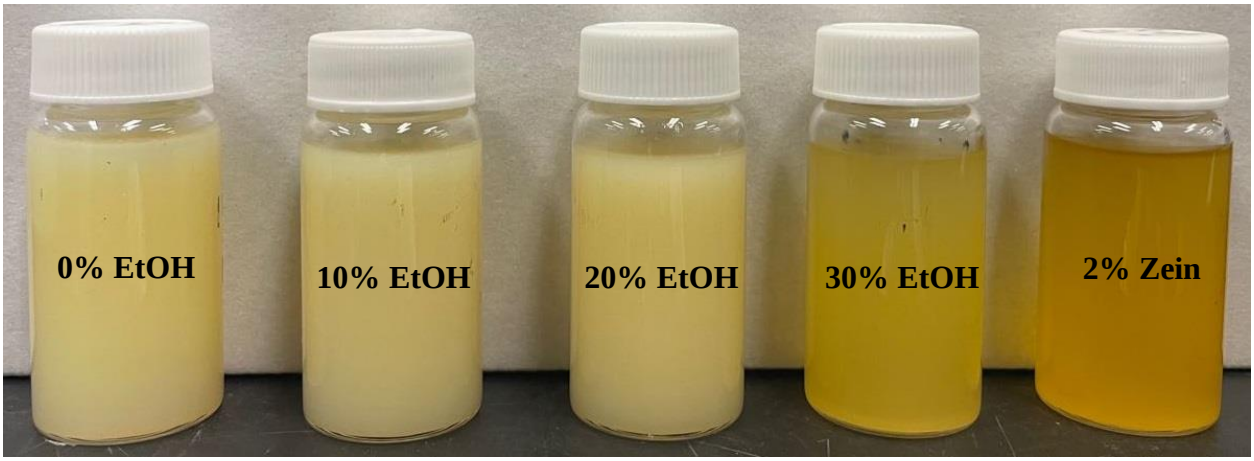

1:2

1:5

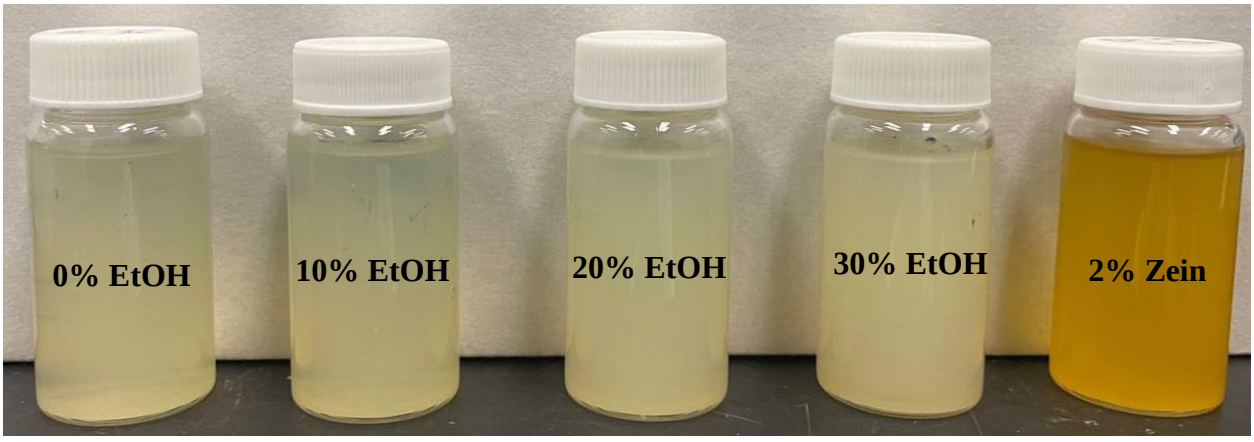

1:10

Fig 5.3 The pictures of the zein nanoparticles suspensions via ultrasonic treatment with various initial ethanol concentrations in the continuous phase and dispersed: continuous phase ratio at the 20% amplitude.

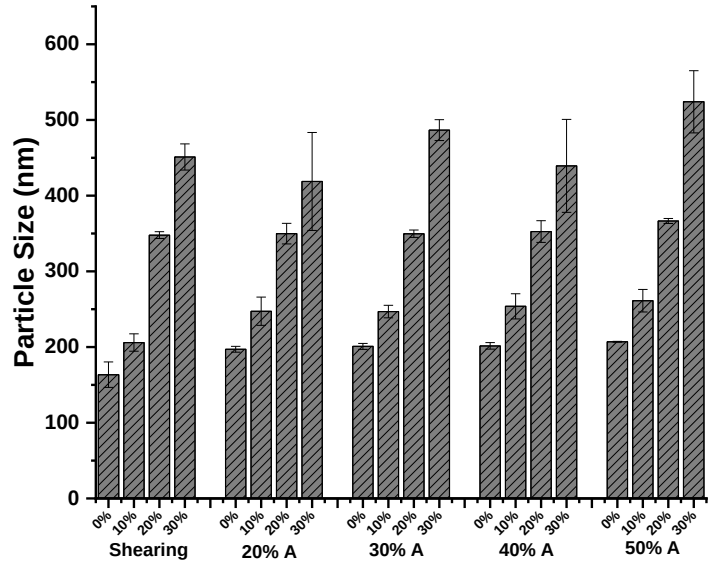

(a)

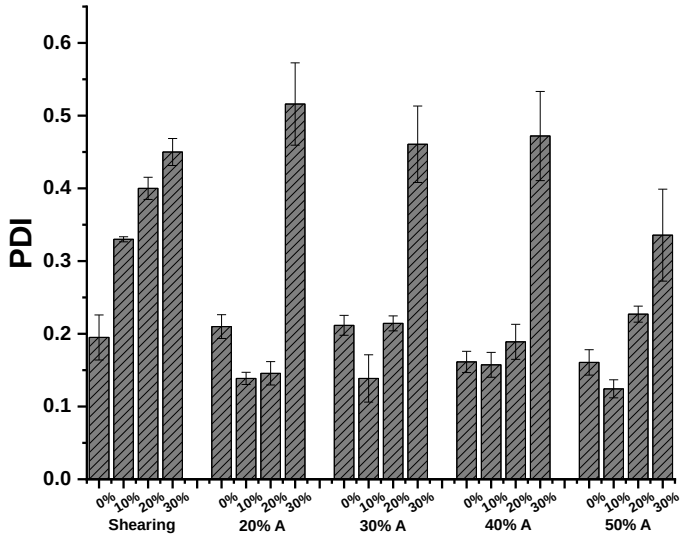

(b)

Fig 5.4 The effective diameter (a) and PDI (b) of 2% zein nanoparticles with various concentrations of ethanol, amplitude (Dispersed phase: Continuous phase = 1:2).

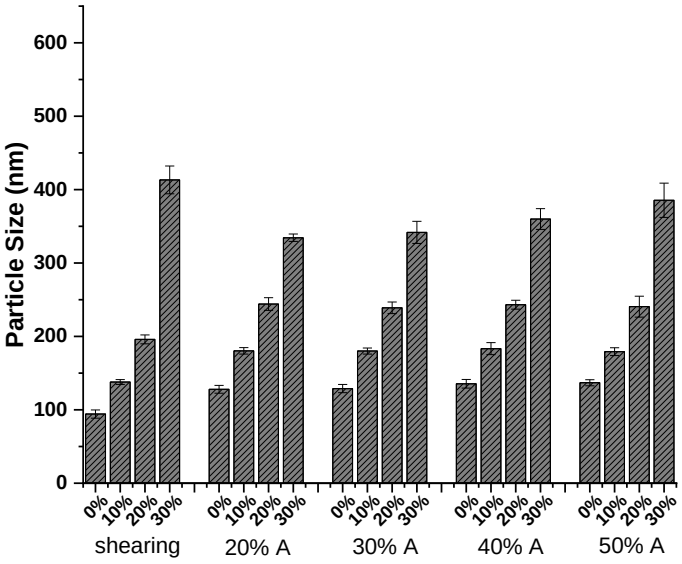

(a)

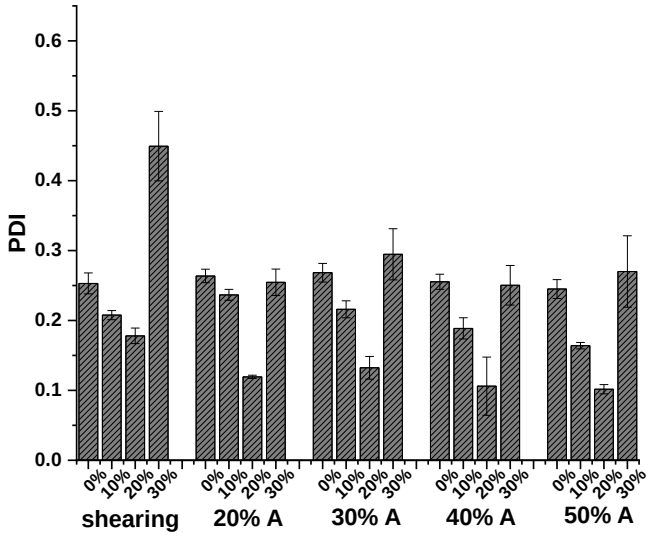

(b)

Fig 5.5 The effective diameter (a) and PDI (b) of 2% zein nanoparticles with various concentrations of ethanol, amplitude (Dispersed phase: Continuous phase = 1:5).

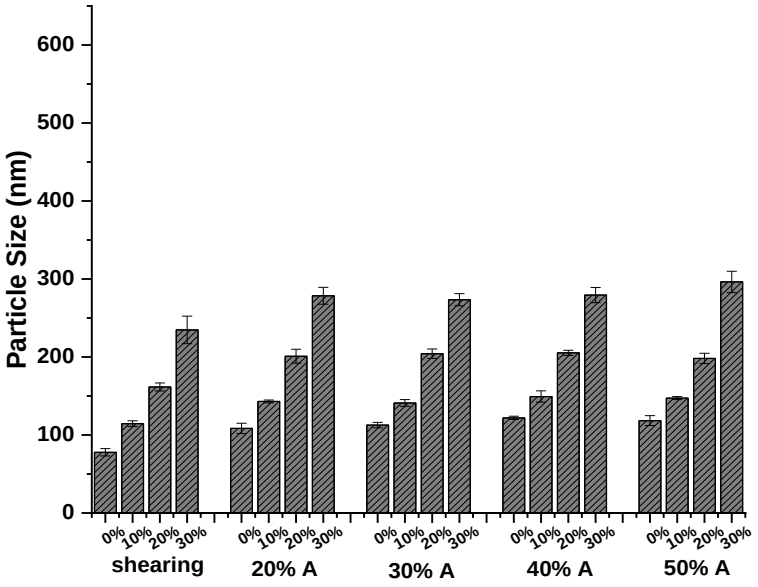

(a)

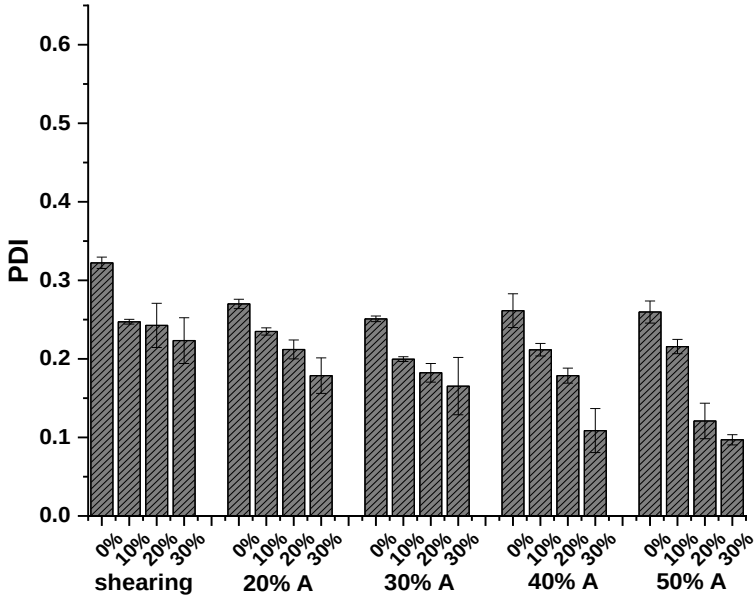

(b)

Fig 5.6 The effective diameter (a) and PDI (b) of 2% zein nanoparticles with various concentrations of ethanol, amplitude (Dispersed phase: Continuous phase = 1:10).

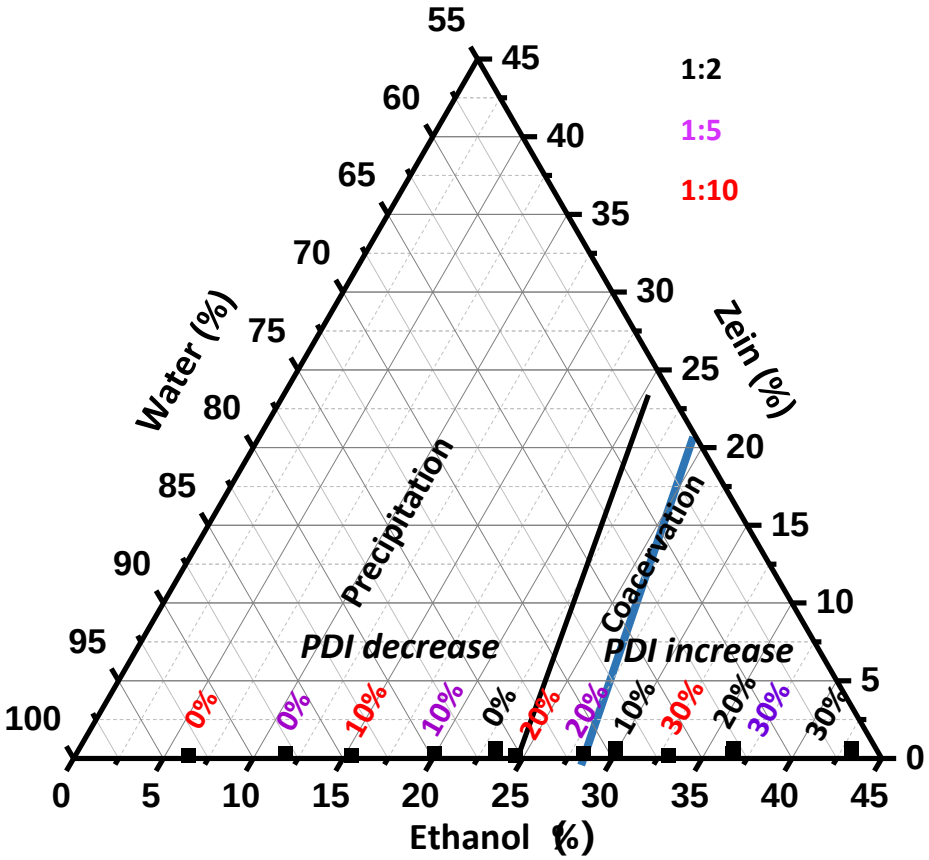

Fig 5.7 Final compositions of the zein nanoparticle dispersions on ternary phase diagram based on the ratio of dispersed to continuous phase and initial ethanol concentration in the continuous phase.

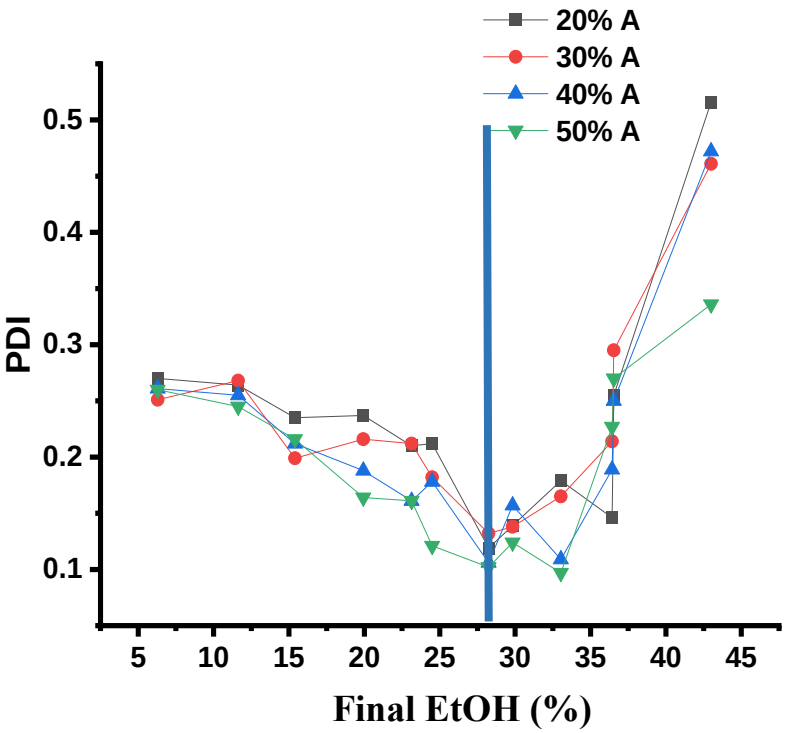

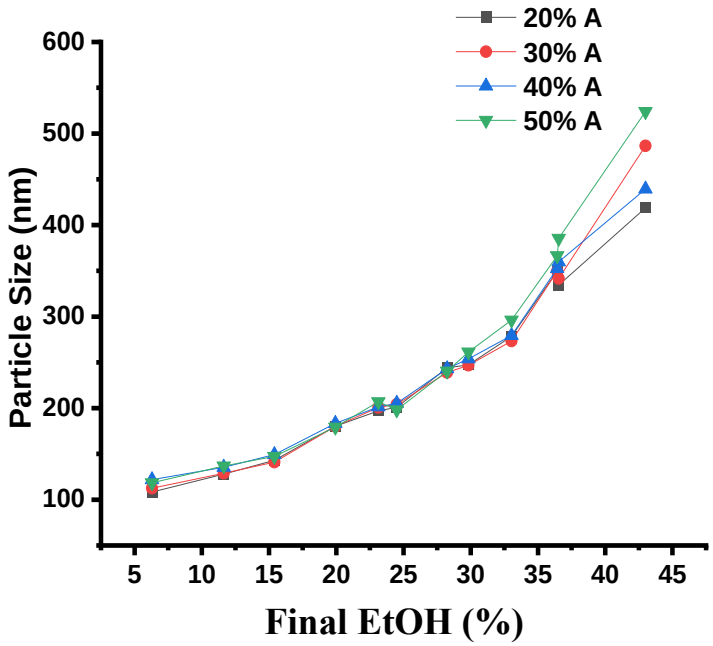

Fig 5.8 The effective diameter (a) and PDI (b) of zein nanoparticles in the various final concentration of ethanol in the zein nanoparticle suspensions.

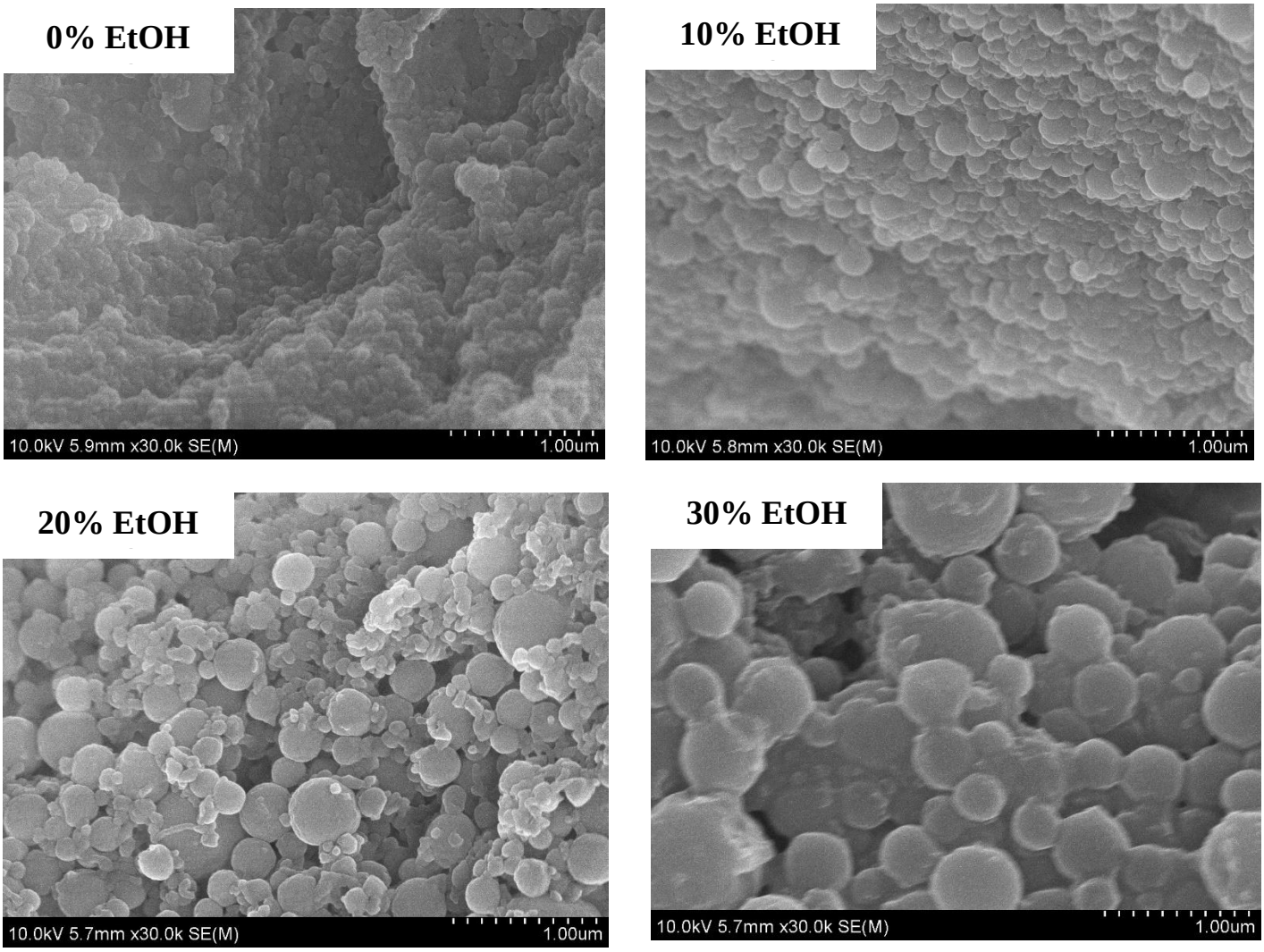

Fig 5.9 The diagram of the zein nanoparticles in the various concentration of ethanol solutions (Dispersed phase: Continuous phase = 1:2).

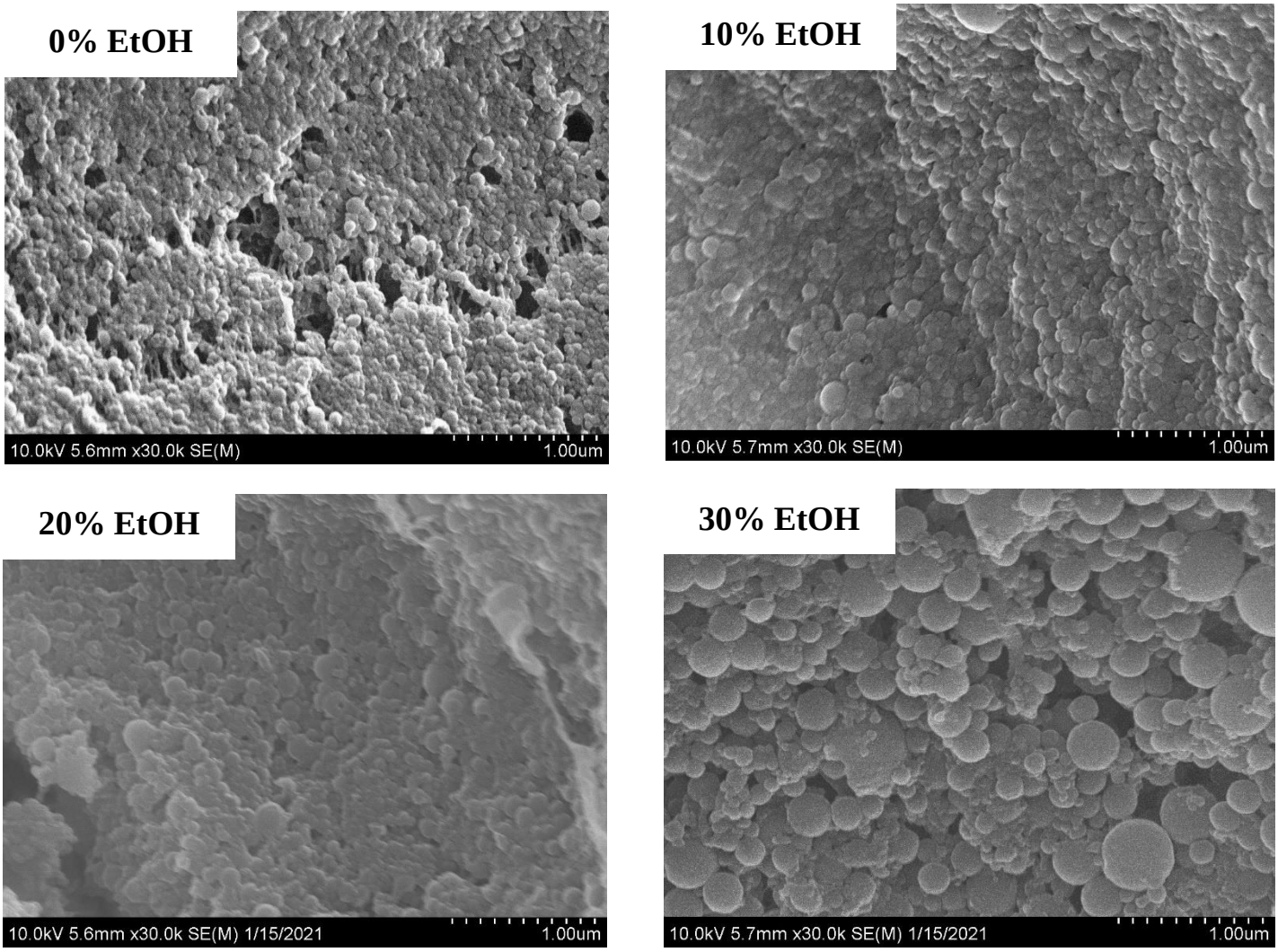

Fig 5.10 The diagram of the zein nanoparticles in the various concentration of ethanol solutions (Dispersed phase: Continuous phase = 1:5).

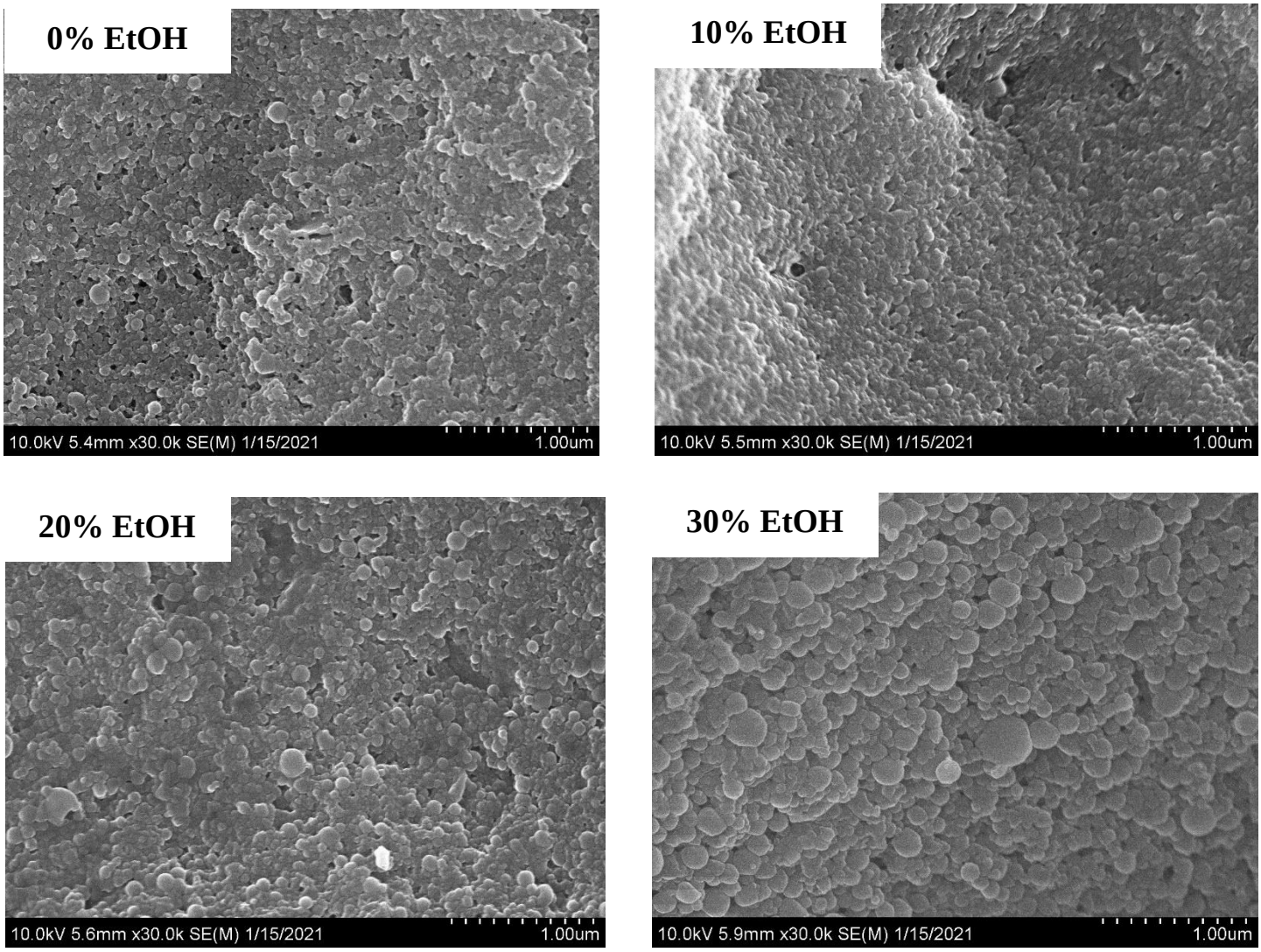

Fig 5.11 The diagram of the zein nanoparticles in the various concentration of ethanol solutions

(Dispersed phase: Continuous phase = 1:10).

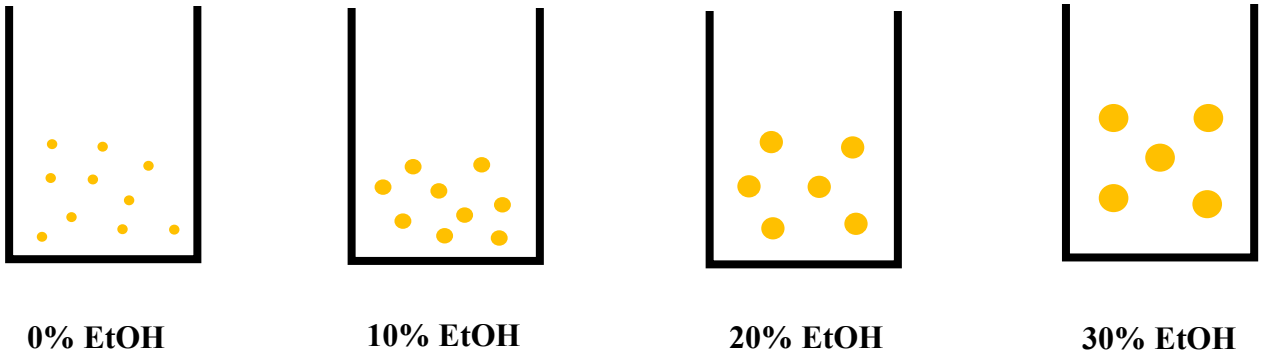

Fig 5.12 The diagram of the zein nanoparticles in the various concentration of ethanol solutions.

Table 5.3 The final composition of the zein, water, and ethanol in nanoparticle dispersion*.

Samples	Ethanol (%, w/v)	Zein (%, w/v)	Water (%, w/v)
0% EtOH-2% Zein-1:2	23.13	0.67	76.2
10% EtOH-2% Zein-1:2	29.83	0.67	69.5
20% EtOH-2% Zein-1:2	36.43	0.67	62.9
30% EtOH-2% Zein-1:2	43	0.67	56.33
0% EtOH-2% Zein-1:5	11.63	0.33	88.04
10% EtOH-2% Zein-1:5	19.93	0.33	79.74
20% EtOH-2% Zein-1:5	28.24	0.33	71.43
30% EtOH-2% Zein-1:5	36.54	0.33	63.13
0% EtOH-2% Zein-1:10	6.3	0.2	93.5
10% EtOH-2% Zein-1:10	15.4	0.2	84.4
20% EtOH-2% Zein-1:10	24.5	0.2	75.3
30% EtOH-2% Zein-1:10	33.03	0.2	66.77

*: 0% EtOH-2% Zein-1:2: 2% zein adding into 0% ethanol solution and the ratio of dispersed phase and continuous phased is 1:2.

5.7 References

Ashokkumar, M. (2015). Applications of ultrasound in food and bioprocessing. *Ultrasonics Sonochemistry*, *25*(1), 17–23. https://doi.org/10.1016/j.ultsonch.2014.08.012

Ba, C., Fu, Y., Niu, F., Wang, M., Jin, B., Li, Z., … Li, X. (2020). Effects of environmental stresses on physiochemical stability of β-carotene in zein-carboxymethyl chitosan-tea polyphenols ternary delivery system. *Food Chemistry*, *311*(November 2019), 125878. https://doi.org/10.1016/j.foodchem.2019.125878

Bhaskaracharya, R. K., Kentish, S., & Ashokkumar, M. (2009). Selected applications of ultrasonics in food processing. *Food Engineering Reviews*, *1*(1), 31–49. https://doi.org/10.1007/s12393-009-9003-7

Boufi, S., Bel Haaj, S., Magnin, A., Pignon, F., Impéror-Clerc, M., & Mortha, G. (2018). Ultrasonic assisted production of starch nanoparticles: Structural characterization and mechanism of disintegration. *Ultrasonics Sonochemistry*, *41*(May 2017), 327–336. https://doi.org/10.1016/j.ultsonch.2017.09.033

Cárcel, J. A., García-Pérez, J. V., Benedito, J., & Mulet, A. (2012). Food process innovation through new technologies: Use of ultrasound. *Journal of Food Engineering*, *110*(2), 200–207. https://doi.org/10.1016/j.jfoodeng.2011.05.038

Chandrapala, J., Oliver, C., Kentish, S., & Ashokkumar, M. (2012). Ultrasonics in food processing - Food quality assurance and food safety. *Trends in Food Science and Technology*, *26*(2), 88–98. https://doi.org/10.1016/j.tifs.2012.01.010

Chang, Y., Yan, X., Wang, Q., Ren, L., Tong, J., & Zhou, J. (2017). High efficiency and low cost preparation of size controlled starch nanoparticles through ultrasonic treatment and precipitation. *Food Chemistry*, *227*, 369–375.

https://doi.org/10.1016/j.foodchem.2017.01.111

Chemat, F., Rombaut, N., Meullemiestre, A., Turk, M., Perino, S., Fabiano-Tixier, A. S., & Abert-Vian, M. (2017). Review of Green Food Processing techniques. Preservation, transformation, and extraction. *Innovative Food Science and Emerging Technologies*, *41*(May), 357–377. https://doi.org/10.1016/j.ifset.2017.04.016

Chemat, F., Zill-E-Huma, & Khan, M. K. (2011). Applications of ultrasound in food technology: Processing, preservation and extraction. *Ultrasonics Sonochemistry*, *18*(4), 813–835. https://doi.org/10.1016/j.ultsonch.2010.11.023

Feng, X., Sun, Y., Yang, Y., Zhou, X., Cen, K., Yu, C., … Tang, X. (2020). Zein nanoparticle stabilized Pickering emulsion enriched with cinnamon oil and its effects on pound cakes. *Lwt*, *122*(January), 109025. https://doi.org/10.1016/j.lwt.2020.109025

Joye, I. J., & McClements, D. J. (2013). Production of nanoparticles by anti-solvent precipitation for use in food systems. *Trends in Food Science and Technology*, *34*(2), 109–123. https://doi.org/10.1016/j.tifs.2013.10.002

Kadam, S. U., Tiwari, B. K., Álvarez, C., & O'Donnell, C. P. (2015). Ultrasound applications for the extraction, identification and delivery of food proteins and bioactive peptides. *Trends in Food Science and Technology*, *46*(1), 60–67. https://doi.org/10.1016/j.tifs.2015.07.012

Kentish, S., & Feng, H. (2014). Applications of Power Ultrasound in Food Processing. *Annual Review of Food Science and Technology*, *5*(1), 263–284. https://doi.org/10.1146/annurev-food-030212-182537

Lawton, J. W. (2002). Zein: A history of processing and use. *Cereal Chemistry*, *79*(1), 1–18. https://doi.org/10.1094/CCHEM.2002.79.1.1

Li, H., Wang, D., Liu, C., Zhu, J., Fan, M., Sun, X., … Cao, Y. (2019). Fabrication of stable zein

nanoparticles coated with soluble soybean polysaccharide for encapsulation of quercetin. *Food Hydrocolloids*, *87*(August 2018), 342–351. https://doi.org/10.1016/j.foodhyd.2018.08.002

Minakawa, A. F. K., Faria-Tischer, P. C. S., & Mali, S. (2019). Simple ultrasound method to obtain starch micro- and nanoparticles from cassava, corn and yam starches. *Food Chemistry*, *283*(January), 11–18. https://doi.org/10.1016/j.foodchem.2019.01.015

Ojha, K. S., Mason, T. J., O'Donnell, C. P., Kerry, J. P., & Tiwari, B. K. (2017). Ultrasound technology for food fermentation applications. *Ultrasonics Sonochemistry*, *34*, 410–417. https://doi.org/10.1016/j.ultsonch.2016.06.001

Patel, A., Hu, Y., Tiwari, J. K., & Velikov, K. P. (2010). Synthesis and characterisation of zein-curcumin colloidal particles. *Soft Matter*, *6*(24), 6192–6199. https://doi.org/10.1039/c0sm00800a

Patel, A. R., & Velikov, K. P. (2014). Zein as a source of functional colloidal nano- and microstructures. *Current Opinion in Colloid and Interface Science*, *19*(5), 450–458. https://doi.org/10.1016/j.cocis.2014.08.001

Ren, X., Hou, T., Liang, Q., Zhang, X., Hu, D., Xu, B., … Ma, H. (2019). Effects of frequency ultrasound on the properties of zein-chitosan complex coacervation for resveratrol encapsulation. *Food Chemistry*, *279*(May 2018), 223–230. https://doi.org/10.1016/j.foodchem.2018.11.025

Shukla, R., & Cheryan, M. (2001). Zein: The industrial protein from corn. *Industrial Crops and Products*, *13*(3), 171–192. https://doi.org/10.1016/S0926-6690(00)00064-9

Sun, X., Pan, C., Ying, Z., Yu, D., Duan, X., Huang, F., … Ouyang, X. kun. (2020). Stabilization of zein nanoparticles with k-carrageenan and tween 80 for encapsulation of curcumin.

International Journal of Biological Macromolecules, *146*, 549–559. https://doi.org/10.1016/j.ijbiomac.2020.01.053

Tiwari, B. K. (2015). Ultrasound: A clean, green extraction technology. *TrAC - Trends in Analytical Chemistry*, *71*, 100–109. https://doi.org/10.1016/j.trac.2015.04.013

Wang, Y., & Padua, G. W. (2012). Nanoscale characterization of zein self-assembly. *Langmuir*, *28*(5), 2429–2435. https://doi.org/10.1021/la204204j

Zhang, H., Fu, Y., Xu, Y., Niu, F., Li, Z., Ba, C., … Li, X. (2019). One-step assembly of zein/caseinate/alginate nanoparticles for encapsulation and improved bioaccessibility of propolis. *Food and Function*, *10*(2), 635–645. https://doi.org/10.1039/c8fo01614c

Zhang, Yong, Cui, L., Li, F., Shi, N., Li, C., Yu, X., … Kong, W. (2016). Design, fabrication and biomedical applications of zein-based nano/micro-carrier systems. *International Journal of Pharmaceutics*, *513*(1–2), 191–210. https://doi.org/10.1016/j.ijpharm.2016.09.023

Zhang, Yuanhong, Zhou, F., Zhao, M., Lin, L., Ning, Z., & Sun, B. (2018). Soy peptide nanoparticles by ultrasound-induced self-assembly of large peptide aggregates and their role on emulsion stability. *Food Hydrocolloids*, *74*, 62–71. https://doi.org/10.1016/j.foodhyd.2017.07.021

CHAPTER 6: Encapsulation of curcumin in zein nanoparticles via ultrasonic treatment

6.1 Abstract

Zein is the prolamine that is extracted from corn. Zein can be used as a food delivery system to encapsulate bioactive compounds due to its anti-solvent precipitation properties. Curcumin is a natural bioactive polyphenolic compound that has the health benefits for humans, such as antioxidant, antimicrobial, and anticancer properties. However, curcumin has low water solubility and sensitive to heat and light. The objective of this study was to encapsulate curcumin into the zein nanoparticles via ultrasonic treatment to increase the stability of curcumin.

Zein-curcumin nanoparticles were fabricated by ultrasonic treatment with four different initial ethanol concentration (0%, 10%, 20%, and 30%) in the continuous phase, the ratio of the dispersed phase to continuous was 1:5, and three different ultrasound amplitude (0%, 20%, and 50%). The particle size, polydispersity index, encapsulation efficiency, loading capacity, thermal stability, photostability, and XRD of zein nanoparticles encapsulated curcumin were analyzed. The results showed that as the concentration of ethanol increased, the particle size increased. Compared with the shearing treatment, the ultrasonic treatment group had a higher encapsulation efficiency and loading capacity. In addition, the encapsulated curcumin was more stable toward heat and light than free curcumin. The findings of this research proved that the encapsulation of bioactive compounds such as curcumin is possible using ultrasound treatment and the properties of nanoparticles can be controlled.

Keywords zein nanoparticles, curcumin, stability, ultrasonic treatment

6.2 Introduction

Curcumin is a natural polyphenolic compound that is extracted from *curcuma longa* (Artiga-Artigas, Lanjari-Pérez, & Martín-Belloso, 2018; Ubeyitogullari & Ciftci, 2019). *Curcuma longa* contains 3-5% curcuminoids (consisting of 77% curcumin, 17% demethoxycurcumin, 3% bisdemethoxycurcumin, and 3% cyclocurcumin) (Araiza-Calahorra, Akhtar, & Sarkar, 2018). As the majority component of curcuminoids in *curcuma longa*, curcumin is a yellowish powder with a high order crystal structure, including monoclinic, orthorhombic, and amorphous structures (Thorat & Dalvi, 2014). Curcumin exists in the equilibrium between keto and enol form under the different environments. The health benefits of curcumin are widely acknowledged, such as antioxidant, antimicrobial, and anticancer properties. However, curcumin has a limitation for application because of biochemical/structural degradation due to some external environmental factors such as light and high temperature (Artiga-Artigas et al., 2018). In addition, curcumin has a low bioavailability because of its high degree of crystallinity and low water solubility (Ubeyitogullari & Ciftci, 2019). To overcome these limitations, various delivery systems can be used to carry curcumin, such as oil-in-water (O/W) emulsions, Pickering emulsions, and nanoemulsions (Chang, Wang, Hu, & Luo, 2017; Chen, Han, et al., 2020; Chen et al., 2018; Dai et al., 2018; Silva et al., 2018; Ubeyitogullari & Ciftci, 2019). Among these delivery systems, nanoparticles have received increasing attention in the food industry for applications such as food packaging, sensor, and encapsulation. Nanoparticles are nanometer-sized (1 nm to 1 μm) ultrafine particles with unique properties due to their large surface area. The anti-solvent precipitation is an attractive technology to form nanoparticles for a delivery system because of the low-energy and well-controlled environment.

Zein is the prolamine corn storage protein and more than 50% of amino acids are hydrophobic including alanine, proline, and leucine (Shukla & Cheryan, 2001). Zein particles can be fabricated using anti-solvent precipitation from 55%-95% (v/v) ethanol to a low concentration of ethanol or water because of its solubility differences (H. Zhang et al., 2019). The stability of zein nanoparticles is affected by alcohol type, surface chemistry, and structure, mixing methods (Y. Zhang et al., 2016), and the initial concentration of ethanol in the continuous phase. Many lipophilic bioactive compounds can be encapsulated into zein nanoparticles, including β-carotene (Ba et al., 2020), resveratrol (Khan et al., 2019), luteolin (Shinde, Agraval, Singh, Yadav, & Kumar, 2019) by stirring zein suspension during anti-solvent precipitation processes. However, to date, few studies have been reported using the different initial concentrations of ethanol in the continuous phase and mixing methods to increase the stability of zein nanoparticles. So, in this study, the various initial concentration of ethanol in the continuous phase and the amplitude of ultrasound waves were used to fabricate zein nanoparticles.

Ultrasound is an emerging and non-thermal technology. In the food industry, ultrasound has been used for bio-compounds extraction, food quality assurance, viscosity modification, emulsification, surface cleaning for many years. Besides that, the ultrasound can be used as a mixing method to assist nanoparticle formation, such as starch nanoparticles (Minakawa, Faria-Tischer, & Mali, 2019) and protein nanoparticles (Ren et al., 2019). The results showed that ultrasonic treatment decreased the viscosity and molecular weight of starch and increased the stability of the protein nanoparticles.

In this study, zein nanoparticles were fabricated at different initial concentrations of ethanol (0%, 10%, 20%, and 30%) in the continuous via ultrasonic treatment with different amplitude (20%,

50%) to encapsulate curcumin. It was hypothesized that the ultrasonic treatment would increase the stability of zein nanoparticles and increased the encapsulation efficiency of curcumin.

6.3 Materials and methods

6.3.1 Materials

Zein (purified) was purchased from Sigma–Aldrich (St. Louis, MO). Ethanol (200 proof) was purchased from Decon Labs (King of Prussia, PA) and curcumin (98+% curcumin) was purchased from Fisher Scientific (Pittsburgh, PA).

6.3.2 Sample preparation and characterization of nanoparticles

The zein-curcumin nanoparticles were prepared by ultrasonic treatment and stirring treatment. The continuous phase with an ethanol concentration of 0%, 10 %, 20%, and 30% was prepared and the pH was adjusted to 3. Two grams of zein and one hundred milligrams of curcumin were dissolved into 100 ml of 70% ethanol stirring overnight to reach 2% w/w of zein. The mass ratio of zein and curcumin was 20:1. Six milliliters of the zein-curcumin solution were dropped into 30 ml of 0% (deionized water), 10%, 20%, and 30% ethanol using a 20 ml syringe and a syringe pump (Harvard Apparatus, Holliston, MA). The flow rate was 0.6 mL/min and the ultrasound amplitude setting was 20% and 50%. The ratio of dispersed to continuous was 1:5. A needle (23G: 0.6 mm×25 mm) was located directly above the center of a 100 mL beaker. In addition, for the stirring treatment, the same volume (6 mL) of the zein-curcumin solution was dropped into 30 mL of deionized (DI) water at the 600-rpm stirring rate on a stirring plate (MIX 15 eco model, 2Mag magnetic eMotion). The zein-curcumin particle suspensions were placed into a rotary evaporator (Heidolph 2-Collegiate, Germany) at 40 ℃ for 10 min to remove the remained ethanol in the zein-curcumin nanoparticles suspension.

Particle size and polydispersity index determination

The samples were diluted at 1:40 using deionized (DI) water and the effective diameter was measured by a Dynamic Light Scattering (DLS) particle size analyzer (Brookhaven Instruments, Holtsville, NY). The effective diameters were reported as the surface average diameter ($D_{3,2}$) and the equation was expressed as follow:

$$D_{3,2} = \frac{\Sigma nidi^3}{\Sigma nidi^2} \qquad (1)$$

where ni is the number of particles with diameter di. The three replicated readings were taken for each sample and the average was calculated. The polydispersity index (PDI) was also collected by the DLS and three replicated readings were averaged.

Scanning electron microscopy

Zein nanoparticles were prepared via ultrasonic treatment at 20% amplitude with different concentrations of ethanol (0%, 10%, 20%, and 30%) and stirring treatment (600 rpm). Freshly prepared nanoparticle suspensions were converted into a powder using freeze-drying. The dried nanoparticles were imaged using scanning electron microscopy with an acceleration potential of 10 kV using a high vacuum mode. A layer of gold coating (15 nm) was applied to the mounted sample before analysis.

The encapsulation efficiency and loading capacity of curcumin in the zein nanoparticles

For separating the encapsulated curcumin and the free curcumin, the nanoparticle dispersions were centrifuged at 10,000 rpm for 60 min (IEC Centra CL2, Thermo Scientific Co., Waltham, MA). Then the supernatants were collected and diluted 10 times using the 70% ethanol solution to measure free curcumin. The content of the free curcumin was measured by a spectrophotometer (Genesys5, Thermo Scientific Co., Waltham, MA) using absorbance at 426 nm. The total amount of curcumin was 100 mg, which was added to the zein solution. The equation of encapsulation efficiency was expressed as follow:

$$\text{EE (\%)} = \frac{Encapsulated\ curcumin\ (mg)}{Total\ amount\ of\ the\ curcumin\ (mg)} * 100 = \frac{Total\ amount\ of\ the\ curcumin\ (mg) - Free\ curcumin\ (mg)}{Total\ amount\ of\ the\ curcumin\ (mg)} * 100 \quad (2)$$

The equation of loading capacity was expressed as follow:

$$\text{LC (\%)} = \frac{Encapsulated\ curcumin}{Total\ mass\ of\ nanoparticles} * 100 = \frac{Total\ amount\ of\ the\ curcumin\ (mg) - Free\ curcumin\ (mg)}{Total\ mass\ of\ nanoparticles} * 100 \quad (3)$$

Thermal stability

Five milliliters of freshly prepared zein-curcumin nanoparticle suspension and free curcumin were placed into 15 mL centrifuged tubes and incubated in a water bath at 63 °C for 30 min then cooled down to room temperature immediately. 300 µL of nanocapsule suspension was mixed with 700 µL of 100% ethanol to disrupt nanocapsules and release curcumin. The quantity of curcumin was determined by spectrophotometer as described before.

Photostability

Two milliliters of freshly prepared zein-curcumin nanoparticle suspensions and free curcumin were placed into UV lightbox for 30 min, 60 min, 90 min and cool down to room temperature. 300 µL of nanocapsule suspension was mixed with 700 µL of 100% ethanol to disrupt nanocapsules and release curcumin. The quantity of curcumin was determined by spectrophotometer as described before.

DPPH· scavenging capacity

Two milliliters of a 100 µM DPPH· ethanol solution were mixed with equivalent volume aliquots of encapsulated curcumin, ethanol-dissolved free curcumin, and 70% ethanol solution. The mixture was incubated at room temperature in the dark. After 30min, the absorbance of the reaction solution was measured at 517nm. The free radical scavenging activity was calculated by the equation as follows:

$$\text{DPPH· Scavenging (\%)} = \frac{(A_{S1} - A_{S2})}{A_c} \times 100\% \quad (4)$$

where A_c is the absorbance of the control (DPPH· mixed with ethanol), A_{s1}, A_{s2} is the absorbance of the sample before and after incubated at room temperature in the dark, respectively.

X-Ray Diffraction

Freshly prepared nanoparticle suspensions were converted into a powder using freeze-drying. X-ray powder diffraction patterns (XRD) were obtained using an X-ray diffractometer (Brucker D8, Odelzhausen, Germany) based with a rotating Cu anode operating at 1200 W. The X-ray intensity covered from 5.0° to 40.0° as a function of the 2θ angle.

Statistical analysis

All the experimental results were conducted in triplicate. The results were expressed as mean ± standard deviation (n=3). The significant differences of the results among the different treatments were assessed by one-way ANOVA ($P< 0.5$), and the averages were compared using Tukey's test.

6.4 Results and Discussion

Particle size and polydispersity index (PDI) determination

The pictures of zein-curcumin nanoparticles with different ratios of the continuous phase and dispersed phase and different concentrations of ethanol (0%, 10%, 20%, and 30%) were shown in Fig 6.1. And as the concentration of ethanol increased, the zein curcumin nanoparticles were closer to the solution phase.

The particle size and PDI of the zein-curcumin nanoparticles with the different initial ethanol concentrations in the continuous phase are presented in Fig 6.2. The particle size ranged from 100 nm to 450 nm and the ultrasound treatment resulted in smaller particle sizes than the stirring treatment. As the concentration of the initial concentration of ethanol in the continuous phase increased, the particle size of zein-curcumin nanoparticles increased with both mixing methods: ultrasound and stirring. The particle size showed similar ranged and trends with the zein

nanoparticles without curcumin in them (Chapter 5). For the PDI, in the ultrasonic treatment, as the concentration of ethanol increased, the PDI increased and then decreased, but in the stirring treatment, the PDI showed a different trend: decreased and then increased. The results indicated that the zein self-assembly kinetics between the ultrasonic treatment and stirring were different. Compared with the PDI results, ranged from 0.1 to 0.3, from Chapter 5 for only zein nanoparticles, the PDI for the zein curcumin nanoparticles increased to the range from 0.24 to 0.35. The difference indicates that the zein self-assembly kinetics was altered by the inclusion of curcumin. Compared with the only zein, the zein curcumin nanoparticle formation may be slowed down due to the presence of curcumin. The crtical ethaol concentration for self assembly of zein proposed in Chapter 5 was not clear from the PDI results, however it may be apparent from the encapsulation efficiency and curcumin loading results which to be discussed next

Scanning electron microscopy

The SEM pictures of zein curcumin nanoparticles with the different initial ethanol concentrations (0%, 10%, 20%, and 30%), 20% amplitude ultrasonic treatment, and stirring treatment were shown in Fig 6.3 and Fig 6.4. For both treatments, as the initial concentration of ethanol increased, the particle size of the zein curcumin nanoparticles increased. These findings were consistent with the findings in Chapter 5. As the initial concentration of ethanol increased, the degree of supersaturation decreased, and the radius of zein nanoparticles increased.

The encapsulation efficiency

The standard curve of curcumin concentration in ethanol was showed in Fig 6.5. As the concentration of curcumin increased, the absorbance at 517 nm increased. In addition, the standard curve equation was:

$$Y= 0.15796X-0.00354$$

Where Y is absorbance and X is the concentration of curcumin in the ethanol. And the R^2 of this standard curve is 0.99993. The encapsulation efficiency of curcumin in the zein nanoparticles with the different amplitude (20% and 50%) of ultrasonic treatment and different initial concentrations of ethanol (0%, 10%, 20%, and 30%) in the continuous phase were shown in Fig 6.6. As the initial concentration of ethanol increased, the encapsulation efficiency increased and then decreased. The particle size of zein-curcumin nanoparticles increased as the initial concentration of ethanol increased and more space for the curcumin to be encapsulated. However, for the 30% ethanol treatment, the final ethanol concentration reached around 36% and the zein-curcumin nanoparticles were close to the boundary of solution and coacervation as showed in Fig 6.7. The final ethanol concentration of 36% was greater than the critical ethanol concentration of 28% proposed in Chapter 5. The ethanol concentration was close to the solution condition of zein, zein was not able to encapsulate curcumin effectively. Compared with the stirring treatment sampled, the ultrasonic treatment samples had a significantly higher encapsulation efficiency.

Loading capacity

The loading capacity of curcumin in the zein nanoparticles with different amplitude (20% and 50%) ultrasonic treatment and different concentrations of ethanol are shown in Fig 6.8. As the concentration of ethanol increased, the loading capacity increased and then decreased. It showed a similar trend with the initial ethanol concentration as the encapsulation efficiency and indicated the presence of the critical ethanol concentration. The theoretical loading capacity is 4.67% and the maximum loading capacity reached 4%. Compared with the stirring treatment samples, the ultrasonic treatment samples had a significantly higher loading capacity.

Thermal stability

The thermal stability of curcumin at 63℃ for 30 min was shown in Fig 6.9. After the heat treatment, free curcumin remained about 83% and the encapsulated curcumin was saved almost all, close to 1005. There were no significant differences in the retention of the encapsulated curcumin with the different amplitude (20% and 50%) and different initial concentrations of ethanol (0%, 10%, 20%, and 30%). The results can be explained by the zein nanoparticles encapsulation. The free curcumin is heat sensitive and easily degraded under external environmental stress such as high temperature. However, when the free curcumin is encapsulated into the zein nanoparticles, a self-assembled zein matrix can protect curcumin against adverse environmental factors.

Photostability

The photostability of curcumin under UV light treatment for 30 min, 60 min, and 90 min was shown in Fig 6.10. As the treatment time increased, the retention of curcumin decreased for all the samples. The photo-degradation of curcumin in the organic solvent has been reported with the different degradation products (Priyadarsini, 2009). Compared with the free curcumin, all of the curcumin encapsulated in the zein nanoparticles had a significantly higher retention rate. The retention rate of curcumin in the zein nanoparticles was increased and then decreased with the increase of the initial ethanol concentration. In addition, compared with the stirring treatment group, the ultrasonic treatment retained more curcumin against UV irradiation. After 90 min of UV treatment, more than 60% of curcumin was retained in the zein nanoparticles with the 0%, 10%, and 20% ethanol with 20% and 50% amplitude as compared to around 20% retention for free curcumin, stirring treatment and ultrasonic treatment with 30% initial ethanol concentration., The encapsulated curcumin has a higher retention rate than free curcumin because the double bonds and aromatic side groups in zein nanoparticles can absorb UV light (Dai et al., 2017). Compared

with the stirring treatment samples, the formation of zein curcumin nanoparticles via ultrasonic treatment can be well controlled and lead to more stable nanoparticles and a higher retention rate of curcumin.

DPPH· scavenging capacity

The DPPH· scavenging capacity of free curcumin and the encapsulated curcumin in the zein nanoparticles with different treatments were shown in Fig 6.11. As the initial concentration of ethanol increased, the DPPH· scavenging capacity increased and then decreased both in the ultrasonic treatment and stirring treatment groups. The DPPH· is a stable radical, which absorbs at 517 nm, but the absorption will decrease by the addition of antioxidants (Ak & Gülçin, 2008). As the initial concentration of ethanol increased, the encapsulation efficiency of curcumin in the zein nanoparticles increased and then decreased. These findings indicate that the encapsulated curcumin was more efficient to scavenge DPPH· than free curcumin in the ethanol solution which is in good agreement with a previous study (Huang et al., 2016).

X-Ray Diffraction

The crystalline diffraction patterns of zein, free curcumin, zein-curcumin nanoparticles, and the physical mixture of zein and curcumin are shown in Fig 6.12. Zein had two flat peaks at diffraction angles 2θ of 8.97° and 19.47°, indicating the amorphous nature of the protein, which is in good agreement with the previous studies (Chen, Li, et al., 2020; Khan et al., 2019; Wei et al., 2019). Pure curcumin was in a highly crystallized state and had several sharp diffraction peaks at 2θ from 5° to 40° as reported previously (Dai et al., 2017). The physical mixture (dry blend) of zein and curcumin showed X-ray diffraction patterns with sharp peaks, which appeared at the same diffraction angle from 5° to 40° as the free curcumin. However, there were no typical diffraction peaks belongs to the free curcumin in the zein-curcumin nanoparticles indicating that the curcumin

was encapsulated in the zein nanoparticles and lost its crystallinity. Due to its low water solubility and crystalline structure, the bioavailability of curcumin is very low (Ubeyitogullari & Ciftci, 2019). The zein-curcumin nanoparticles altered the physical state of curcumin from a crystallized state to an amorphous state, which can increase the bioavailability of curcumin.

6.5 Conclusions

In this study, curcumin encapsulated in the zein nanoparticles were fabricated by ultrasonic treatment and stirring treatment with the different initial concentration of ethanol (0%, 10%, 20%, and 30%) in a continuous phase. The properties of zein curcumin nanoparticles were characterized by particle size, polydispersity index, SEM, photo- and thermal-stability, XRD, encapsulation efficiency, loading capacity, and DPPH· scavenging capacity. The results showed that as the initial concentration of ethanol increased, the particle size of zein-curcumin nanoparticles increased, the encapsulation efficiency and loading capacity increased, and then decreased, which indicated the presence of the critical ethanol concentration. The zein matrix was able to protect the encapsulated curcumin from degradation against heat and UV light. The physical state of curcumin was altered from crystalline to amorphous by the encapsulation of the zein nanoparticles. These findings can be used to improve the encapsulation of curcumin in zein nanoparticles for a delivery system.

6.6 Tables and figures

Fig 6.1 The pictures of the encapsulated curcumin in the zein nanoparticles via ultrasonic treatment with various ethanol concentrations and dispersed: continuous phase ratio at the 20% amplitude (Dispersed phase: Continuous phase = 1:5).

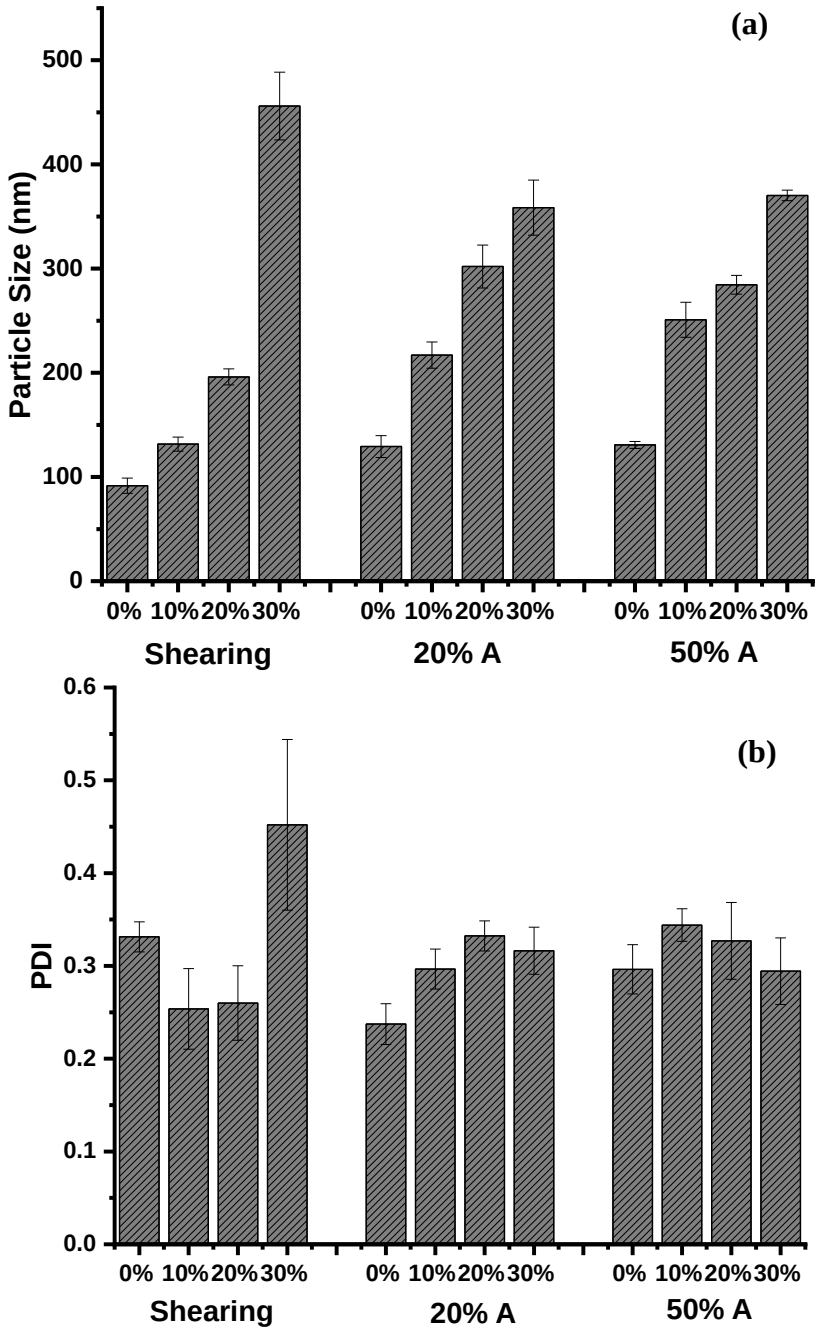

Fig 6.2 The effective diameter (a) and PDI (b) of curcumin-encapsulated zein nanoparticles with various concentrations of ethanol, amplitude (Dispersed phase: Continuous phase = 1:5).

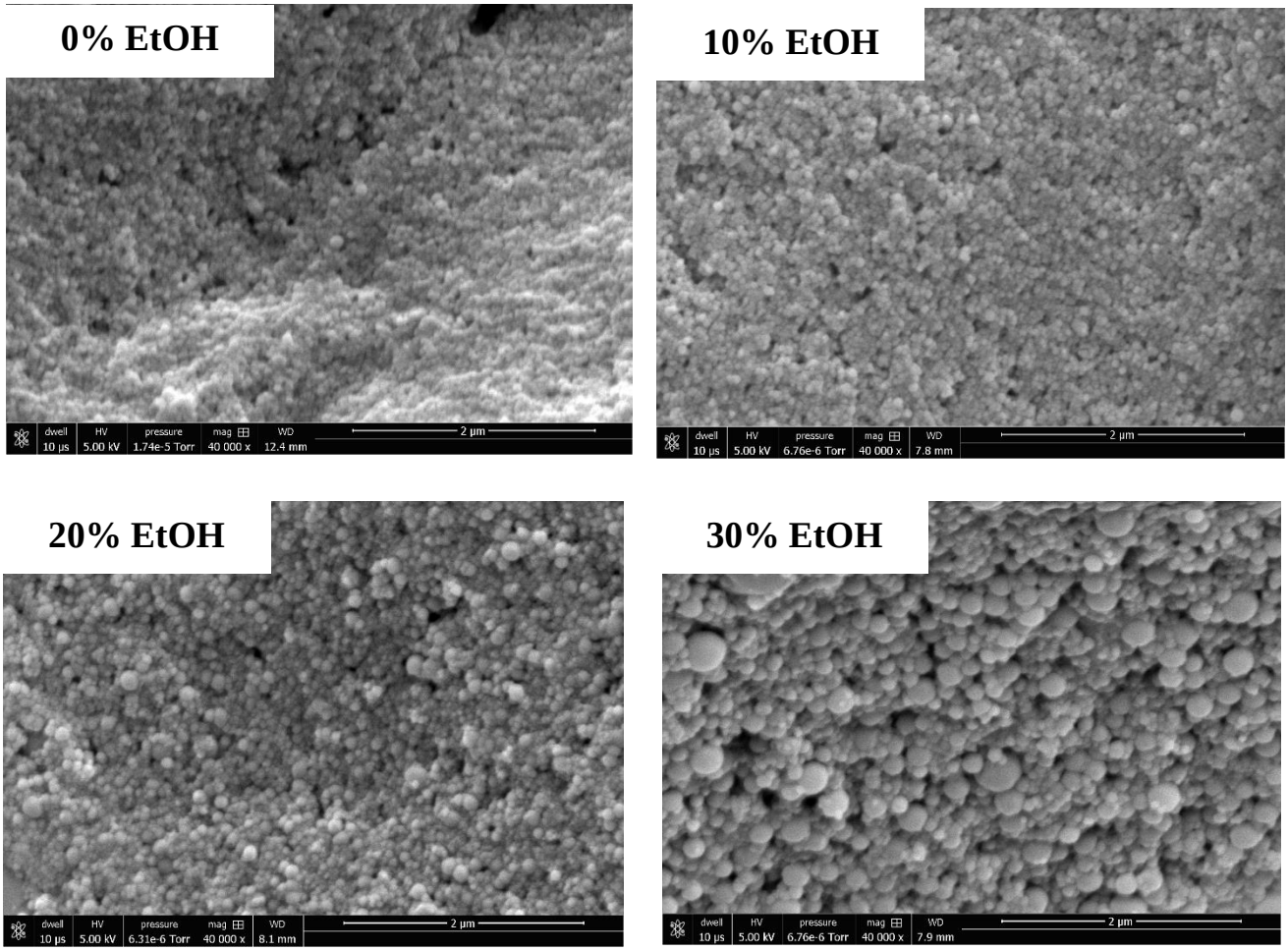

Fig 6.3 The SEM diagram of the zein curcumin nanoparticles in the various concentration of ethanol solutions via shearing treatment (Dispersed phase: Continuous phase = 1:5).

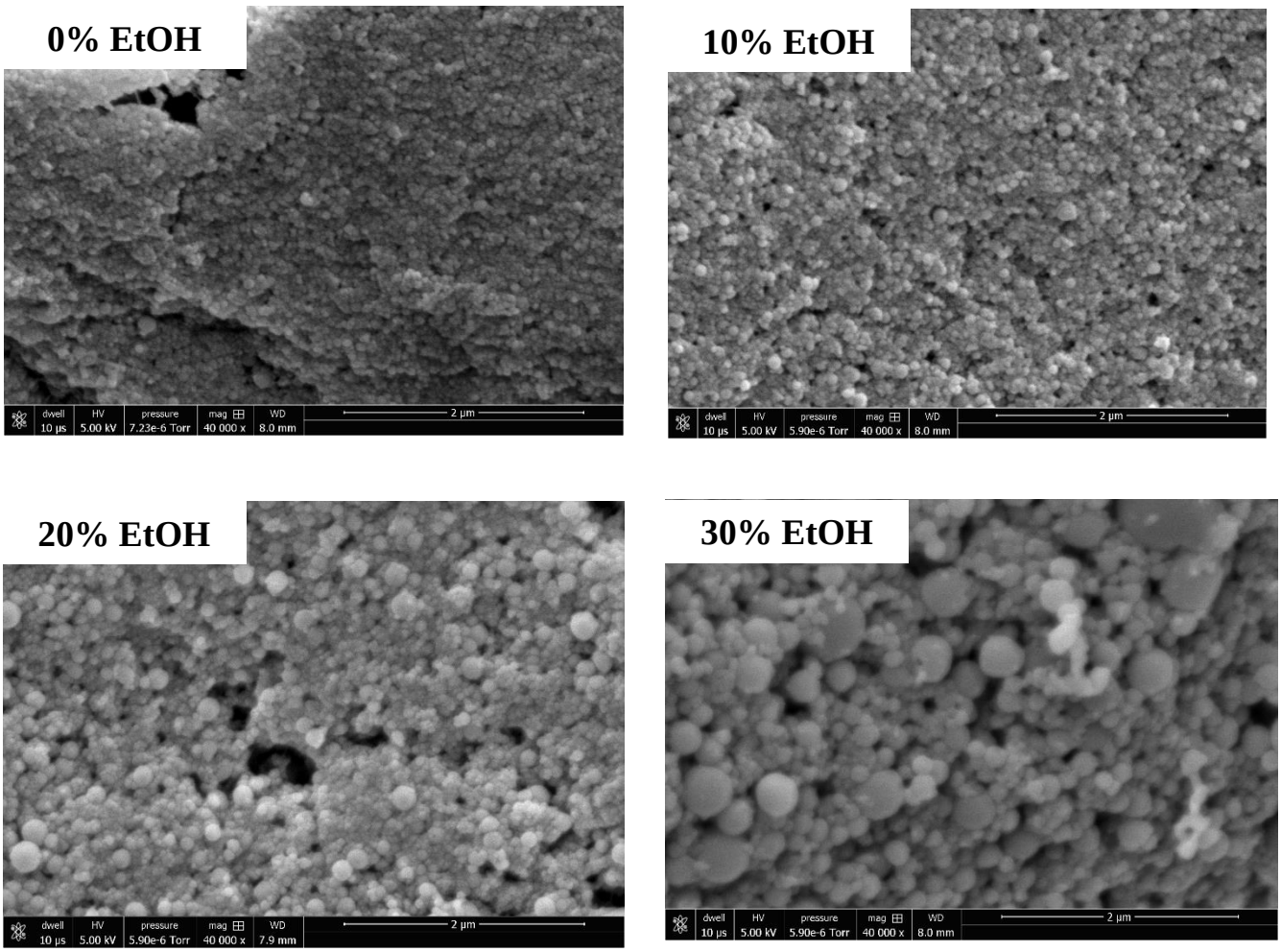

Fig 6.4 The SEM diagram of the zein curcumin nanoparticles in the various concentration of ethanol solutions via ultrasonic treatment at 20 % amplitude (Dispersed phase: Continuous phase = 1:5).

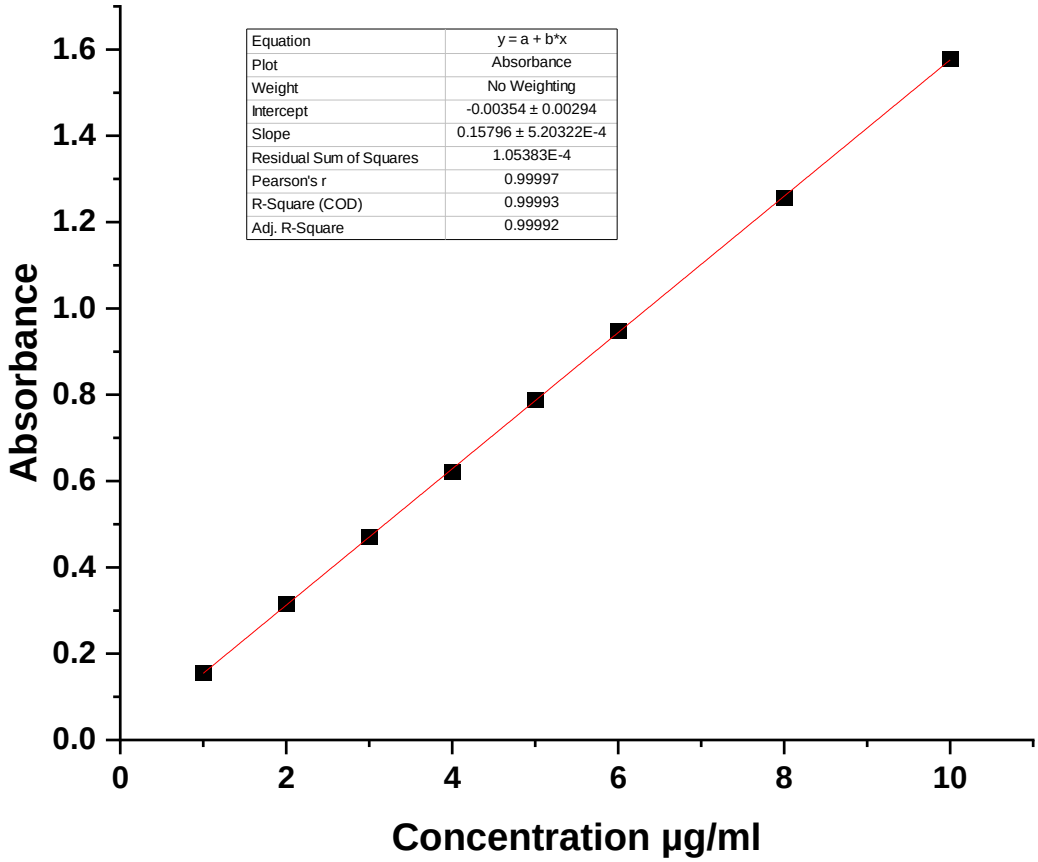

Fig 6.5 The standard curve of curcumin in 70% ethanol solution.

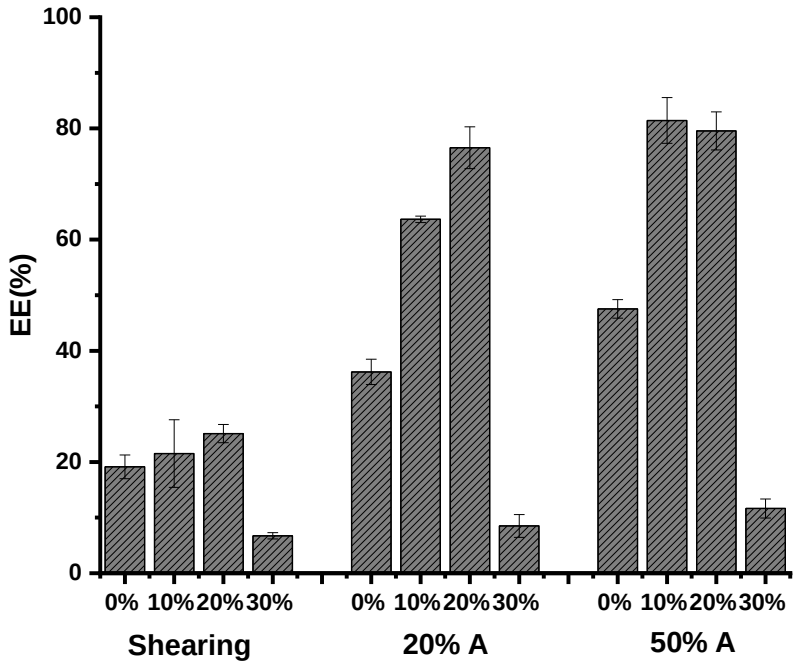

Fig 6.6 The encapsulation efficiency of curcumin in zein nanoparticles with various concentrations of ethanol, amplitude (Dispersed phase: Continuous phase = 1:5).

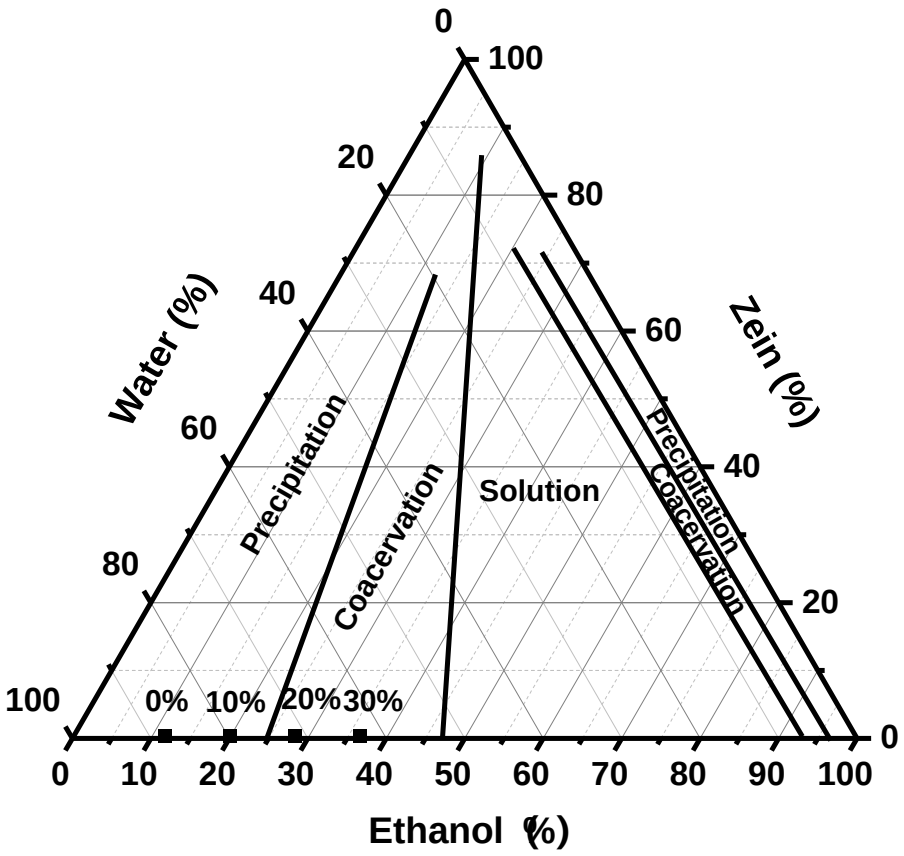

Fig 6.7 The ternary diagram of zein nanoparticles in the water and ethanol solution with the different treatments (different concentrations of ethanol and different ratio of the dispersed phase and continuous phase).

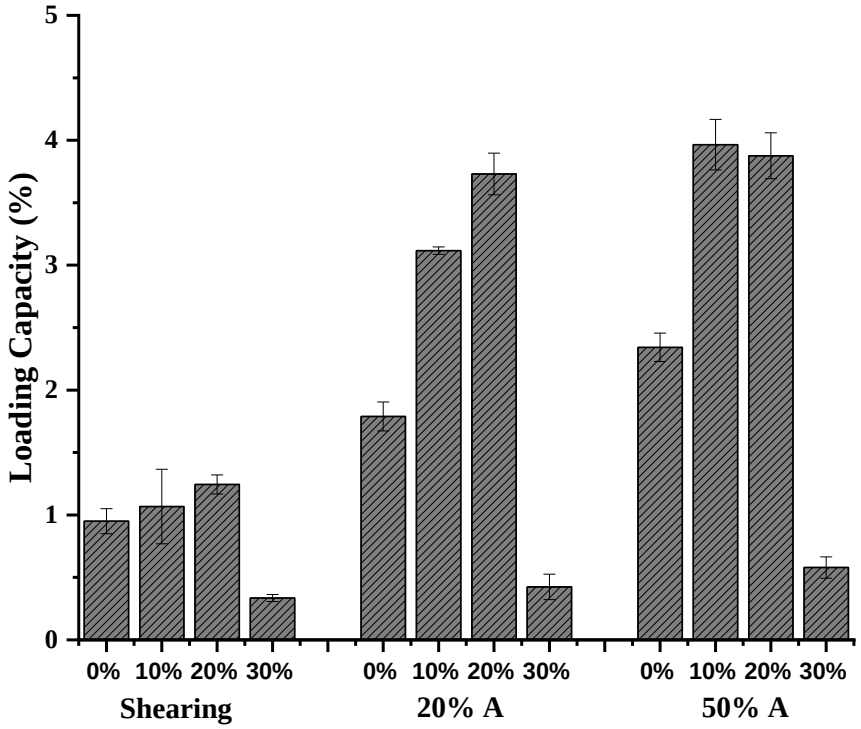

Fig 6.8 The loading capacity of curcumin in zein nanoparticles with various concentrations of ethanol, amplitude (Dispersed phase: Continuous phase = 1:5).

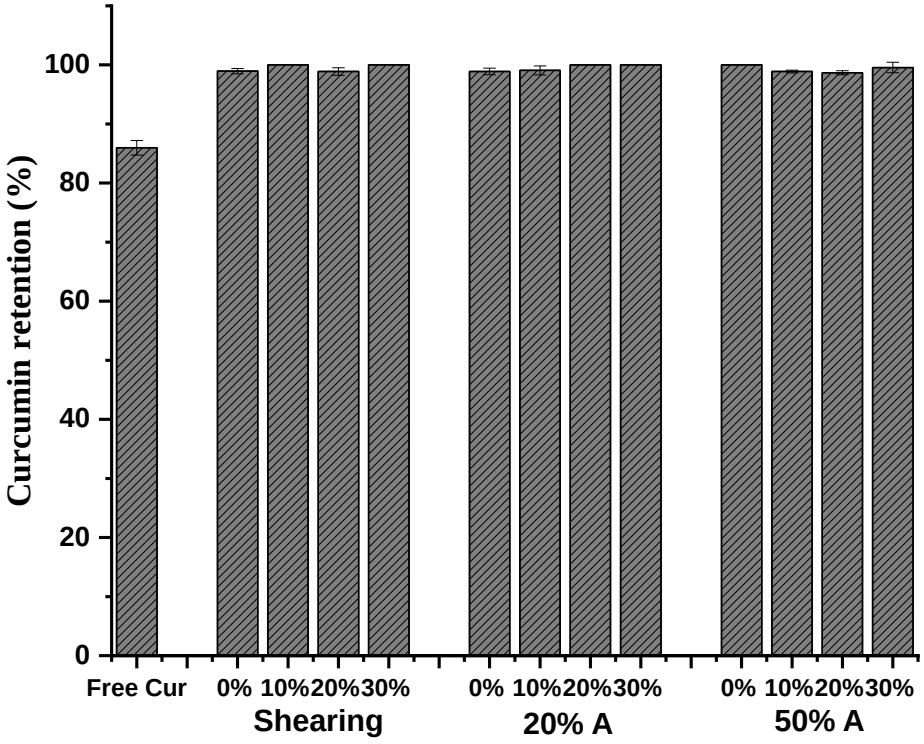

Fig 6.9 The thermal stability of curcumin in zein nanoparticles with various concentrations of ethanol and amplitude at 63 ℃, 30 min (Dispersed phase: Continuous phase = 1:5).

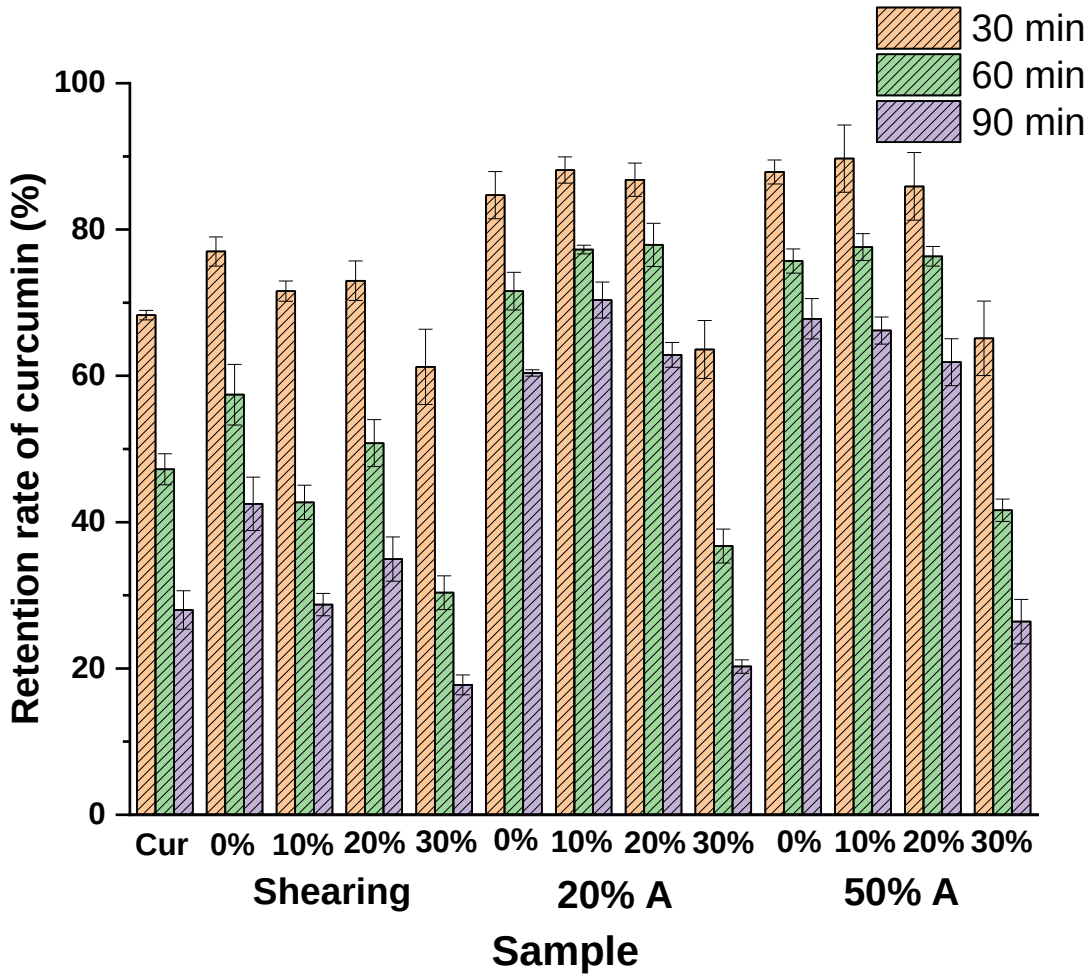

Fig 6.10 The photostability of curcumin in zein nanoparticles with various concentrations of ethanol and amplitude at UV light treatment 30, 60, and 90 min (Dispersed phase: Continuous phase = 1:5).

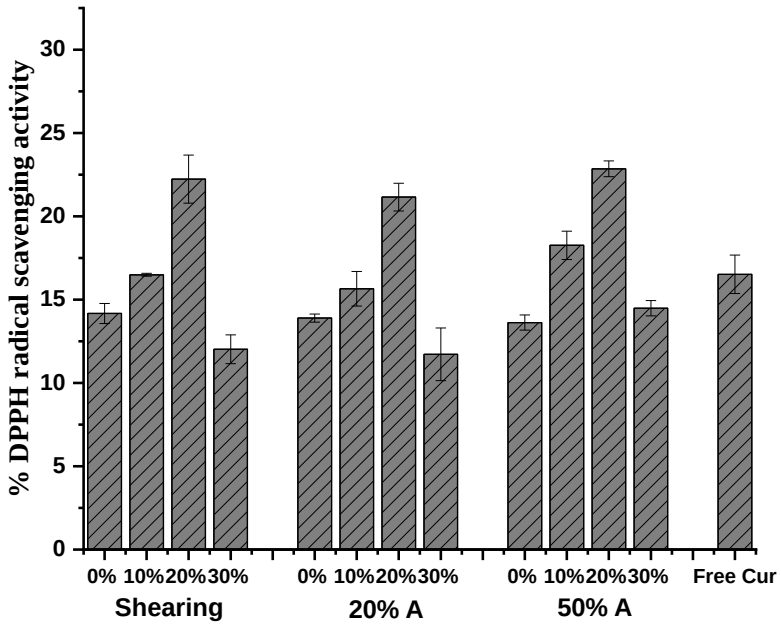

Fig 6.11 The DPPH radical scavenging activity of curcumin in zein nanoparticles with various concentrations of ethanol, amplitude (Dispersed phase: Continuous phase = 1:5).

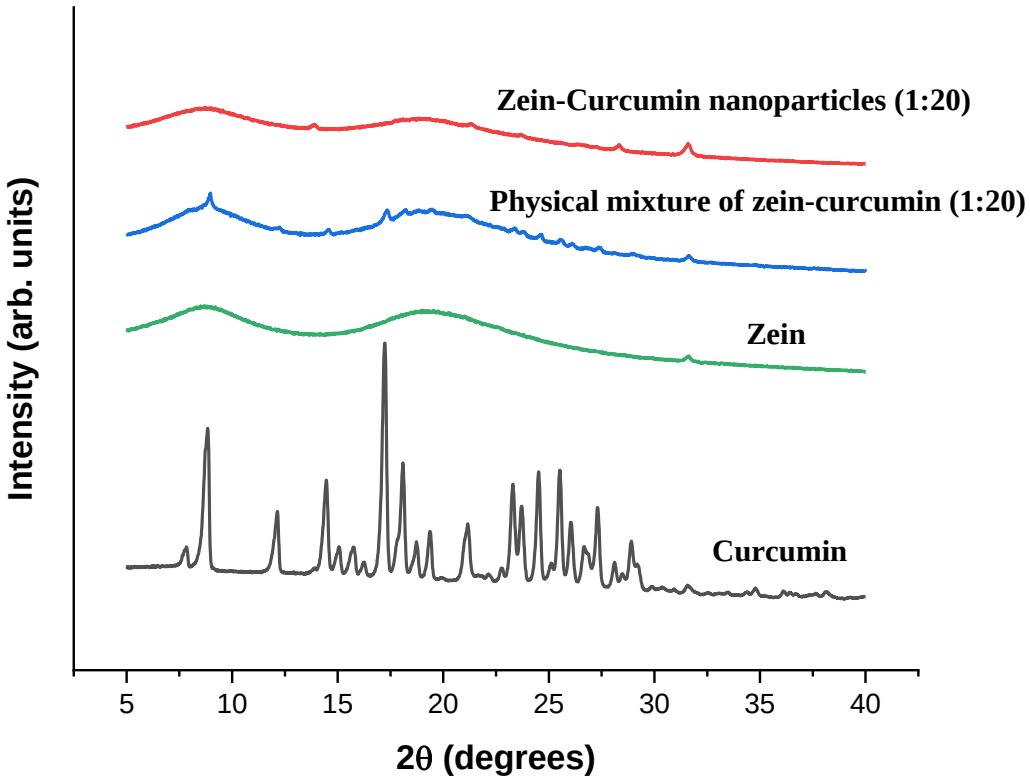

Fig 6.12 The X-ray diffraction graphs of zein, free curcumin, zein-curcumin nanoparticles, and physical mixture of zein-curcumin.

6.7 References

Ak, T., & Gülçin, I. (2008). Antioxidant and radical scavenging properties of curcumin. *Chemico-Biological Interactions*, *174*(1), 27–37. https://doi.org/10.1016/j.cbi.2008.05.003

Araiza-Calahorra, A., Akhtar, M., & Sarkar, A. (2018). Recent advances in emulsion-based delivery approaches for curcumin: From encapsulation to bioaccessibility. *Trends in Food Science and Technology*, *71*(July 2017), 155–169. https://doi.org/10.1016/j.tifs.2017.11.009

Artiga-Artigas, M., Lanjari-Pérez, Y., & Martín-Belloso, O. (2018). Curcumin-loaded nanoemulsions stability as affected by the nature and concentration of surfactant. *Food Chemistry*, *266*(June), 466–474. https://doi.org/10.1016/j.foodchem.2018.06.043

Ba, C., Fu, Y., Niu, F., Wang, M., Jin, B., Li, Z., … Li, X. (2020). Effects of environmental stresses on physiochemical stability of β-carotene in zein-carboxymethyl chitosan-tea polyphenols ternary delivery system. *Food Chemistry*, *311*(November 2019), 125878. https://doi.org/10.1016/j.foodchem.2019.125878

Chang, C., Wang, T., Hu, Q., & Luo, Y. (2017). Caseinate-zein-polysaccharide complex nanoparticles as potential oral delivery vehicles for curcumin: Effect of polysaccharide type and chemical cross-linking. *Food Hydrocolloids*, *72*, 254–262. https://doi.org/10.1016/j.foodhyd.2017.05.039

Chen, S., Han, Y., Jian, L., Liao, W., Zhang, Y., & Gao, Y. (2020). Fabrication, characterization, physicochemical stability of zein-chitosan nanocomplex for co-encapsulating curcumin and resveratrol. *Carbohydrate Polymers*, *236*(February), 116090. https://doi.org/10.1016/j.carbpol.2020.116090

Chen, S., Han, Y., Sun, C., Dai, L., Yang, S., Wei, Y., … Gao, Y. (2018). Effect of molecular weight of hyaluronan on zein-based nanoparticles: Fabrication, structural characterization

and delivery of curcumin. *Carbohydrate Polymers*, *201*(17), 599–607. https://doi.org/10.1016/j.carbpol.2018.08.116

Chen, S., Li, Q., McClements, D. J., Han, Y., Dai, L., Mao, L., & Gao, Y. (2020). Co-delivery of curcumin and piperine in zein-carrageenan core-shell nanoparticles: Formation, structure, stability and in vitro gastrointestinal digestion. *Food Hydrocolloids*, *99*(August 2019), 105334. https://doi.org/10.1016/j.foodhyd.2019.105334

Dai, L., Li, R., Wei, Y., Sun, C., Mao, L., & Gao, Y. (2018). Fabrication of zein and rhamnolipid complex nanoparticles to enhance the stability and in vitro release of curcumin. *Food Hydrocolloids*, *77*, 617–628. https://doi.org/10.1016/j.foodhyd.2017.11.003

Dai, L., Sun, C., Li, R., Mao, L., Liu, F., & Gao, Y. (2017). Structural characterization, formation mechanism and stability of curcumin in zein-lecithin composite nanoparticles fabricated by antisolvent co-precipitation. *Food Chemistry*, *237*, 1163–1171. https://doi.org/10.1016/j.foodchem.2017.05.134

Huang, X., Huang, X., Gong, Y., Xiao, H., McClements, D. J., & Hu, K. (2016). Enhancement of curcumin water dispersibility and antioxidant activity using core-shell protein-polysaccharide nanoparticles. *Food Research International*, *87*, 1–9. https://doi.org/10.1016/j.foodres.2016.06.009

Khan, M. A., Yue, C., Fang, Z., Hu, S., Cheng, H., Bakry, A. M., & Liang, L. (2019). Alginate/chitosan-coated zein nanoparticles for the delivery of resveratrol. *Journal of Food Engineering*, *258*(March), 45–53. https://doi.org/10.1016/j.jfoodeng.2019.04.010

Minakawa, A. F. K., Faria-Tischer, P. C. S., & Mali, S. (2019). Simple ultrasound method to obtain starch micro- and nanoparticles from cassava, corn and yam starches. *Food Chemistry*, *283*(January), 11–18. https://doi.org/10.1016/j.foodchem.2019.01.015

Priyadarsini, K. I. (2009). Photophysics, photochemistry and photobiology of curcumin: Studies from organic solutions, bio-mimetics and living cells. *Journal of Photochemistry and Photobiology C: Photochemistry Reviews*, *10*(2), 81–95. https://doi.org/10.1016/j.jphotochemrev.2009.05.001

Ren, X., Hou, T., Liang, Q., Zhang, X., Hu, D., Xu, B., … Ma, H. (2019). Effects of frequency ultrasound on the properties of zein-chitosan complex coacervation for resveratrol encapsulation. *Food Chemistry*, *279*(May 2018), 223–230. https://doi.org/10.1016/j.foodchem.2018.11.025

Shinde, P., Agraval, H., Singh, A., Yadav, U. C. S., & Kumar, U. (2019). Synthesis of luteolin loaded zein nanoparticles for targeted cancer therapy improving bioavailability and efficacy. *Journal of Drug Delivery Science and Technology*, *52*(April), 369–378. https://doi.org/10.1016/j.jddst.2019.04.044

Shukla, R., & Cheryan, M. (2001). Zein: The industrial protein from corn. *Industrial Crops and Products*, *13*(3), 171–192. https://doi.org/10.1016/S0926-6690(00)00064-9

Silva, A. C. da, Santos, P. D. de F., Silva, J. T. do P., Leimann, F. V., Bracht, L., & Gonçalves, O. H. (2018). Impact of curcumin nanoformulation on its antimicrobial activity. *Trends in Food Science and Technology*, *72*(January 2017), 74–82. https://doi.org/10.1016/j.tifs.2017.12.004

Thorat, A. A., & Dalvi, S. V. (2014). Particle formation pathways and polymorphism of curcumin induced by ultrasound and additives during liquid antisolvent precipitation. *CrystEngComm*, *16*(48), 11102–11114. https://doi.org/10.1039/c4ce02021a

Ubeyitogullari, A., & Ciftci, O. N. (2019). A novel and green nanoparticle formation approach to forming low-crystallinity curcumin nanoparticles to improve curcumin's bioaccessibility.

Scientific Reports, *9*(1), 1–11. https://doi.org/10.1038/s41598-019-55619-4

Wei, Y., Yu, Z., Lin, K., Sun, C., Dai, L., Yang, S., … Gao, Y. (2019). Fabrication and characterization of resveratrol loaded zein-propylene glycol alginate-rhamnolipid composite nanoparticles: Physicochemical stability, formation mechanism and in vitro digestion. *Food Hydrocolloids*, *95*(17), 336–348. https://doi.org/10.1016/j.foodhyd.2019.04.048

Zhang, H., Fu, Y., Xu, Y., Niu, F., Li, Z., Ba, C., … Li, X. (2019). One-step assembly of zein/caseinate/alginate nanoparticles for encapsulation and improved bioaccessibility of propolis. *Food and Function*, *10*(2), 635–645. https://doi.org/10.1039/c8fo01614c

Zhang, Y., Cui, L., Li, F., Shi, N., Li, C., Yu, X., … Kong, W. (2016). Design, fabrication and biomedical applications of zein-based nano/micro-carrier systems. *International Journal of Pharmaceutics*, *513*(1–2), 191–210. https://doi.org/10.1016/j.ijpharm.2016.09.023

CHAPTER 7: Conclusions and future directions

Nanoscale delivery systems, nanoparticles have received increasing attention in the food industry for applications like food packaging, sensor, and encapsulation. In this study, zein nanoparticles formed via a microfluidic fabrication and ultrasonic treatment and encapsulated nisin and curcumin, respectively. The findings of this study showed that for the microfluidic chip zein nanoparticles, OSA modified increased the stability of nanoparticles. And as the concentration of OSA modified starch increased, the encapsulation efficiency and anti-microbial activity of nisin increased. And for the ultrasonic treatment of zein nanoparticles, as the concentration of ethanol concentration in the continuous phase increased, the particle size increased. PDI results revealed that as the concentration of ethanol in the continuous increased, the PDI decreased and then increased. Besides, the presence of zein protected curcumin from degradation under heat and UV light treatment.

Because of precisely controlled particle size and small reagents, a microfluidic chip is suitable for delicate materials. However, the sample collection in the microfluidic chip is time-consuming due to the micro-scales dimension channel and the flow rate of the continuous phase and dispersed phase cannot be very high. For future studies, the continuous system for the formation of nanoparticles via microfluidic chip can be fabricated to increase the throughput. What's more, microfluidic chips are easy to clog, especially for the biomaterials, such as zein. The other direction for the microfluidic chips future study could focus on decreasing clogging during the formation of the nanoparticles.

For the nanoparticles via ultrasonic treatment, the challenge associated with the heat produce by high amplitude. In this study, the results showed that when the amplitude is more than 50%, the heat produce by ultrasonic treatment is obvious and even affects the properties of materials. The

future study could focus on avoiding heat transfer to affect materials under the high amplitude treatment. Although the zein can form the self-assembled nanoparticles via ultrasonic treatment, mass production is still a major obstacle for future application in the food industry. So the future study could focus on creating a continuous system to fabricate zein nanoparticles formation system via ultrasonic treatment with other technologies, such as spray drying.

APPENDIX

Table A.1 The effective diameter of the 1%, and 2% zein nanoparticles with various concentrations of modified starch.

The Sample Code	Effective Diameter (nm)
MS0-Zein1	117.8±14.5[a]
MS0-Zein2	150.53±3.48[b]
MS1-Zein1	140.3±6.5[ab]
MS1-Zein2	186.13±4.3[cd]
MS2.5-Zein1	145.87±5.51[ab]
MS2.5-Zein2	205.63±5.12[c]
MS5-Zein1	158.9±14.33[b]
MS5-Zein2	251.1±3.38[e]
MS7.5-Zein1	181.9±7.74[d]
MS7.5-Zein2	281.87±7.38[f]
MS10-Zein1	198.7±13.9[cd]
MS10-Zein2	317.6±3.4[g]

Values with different letters in the same column are significantly different ($P < 0.05$).

Table A.2 The PDI of the 1%, and 2% zein nanoparticles with various concentrations of modified starch.

The Sample Code	PDI
MS0-Zein1	0.31 ± 0.012^{abc}
MS0-Zein2	0.29 ± 0.02^{ab}
MS1-Zein1	0.272 ± 0.02^{a}
MS1-Zein2	0.285 ± 0.012^{ab}
MS2.5-Zein1	0.296 ± 0.007^{ab}
MS2.5-Zein2	0.288 ± 0.014^{ab}
MS5-Zein1	0.33 ± 0.011^{bc}
MS5-Zein2	0.316 ± 0.026^{abc}
MS7.5-Zein1	0.325 ± 0.007^{bc}
MS7.5-Zein2	0.31 ± 0.014^{abc}
MS10-Zein1	0.343 ± 0.012^{c}
MS10-Zein2	0.313 ± 0.023^{abc}

Values with different letters in the same column are significantly different ($P< 0.05$).

Table A.3 The encapsulation efficiency of the nisin encapsulated zein nanoparticle with 0, 5, and 10% modified starch.

The Sample Code	Encapsulation Efficiency
MS0-Zein1	10.23 ± 3.33^{a}
MS0-Zein2	22.4 ± 4.81^{b}
MS5-Zein1	21.08 ± 3.04^{b}
MS5-Zein2	50.69 ± 7.91^{c}
MS10-Zein1	40.14 ± 5.57^{d}
MS10-Zein2	52.25 ± 7.73^{c}

Values with different letters in the same column are significantly different ($P< 0.05$).

Table A.4 Antimicrobial activity nisin encapsulated zein nanoparticle with 0, 5, and 10% modified starch.

The Sample Code	*L.monocytogenes* (Log CFU/g)				
	Day 0	Day 3	Day 5	Day 7	Day 14
Non-antimicrobial	3.44±0.167^{a}	3.78±0.047^{b}	4.32±0.009^{c}	4.65±0.009^{c}	5.37±0.100^{d}
Free Nisin	3.44±0.167^{a}	3.54±0.141^{ab}	4.17±0.030^{c}	4.44±0.094^{c}	5.29±0.096^{d}
MS0-Zein1	3.44±0.167^{a}	3.46±0.093^{ab}	3.93±0.095^{bc}	4.28±0.046^{c}	5.05±0.096^{d}
MS0-Zein2	3.44±0.167^{a}	3.29±0.046^{a}	3.74±0.015^{b}	4.08±0.030^{bc}	4.90±0.096^{d}
MS5-Zein1	3.44±0.167^{a}	3.59±0.081^{ab}	4.02±0.039^{c}	4.46±0.059^{c}	5.17±0.067^{d}
MS5-Zein2	3.44±0.167^{a}	3.42±0.028^{a}	3.65±0.053^{ab}	4.22±0.013^{c}	4.88±0.061^{cd}
MS10-Zein1	3.44±0.167^{a}	3.38±0.081^{a}	3.71±0.148^{ab}	4.24±0.065^{c}	5.17±0.263^{d}
MS10-Zein2	3.44±0.167^{a}	3.29±0.170^{a}	3.56±0.058^{ab}	4.07±0.067^{bc}	4.82±0.056^{cd}

Values with different letters in the same column are significantly different ($P< 0.05$).

Table A.5 The effective diameter of 2% zein nanoparticles with various concentrations of ethanol, amplitude (Dispersed phase: Continuous phase = 1:2).

Treatment	Ethanol Concentration (%, w/v)	Effective Diameter (nm)
Shearing	0	163.51±16.8[a]
	10	205.97±11.47[b]
	20	347.87±4.53[d]
	30	451.03±17.28[e]
20% Amplitude	0	197.13±3.85[b]
	10	247.33±18.63[c]
	20	349.77±13.59[d]
	30	418.77±64.77[e]
30% Amplitude	0	200.83±3.98[b]
	10	246.86±8.31[c]
	20	349.71±4.84[d]
	30	486.57±13.8[e]
40% Amplitude	0	201.5±4.3[b]
	10	253.8±16.69[c]
	20	352.6±14.39[d]
	30	439.37±61.45[e]
50% Amplitude	0	206.97±0.5[b]
	10	261.3±14.89[c]
	20	366.57±3.30[d]
	30	524±41.1[f]

Values with different letters in the same column are significantly different ($P < 0.05$).

Table A.6 The PDI of 2% zein nanoparticles with various concentrations of ethanol, amplitude (Dispersed phase: Continuous phase = 1:2).

Treatment	Ethanol Concentration (%, w/v)	PDI
Shearing	0	0.195 ± 0.031^{b}
	10	0.33 ± 0.003^{c}
	20	0.4 ± 0.015^{d}
	30	0.45 ± 0.018^{e}
20% Amplitude	0	0.21 ± 0.0164^{b}
	10	0.138 ± 0.0084^{a}
	20	0.146 ± 0.016^{ab}
	30	0.516 ± 0.057^{f}
30% Amplitude	0	0.212 ± 0.013^{b}
	10	0.138 ± 0.033^{a}
	20	0.214 ± 0.01^{b}
	30	0.461 ± 0.053^{e}
40% Amplitude	0	0.161 ± 0.015^{ab}
	10	0.157 ± 0.017^{ab}
	20	0.189 ± 0.024^{b}
	30	0.472 ± 0.061^{e}
50% Amplitude	0	0.161 ± 0.017^{a}
	10	0.124 ± 0.012^{a}
	20	0.227 ± 0.011^{b}
	30	0.335 ± 0.063^{c}

Values with different letters in the same column are significantly different ($P< 0.05$).

Table A.7 The effective diameter of 2% zein nanoparticles with various concentrations of ethanol, amplitude (Dispersed phase: Continuous phase = 1:5).

Treatment	Ethanol Concentration (%, w/v)	Effective Diameter (nm)
Shearing	0	94.21±5.63[a]
	10	137.9±3.29[b]
	20	195.93±6.08[c]
	30	413.23±19.02[f]
20% Amplitude	0	127.93±5.35[b]
	10	180.33±4.39[c]
	20	244.06±8.65[d]
	30	334.43±5.08[e]
30% Amplitude	0	128.93±5.59[b]
	10	180.06±4.18[c]
	20	238.97±7.96[d]
	30	341.67±15.09[e]
40% Amplitude	0	135.46±5.84[b]
	10	183.3±8.15[c]
	20	243.16±6.02[d]
	30	359.87±14.15[e]
50% Amplitude	0	136.87±4.21[b]
	10	179.27±5.35[c]
	20	240.57±14.20[d]
	30	385.53±23.37[e]

Values with different letters in the same column are significantly different ($P < 0.05$).

Table A.8 The PDI of 2% zein nanoparticles with various concentrations of ethanol, amplitude (Dispersed phase: Continuous phase = 1:5).

Treatment	Ethanol Concentration (%, w/v)	PDI
Shearing	0	0.253 ± 0.015^{d}
	10	0.208 ± 0.006^{c}
	20	0.178 ± 0.011^{b}
	30	0.449 ± 0.050^{e}
20% Amplitude	0	0.264 ± 0.009^{d}
	10	0.236 ± 0.008^{dc}
	20	0.119 ± 0.002^{a}
	30	0.254 ± 0.019^{dc}
30% Amplitude	0	0.268 ± 0.013^{d}
	10	0.216 ± 0.012^{c}
	20	0.132 ± 0.016^{a}
	30	0.294 ± 0.036^{d}
40% Amplitude	0	0.255 ± 0.011^{d}
	10	0.188 ± 0.015^{c}
	20	0.106 ± 0.041^{a}
	30	0.251 ± 0.028^{d}
50% Amplitude	0	0.245 ± 0.013^{d}
	10	0.164 ± 0.005^{c}
	20	0.102 ± 0.006^{a}
	30	0.27 ± 0.051^{d}

Values with different letters in the same column are significantly different ($P< 0.05$).

Table A.9 The effective diameter of 2% zein nanoparticles with various concentrations of ethanol, amplitude (Dispersed phase: Continuous phase = 1:10).

Treatment	Ethanol Concentration (%, w/v)	Effective Diameter (nm)
Shearing	0	77.84±4.69[a]
	10	114.55±3.68[b]
	20	161.57±5.18[c]
	30	234.73±17.71[e]
20% Amplitude	0	108.38±6.63[b]
	10	143.03±1.78[bc]
	20	201±8.98[d]
	30	278.46±10.78[e]
30% Amplitude	0	112.63±3.51[b]
	10	141.07±4.31[bc]
	20	204.27±6.07[d]
	30	273.4±7.76[e]
40% Amplitude	0	121.97±2.06[b]
	10	149.33±7.20[bc]
	20	205.37±3.26[d]
	30	279.43±9.72[e]
50% Amplitude	0	118.43±6.33[b]
	10	147.3±1.93[bc]
	20	198.23±6.60[d]
	30	296.23±13.71[e]

Values with different letters in the same column are significantly different ($P < 0.05$).

Table A.10 The PDI of 2% zein nanoparticles with various concentrations of ethanol, amplitude (Dispersed phase: Continuous phase = 1:10).

Treatment	Ethanol Concentration (%, w/v)	PDI
Shearing	0	0.322 ± 0.007^{e}
	10	0.247 ± 0.003^{d}
	20	0.242 ± 0.028^{d}
	30	0.223 ± 0.029^{d}
20% Amplitude	0	0.27 ± 0.006^{de}
	10	0.235 ± 0.004^{d}
	20	0.212 ± 0.012^{d}
	30	0.178 ± 0.022^{c}
30% Amplitude	0	0.251 ± 0.003^{d}
	10	0.199 ± 0.003^{c}
	20	0.182 ± 0.012^{c}
	30	0.165 ± 0.036^{c}
40% Amplitude	0	0.261 ± 0.022^{d}
	10	0.212 ± 0.008^{c}
	20	0.178 ± 0.009^{c}
	30	0.108 ± 0.028^{b}
50% Amplitude	0	0.260 ± 0.014^{d}
	10	0.215 ± 0.009^{c}
	20	0.121 ± 0.022^{b}
	30	0.097 ± 0.006^{a}

Values with different letters in the same column are significantly different ($P< 0.05$).

Table A.11 The effective diameter of curcumin-encapsulated zein nanoparticles with various concentrations of ethanol, amplitude (Dispersed phase: Continuous phase = 1:5).

Treatment	Ethanol Concentration (%, w/v)	Effective Diameter (nm)
Shearing	0	91.63±7.29[a]
	10	131.53±6.79[b]
	20	196.03±7.7[c]
	30	456.1±32.52[f]
20% Amplitude	0	129.2±10.45[b]
	10	216.97±12.59[c]
	20	302±20.63[d]
	30	358.5±26.43[e]
50% Amplitude	0	130.8±3.34[b]
	10	250.87±16.77[cd]
	20	284.5±9.01[d]
	30	370.27±5.12[e]

Values with different letters in the same column are significantly different ($P < 0.05$).

Table A.12 The PDI of curcumin-encapsulated zein nanoparticles with various concentrations of ethanol, amplitude (Dispersed phase: Continuous phase = 1:5).

Treatment	Ethanol Concentration (%, w/v)	PDI
Shearing	0	0.331 ± 0.016^{c}
	10	0.253 ± 0.044^{b}
	20	0.26 ± 0.04^{b}
	30	0.452 ± 0.092^{e}
20% Amplitude	0	0.237 ± 0.022^{a}
	10	0.297 ± 0.02^{bc}
	20	0.332 ± 0.016^{c}
	30	0.316 ± 0.025^{bc}
50% Amplitude	0	0.296 ± 0.026^{bc}
	10	0.344 ± 0.017^{c}
	20	0.327 ± 0.04^{c}
	30	0.294 ± 0.036^{bc}

Values with different letters in the same column are significantly different ($P< 0.05$).

Table A.13 The encapsulation efficiency of curcumin in zein nanoparticles with various concentrations of ethanol, amplitude (Dispersed phase: Continuous phase = 1:5).

Treatment	Ethanol Concentration (%, w/v)	Encapsulation Efficiency (%)
Shearing	0	19.14±2.13[c]
	10	21.52±6.07[c]
	20	25.13±1.62[c]
	30	6.73±0.57[a]
20% Amplitude	0	36.20±2.27[d]
	10	63.65±0.58[f]
	20	76.51±3.76[g]
	30	8.5±2.06[a]
50% Amplitude	0	47.55±1.67[e]
	10	81.43±4.12[g]
	20	79.55±3.42[g]
	30	11.64±1.71[b]

Values with different letters in the same column are significantly different ($P < 0.05$).

Table A.14 The loading capacity of curcumin in zein nanoparticles with various concentrations of ethanol, amplitude (Dispersed phase: Continuous phase = 1:5).

Treatment	Ethanol Concentration (%, w/v)	Loading Capacity
Shearing	0	0.95 ± 0.100^{b}
	10	1.07 ± 0.298^{b}
	20	1.24 ± 0.075^{b}
	30	0.34 ± 0.028^{a}
20% Amplitude	0	1.79 ± 0.116^{c}
	10	3.12 ± 0.029^{e}
	20	3.73 ± 0.167^{f}
	30	0.42 ± 0.101^{a}
50% Amplitude	0	2.34 ± 0.114^{d}
	10	3.96 ± 0.202^{f}
	20	3.87 ± 0.184^{f}
	30	0.58 ± 0.08^{a}

Values with different letters in the same column are significantly different ($P< 0.05$).

Table A.15 The thermal stability of curcumin in zein nanoparticles with various concentrations of ethanol and amplitude at 63 ℃, 30 min (Dispersed phase: Continuous phase = 1:5).

Treatment	Ethanol Concentration (%, w/v)	Curcumin Retention (%)
Free Curcumin	-	85.98±1.23[a]
Shearing	0	98.95±0.45[b]
	10	100[b]
	20	98.89±0.639[b]
	30	100[b]
20% Amplitude	0	98.89±0.562[b]
	10	99.07±0.752[b]
	20	100[b]
	30	100[b]
50% Amplitude	0	100[b]
	10	98.89±0.234[b]
	20	98.67±0.342[b]
	30	99.56±0.892[b]

Values with different letters in the same column are significantly different ($P < 0.05$).

Table A.16 The DPPH radical scavenging activity of curcumin in zein nanoparticles with various concentrations of ethanol, amplitude (Dispersed phase: Continuous phase = 1:5).

Treatment	Ethanol Concentration (%, w/v)	DPPH Radical Scavenging activity (%)
Free Curcumin	-	16.52 ± 1.15^{c}
Shearing	0	14.17 ± 0.60^{b}
	10	16.49 ± 0.08^{c}
	20	22.23 ± 1.44^{e}
	30	12.02 ± 0.86^{a}
20% Amplitude	0	13.89 ± 0.24^{b}
	10	15.65 ± 1.04^{c}
	20	21.16 ± 0.83^{e}
	30	11.72 ± 1.58^{a}
50% Amplitude	0	13.62 ± 0.45^{b}
	10	18.26 ± 0.85^{d}
	20	22.85 ± 0.47^{e}
	30	14.48 ± 0.46^{bc}

Values with different letters in the same column are significantly different ($P< 0.05$).